THE CHEMILUMINESCENCE OF LUCIGENIN

by

Kenneth D. Legg

B.S. Union College

(1964)

Submitted in Partial Fulfillment

of the Requirements of the

Degree of

DOCTOR OF PHILOSOPHY

at the

MASSACHUSETTS INSTITUTE OF TECHNOLOGY

August, 1969

Signature of Author _____
Department of Chemistry, August 6, 1969

Certified by _____
Thesis Supervisor

Accepted by _____
Chairman, Departmental Committee on Graduate Students

This doctoral thesis has been examined by a Committee of the Department of Chemistry as follows:

Professor David N. Hume _____ Chairman

Professor David M. Hercules _____ Thesis Supervisor

Professor Kerry W. Bowers _____

The Chemiluminescence of Lucigenin

Kenneth D. Legg

Submitted to the Department of Chemistry on 6 August 1969 in partial fulfillment of the requirement for the degree of Doctor of Philosophy.

Abstract

The electrochemical behavior of lucigenin has been studied in both aqueous and non-aqueous systems. The initial reduction of lucigenin has been shown to proceed by a one-electron charge transfer step leading to the mono-cation radical of lucigenin. The charge transfer step is followed by a rapid disproportionation of the radical yielding dimethyl biacridene (DBA) as the end product. The rate constant of the following disproportionation step has been estimated as 8×10^3 1/M-sec. The oxidation of DBA has been shown to proceed *via* two, consecutive one-electron oxidations, occurring at the same potential, yielding lucigenin as the product.

The electrochemically generated chemiluminescence (ECL) of lucigenin has been studied in both aqueous and non-aqueous media. The non-aqueous ECL has been shown to arise from the reaction of superoxide with lucigenin. The spectral characteristics of the ECL, when compared with the fluorescence spectra and quantum efficiencies of N-methyl acridone (NMA), DBA and lucigenin allow identification of the emitting species. NMA is the primary emitter formed in the excited state by the reaction of superoxide with lucigenin. In several systems a second, longer wavelength component of emission was observed. This was the fluorescence of either DBA or lucigenin, depending on their respective concentrations and quantum efficiencies. Both DBA and lucigenin act as energy acceptors from excited NMA *via* singlet-singlet energy transfer.

Chemiluminescence has been observed in three non-aqueous solvents (DMSO, DMF and acetonitrile) from the reaction of potassium tert-butoxide with lucigenin and oxygen. Spectra of this chemiluminescence show the same gross behavior as those observed in the ECL studies. The same considerations as to extent of reaction, quantum efficiencies of acceptor fluorescence and energy transfer probabilities may be used to explain these spectra as were used for the ECL spectra. At high base and lucigenin concentrations a third yet unidentified product is formed.

A study has been made of the quenching of lucigenin's fluorescence by various anions, notably chloride. As in the case of amine quenching, a direct relationship between ionization potential of the quencher and its quenching efficiency is seen. Rate constants for the quenching are diffusion controlled and a charge-transfer mechanism is proposed. Photoreaction of lucigenin has been observed and studies have shown this process to occur from the first excited singlet state of lucigenin.

Thesis Supervisor: David M. Hercules
Title: Associate Professor of Chemistry

"THERE IS NOTHING - ABSOLUTELY NOTHING - HALF SO MUCH WORTH DOING AS SIMPLY MESSING ABOUT IN BOATS."

The Water Rat

from

"The Wind in the Willows"

by

Kenneth Grahame

Acknowledgements

The author would like to thank Professor David M. Hercules for his help and encouragement during the course of the research. His willingness to allow the author to follow his own whims in this work is especially appreciated. Thanks are also due to Professors David N. Hume and Kerry W. Bowers for their constructive criticism in preparing the final draft of this thesis.

A special note of thanks goes to Dr. Donald W. Shive for his invaluable aid and suggestions pertaining to the electrochemical measurements. The author is also indebted to Dr. Jack Chang for further aid in the electrochemistry and to Dr. Stanley Ness for building the Image Intensifier Spectrograph without which much of this work would have been impossible. The extent of help of the "group" as a whole cannot be estimated and I am greatly appreciative of their contribution.

The author wishes to thank the National Institutes of Health for a fellowship for the years 1965-1968.

Thanks are due to Miss Louise Harris for typing the manuscript and to Dr. Ness for proof reading the final draft.

Finally, the author would like to extend his most sincere thanks to his able "first mate" for her steady hand at the wheel during the past two years. How she has put up with him during this time is beyond understanding.

Table of Contents

I. Index of Figures 10

II. Index of Tables 12

III. Introduction 14

IV. Experimental 16

A. Chemicals 16

B. Solvents 17

C. Solutions 17

D. Apparatus 17

1. Electrochemical Instrumentation 17

2. Electrochemical Cell 18

3. Spectroscopic Instrumentation 19

E. Procedures 20

1. Current-Voltage Curves 20

a) Current-Voltage Curves 20

b) Oscillograms 20

c) Coulometry 20

d) ESR 23

2. ECL 24

a) Qualitative Observation of ECL 24

b) Measurement of ECL Spectra 24

3. Energy Transfer 25

a) Quantum Efficiency Measurements 25

b) Lifetime Measurements 26

4. Non-Aqueous Chemiluminescence 27

a) Qualitative Observation of Chemiluminescence 27

b) Measurement of Non-Aqueous Chemiluminescence Spectra 27

V. Electrochemical Results 29

A. Cyclic Voltammetry 29

B. Coulometry 32

C. Scan Rate Studies 33

D. ESR 44

VI. Electrochemistry Discussion 47

VII. ECL Results 56

A. Production of Lucigenin ECL 56

B. Spectral Study of Lucigenin ECL 57

1. Non-aqueous ECL Spectra 57

2. Aqueous ECL Spectra 64

C. Summary of ECL Results 64

D. Energy Transfer Studies 79

VIII. ECL Discussion 94

A. Qualitative Observations 94

B. ECL Spectra 95

C. Singlet-Singlet Energy Transfer Studies 101

D. Correlation of ECL Spectra with Quantum Efficiencies of Acceptor Fluorescence, Extent of Reaction and Energy Transfer 103

IX. Preliminary Investigations of the Non-Aqueous Chemiluminescence of Lucigenin 109

A. Results 109

1. Qualitative observations 109

2. Chemiluminescence Spectra 109

B. Discussion 109

1. Qualitative observations 109

2. Chemiluminescence spectra 126

Appendix A. Quenching of Lucigenin Fluorescence 128

References 146

Biographical Note 149

I. Index of Figures

IV-1	Cell used for taking ECL spectra	21
V-1	Current - voltage curves for lucigenin and oxygen in DMSO at platinum and in water at mercury	30
V-2	Current function ($i_p/\nu^{1/2}$) corrected for concentration vs scan rate for lucigenin reduction in DMSO	39
V-3	Current function ($i_p/\nu^{1/2}$) vs scan rate for DBA oxidation in DMSO	42
V-4	Current-voltage curve of lucigenin in DMSO at a scan rate of 80 V/sec.	45
VII-1	ECL spectra in DMSO	58
VII-2	ECL spectra in DMF	60
VII-3	ECL and fluorescence spectra in DMF	62
VII-4	ECL spectra in AN	65
VII-5	ECL spectra in AN at various times of reaction	67
VII-6	ECL and fluorescence spectra in Ethanol	69
VII-7	Sensitivity curve for the Image Intensifier Spectrograph	71
VII-8	ECL spectra in water	73
VII-9	"Classical" CL spectra in water	75
VII-10	Fluorescence and ECL spectra in water	77
VII-11	Fluorescence quenching of NMA by DBA in DMSO	80
VII-12	Stern-Volmer plot for energy transfer from NMA to lucigenin in DMSO	84
VII-13	Overlap of NMA fluorescence with DBA and lucigenin absorption	88
VII-14	Probability plots for energy transfer from NMA to DBA and lucigenin in AN	90
VIII-1	Corrected ECL spectra in AN	96
VIII-2	Comparison of ECL spectra taken on the Aminco-Bowman Spectrofluorometer and the Image Intensifier Spectrograph	99

IX-1	Chemiluminescence Spectra in DMSO	110
IX-2	Chemiluminescence Spectra in DMF	112
IX-3	Chemiluminescence and Fluorescence Spectra in DMF	114
IX-4	Chemiluminescence Spectra in AN	116
IX-5	Chemiluminescence Spectra in AN at Various Flow Rates	118
IX-6	Absorption and Fluorescence Spectra of Compound Formed by Reaction of lucigenin with KOtBu in AN	121
IX-7	NMR Spectrum of lucigenin in trifluoroacetic acid	124
A-1	Relationship between Ionization potential of amines and their efficiency of quenching lucigenin fluorescence	133
A-2	Absorption spectra of lucigenin in water before and after photoreaction	136
A-3	Amount of photoreaction (ΔA) vs lifetime of lucigenin fluorescence at various chloride concentrations	141
A-4	State diagrams showing mode of energy dissipation in fluorescence quenching by chloride ion	144

II. Index of Tables

V-1	Coulometry of Lucigenin Reduction in DMSO	34
V-2	Coulometry of DBA Oxidation in DMSO	35
V-3	Scan Rate Study of Lucigenin Reduction (2.14×10^{-3} M lucigenin in DMSO)	36
V-4	Scan Rate Study of Lucigenin Reduction (1.07×10^{-2} M lucigenin in DMSO)	37
V-5	Scan Rate Study of Lucigenin Reduction (2.14×10^{-2} M lucigenin in DMSO)	38
V-6	Scan Rate Study of DBA Oxidation in DMSO	41
VII-1	Fluorescence Lifetimes and Quantum Efficiencies	82
VII-2	Experimental and Theoretical Rate Constants for Energy Transfer and Critical Radius	86
VII-3	Concentration of Acceptor where Total Probability of Energy Transfer and the "Trivial" Process from NMA Equals 0.5	93
A-1	Anion Quenching of Lucigenin Fluorescence	130
A-2	Quenching of Lucigenin Fluorescence by Amines	131
A-3	Chloride Quenching of Lucigenin Fluorescence in Various Solvents	135
A-4	Photolysis of Lucigenin as a Function of Chloride Concentration	139

Commonly Occurring Structures and their Abbreviations

Structure	Name	Abbreviation
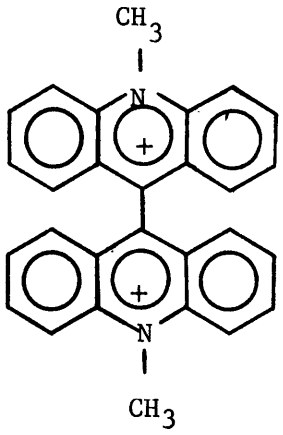	Lucigenin	L^{++}
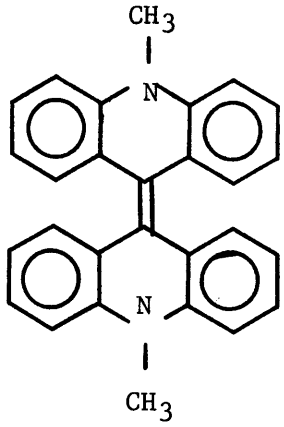	Dimethyl biacridene	DBA
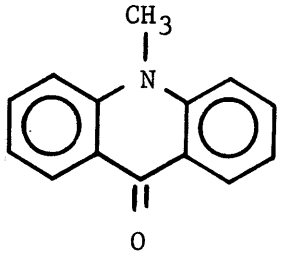	N-methyl acridone	NMA
$(CH_3)_2SO$	Dimethylsulfoxide	DMSO
CH_3CN	Acetonitrile	AN
$(CH_3)_2$ N-COH	Dimethyl Formamide	DMF
$KOC(CH_3)_3$	Potassium tert-butoxide	KOtBu

III Introduction

Chemiluminescence (CL), the production of light from a chemical reaction, is not an unusual phenomenon. Indeed, light emission, albiet low level, has been shown to occur in a seemingly endless number of reactions. The phenomenon is not new since CL was observed from the oxidation of Lophine in 1877 (1). Luminol (2) and lucigenin (3) are two of the best known examples of chemiluminescent reactions and have received a great deal of attention because of their intense emission. Most solution CL studied to date falls into one of four major categories: reactions involving molecular oxygen or peroxides (4), oxidation of anion radicals (5), alternating current electrolysis of aromatic hydrocarbons (6,7) and reduction of ruthenium chelates (8).

The chemiluminescence of lucigenin (dimethyl biacridinium ion) is a reaction involving peroxide, and was first reported in 1935 by Gleu and Petsch (3). They observed intense CL when lucigenin was treated with hydrogen peroxide in basic solution. It was also observed that the emission was either green or blue, depending on the conditions under which the reaction was run. Addition of alcohols, reducing agents or heating caused the emission to change from green to blue (3, 9, 10). N-methyl acridone, the major product of the reaction, was tentatively (10) and later conclusively (11) identified as the primary emitter in the blue CL reaction. Kautsky and Kaiser (9) attributed the green emission to lucigenin fluorescence excited by emission from N-methyl acridone. This was later shown not to be the case by Spruit-van der Berg (10). Until now the green emitter had not been identified.

Since the discovery of the lucigenin CL, numerous studies have been carried out concerning its mechanism (9-16). The subject has been reviewed by McCapra (17) and Gundermann(4). The reaction has been shown to be of a redox type (2, 11, 18) but the exact nature of the redox step has not yet been ascertained. The electrochemistry of lucigenin has been briefly treated by Totter (11) but an extensive analysis of its behavior has not been reported.

The electrochemical generation of lucigenin CL at a platinum electrode in basic solution was reported by Tammamushi and Akiyama (19). They observed light at the platinum cathode, along the path of hydrogen evolution. No further work has been reported concerning the electrochemically generated CL (ECL) of lucigenin.

Driscoll et. al. (20) have reported the observation of lucigenin CL in methanol by reaction with potassium t-butoxide. Observation of this CL in other non-aqueous solvents has not been reported.

The purpose of the present investigation was two-fold. First, it was evident that a detailed study of the electrochemical behaviour of lucigenin would be of interest as applied to redox nature of the CL reaction. The second objective was the production of lucigenin CL in non-aqueous media. It was hoped that, like luminol, the CL process in non-aqueous media would be simpler than that seen in water. The production of lucigenin CL by electrochemical means seemed to be the logical starting place for such studies.

IV. Experimental

A. Chemicals

Lucigenin (nitrate salt) was obtained from Columbia Organic Chemicals and was recrystallized twice from 1:1 methanol-ethanol before use.

N-methyl acridone was obtained as a sample synthesized in the MIT Organic Laboratories (21) and was recrystallized from ethanol until a constant melting point of 202° - 203° C was obtained.

Dimethyl biacridene (DBA) was prepared according to Decker and Petsch (22). 5 grams of lucigenin were dissolved in 75 ml of Glacial Acetic acid. 25 grams of zinc pellets were added and the solution was allowed to stand overnight. The DBA produced is insoluble in the reaction medium and the bulk precipitates out on the zinc surface. The zinc-DBA precipitate was washed thoroughly with water and dried in a vacuum oven at 100°. The DBA was then dissolved in chloroform and, after concentration in a rotary evaporator, recrystallized twice from chloroform. 2.5 grams of DBA were obtained from the recrystallization.

Tetrabutyl ammonium perchlorate was prepared from 1 M tetrabutyl ammonium hydroxide (Southwestern Analytical). 70% perchloric acid (G. Frederick Smith) was diluted 1:1 with water and was added dropwise with stirring to the hydroxide until the solution was acidic (pH ~2). The precipitated perchlorate was collected by filtration and washed several times with hot water tc remove all traces of acid. The perchlorate was then recrystallized twice from 70% H_2O -30% methanol and dried in a vacuum oven at 100°.

Potassium t-butoxide was used as obtained from MSA Research Corporation. It was stored in a dry nitrogen atmosphere to ensure no re-

action with water.

Baker Analyzed Reagent 30% Hydrogen Peroxide was used as obtained.

All other organic and inorganic chemicals used were reagent grade or better.

B. Solvents.

Absolute ethanol (U.S. Industrial Chemicals Co.) was used as obtained.

Dimethyl Sulfoxide, Dimethyl Formamide (Matheson, Coleman and Bell, spectroscopic grade) and Acetonitrile (Eastman Chemicals, spectroscopic grade) were dried over molecular sieves before use.

All other solvents used were of spectroscopic grade when available or reagent grade or better.

C. Solutions.

Solutions of most reagents were made by weighing the reagent and dissolving it in the appropriate volume of solvent. Solutions of DBA were prepared by saturating the solvent with DBA and determining its concentration by its absorption at 420 nm (ε_{max} at 420 nm = 1.66×10^4). H_2O_2 solutions were prepared by appropriate dilution of 30% H_2O_2. Solutions of HCl or NaOH were prepared by dilution of 1 M stock solutions of Accu-Lute reagent.

D. Apparatus.

1. Electrochemical instrumentation.

Potentiostat. A potentiostat constructed by D. W. Shive was used in the direct electrochemical studies. This instrument and its use are described in detail elsewhere (23).

Recorder. A Houston HR-97 X-Y recorder was used to record the current-voltage curves for scan rates up to 0.333 V/sec.

Wave Generator. A Wavetek triangular wave generator was used to drive the potentiostat for scan rates greater than 0.333 V/sec.

Oscillograms. Oscillograms were obtained by use of a Tektronix Model 536 oscilloscope equipped with a Type 53A plug-in unit. The traces were photographed on polaroid film using a Tektronix Model C-12 camera with projected graticule.

Current Integrator. A current integrator (24) was used in the coulometric measurements. This consisted of a Nexus SQ-3 operational amplifier connected to the current amplifier of the potentiostat through a 5 meg ohm resistor. A 10μF capacitor was in the feedback loop of the integrator. The output voltage of this network is a direct function of the coulombs passed and is equal to 5×10^{-2} E_o (in Volts) coulombs. The output voltage of the current integrator was measured on a Hewlett Packard Model 344A digital volt meter.

2. Electrochemical cell.

A standard three electrode cell was used in all electrochemical measurements. The reference electrode was Ag/AgCl in 0.1 M aqueous KCl. The reference electrode was separated from the bulk of the solution in the cell with a porous Vycor plug. The counter electrode consisted of a 2 cm^2 platinum foil and was isolated from the test solution by a fine glass frit. The indicator electrode was a platinum sphere of 5.53×10^{-2} cm^2 area. 0.1 M tetrabutyl ammonium perchlorate was used as supporting electrolyte in non-aqueous solutions and 0.1 M KCl in aqueous media. For coulometric measurements a 2 cm^2 platinum foil working electrode was used. Provision for bubbling with N_2 was provided.

3. Spectroscopic Instrumentation.

Aminco-Bowman Spectrofluorometer. This instrument is described by Lytle (8) and was used without modification. It employs two Aminco grating monochromators (4-8401) mounted on an optical bench. The excitation monochromator is blazed for 300 nm while the emission monochromator is blazed for 500 nm. The sample chamber may be used for either fluorescence or chemiluminescence measurements. The detector is an E.M.I. 9558QA photomultiplier of S-20 response. This particular tube yielded a sensitivity of 300 amps/lumen. Spectra were recorded on a Hewlett Packard Model 7005B X-Y recorder.

Absolute Spectro Fluorometer. For routine fluorescence studies and quantum efficiency measurements a Turner Model 210 absolute spectrofluorometer was used. This instrument and its use are described by the Turner manual (25) and by Turner (26).

Spectrophotometer. Absorption spectra were recorded on a Cary Model 14 spectrophotometer.

Image Intensifier Spectrograph (IIS). An IIS was used to measure ECL spectra. The optical system was constructed according to Bass and Kessler (27), in conjunction with an RCA C70021 HP2 Image Intensifier tube, and is described by Ness and Hercules (28). A Polaroid camera using type 107 film was used to record the spectra. This has the advantage that the results are immediately available. However, since this film is available only in positive form, negatives have to be made before the spectra can be analyzed on a recording densitometer.

Recording Densitometer. A Leeds and Northrup recording microphotometer (L & N 6700 A2) was used to record the IIS spectra. This instrument and its use is described in the L & N manual DB-1325 (29).

Lifetimes. Lifetimes of fluorescence were obtained on a TRW Model

31A nanosecond fluorometry system.

Electrochemical. The potentiostat used consisted of Heath EUA-14-A operational amplifiers along with a Heath EUA-19-2 polarography module. A three electrode cell was used with a platinum counter electrode isolated from the bulk of the solution by a fine glass frit. A reference electrode of Ag/AgCl in 0.1 M KCl was used and was isolated from the test solution by a porous Vycor plug. Both platinum foil and mercury pool indicator electrodes were employed. Provision for bubbling N_2 or O_2 through the solution was included.

The cell used for taking ECL spectra is shown in Figure IV-1. A platinum wire was used as a reference electrode in this cell due to space limitations.

Syringe Drive. The syringe drive-"T" mixer combination used in the flow measurements has been described in detail by Lytle (8).

E. Procedures

1. Electrochemical

a) Current-voltage curves. Standard techniques were used in obtaining current voltage curves for scan rates up to 0.333 V/sec.

b) Oscillograms. For scan rates greater than 0.333 V/sec the Wavetek triangular wave generator was used to drive the potentiostat and the current voltage curves were recorded on an oscilloscope. The scan rates for a given run were calculated by noting the voltage range per cycle and the value of the cycles per second applied from the Wavetek. Residual currents were estimated to subtract capacity currents in obtaining peak currents from these data.

c) Coulometry. The current integrator described above was used in the coulometry measurements to determine n_c for the reduction of

Figure IV-1

Cell Used For Taking ECL Spectra

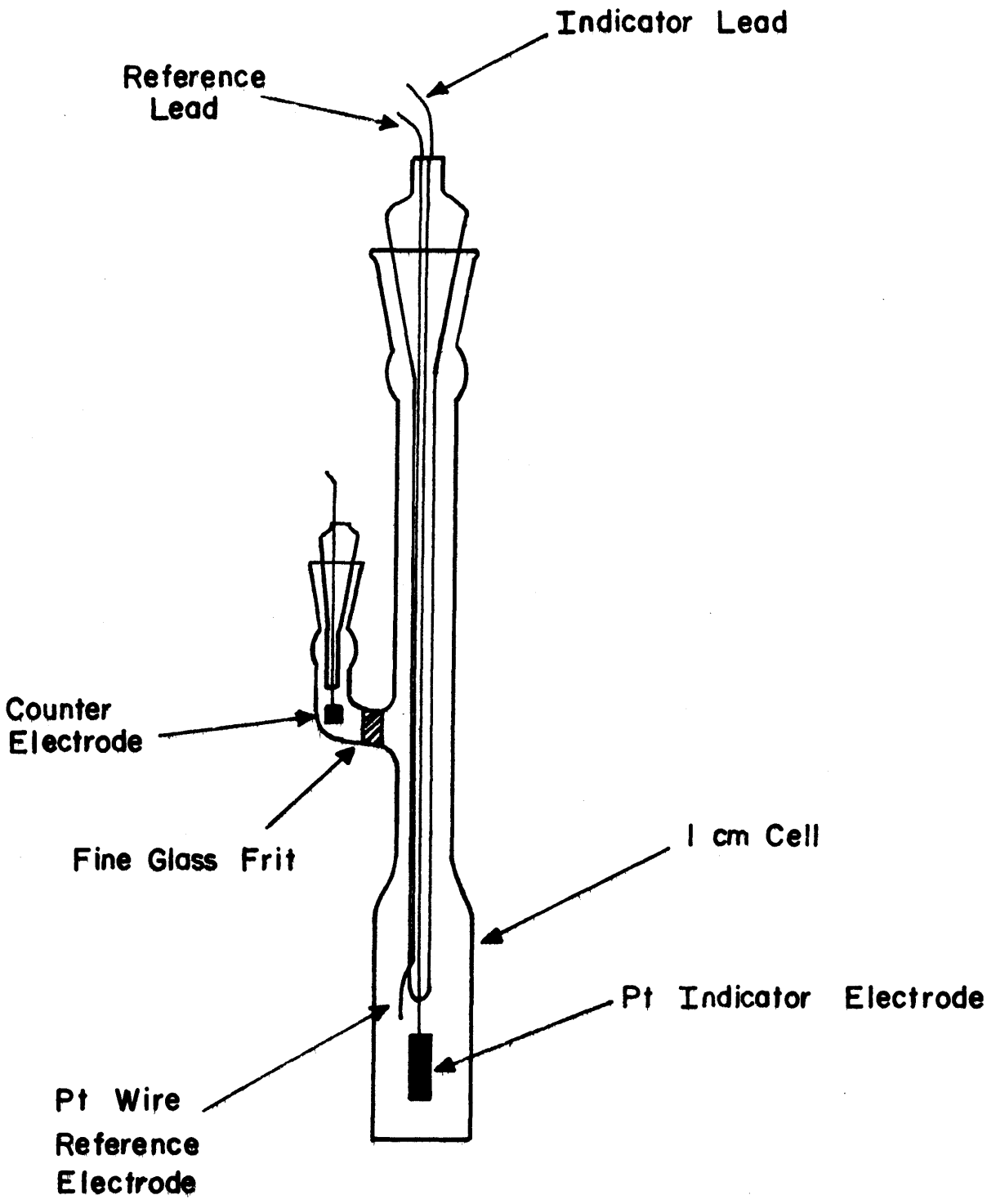
Indicator Lead
Reference Lead
Counter Electrode
Fine Glass Frit
1 cm Cell
Pt Indicator Electrode
Pt Wire Reference Electrode

ECL CELL

lucigenin and n_a for the oxidation of DBA, n being the number of electrons involved in the charge transfer step. 50 ml of a known concentration of lucigenin were introduced into the electrochemical cell. DMSO was used as the solvent to minimize evaporation of solvent during bubbling with N_2. A current-voltage curve was taken using the small spherical indicator electrode. A proportionality constant was then calculated by dividing the known moles of lucigenin present initially by the initial peak current in cm.

The current integrator was then connected, the large working electrode substituted for the platinum sphere and bubbling with nitrogen started. A constant potential of -0.35 V vs Ag/AgCl was then applied. After sufficient electrolysis (~10 min.) the applied potential was shut off and the voltage output of the current integrator was measured with a digital volt meter. The number of coulombs passed during the electrolysis was calculated by the relationship noted above. A second current-voltage curve was then recorded, using the small sphere as the indicator in quiescent solution. The difference in initial and final peak currents, when multiplied by the calculated proportionality constant gives the moles of substance reduced or oxidized. The moles of electrons passed was calculated by dividing the coulombs passed by 9.65×10^4. Dividing the moles of electrons passed by the moles reduced (or oxidized) gives n_c or n_a. The procedure was repeated and n was taken as the average of several runs.

d) ESR. A Varian Model E-3 ESR instrument was used to detect the presence of radicals in the lucigenin reduction. A two electrode cell was used consisting of a platinum wire indicator electrode and a mercury drop reference electrode. Standard techniques were used in observing the ESR signal obtained.

2. ECL

a) Qualitative Observation of ECL. The three electrode cell with Ag/AgCl reference electrode was used in these measurements. Current-voltage curves were recorded on a Houston Model HR-100 X-Y recorder. Solutions were approximately 10^{-3} M in lucigenin and were saturated with oxygen by bubbling for five minutes.

A mercury pool was used as the indicator electrode for aqueous solutions while a platinum foil indicator electrode was used in non-aqueous media. A current-voltage curve for the solution to be studied was recorded and a constant potential was then applied corresponding to the potential at the peak of the oxygen reduction wave. Light emission was observed visually.

b) Measurement of ECL Spectra. Initial measurements were made using the Aminco-Bowman spectrofluorometer in conjunction with the ECL cell shown in Figure VI-1. The excitation source was not used. The slits of the emission monochromator were opened to 3 mm. The photomultiplier was operated at 1750 V for greatest sensitivity. At these settings the signal to noise ratio was 20 to 1. The results of these measurements have been reported by Legg and Hercules (30).

ECL spectra of higher resolution and less distortion were obtained by use of the Image Intensifier Spectrograph (IIS). Exposure times from 5 to 20 seconds gave satisfactory results. Over-exposure of the Polaroid plate resulted in a flattening of the spectra and such spectra were discarded. Since the intensity of the ECL varied over a wide range during and between measurements several pictures of varying exposure times were taken and the best exposure was used.

The Polaroid Camera was mounted on a variable position rack and up to nine exposures could be taken on one photograph. A small mercury

pen lamp (Edmund Scientific Co. No. 70,298) was used to obtain calibration lines. Two sets of calibration lines were taken, one at the top and one at the bottom of the plate.

The slits were set at 3-4 mm for ECL spectra and at 0.01 mm for mercury lines and fluorescence spectra. Exposure times of 1/100 sec. were used in recording fluorescence and calibration spectra.

Fluorescence spectra for comparison with the ECL spectra were also taken on the IIS. The solutions to be studied were excited by the mercury pen lamp with a 380 nm low pass filter between the source and cell.

Photographic negatives were made of the Polaroid positive records of the spectra. These negatives were scanned on the Leeds and Northrup recording densitometer. Calibration lines were also scanned for each spectrum. Since the spectrograph uses a grating for dispersion, the spectra obtained from the densitometer are linear in wavelength and were plotted as such. Care had to be taken that the negative was placed in the plate holder so the spectra were exactly horizontal. This was facilitated by having the calibration lines at the top and bottom of the negative and alignment was assured by keeping the 3650 Å Hg lines (top and bottom) on the same vertical line.

3. Energy Transfer.

a) Quantum Efficiency Measurements. Quantum efficiencies of fluorescence were measured on a Turner Model 210 absolute spectrofluorometer. The method of determining quantum efficiencies with this instrument has been described by Turner (26). Absorbances of the solutions were measured on a Cary Model 14 spectrophotometer. Care

was taken that all solutions showed absorbances less than 0.22, to eliminate distortion of the fluorescence spectra due to self absorption. Quinine sulfate in 0.1 M H_2SO_4, $\phi_f = 0.55$ (31) was used as a standard. Integrated fluorescence intensities were measured using a planimeter. The quantum efficiency was calculated by:

$$\phi_u = \phi_s \frac{S_s A_u \lambda_{exs} D_s}{S_u A_s \lambda_{exu} D_u}$$

where ϕ_u and ϕ_s are the quantum efficiencies of the unknown and standard respectively, λ_{exu} and λ_{exs} their excitation wavelengths, S_u and S_s their sensitivity settings on the spectrofluorometer, A_u and A_s the respective areas of fluorescence and D_u and D_s the absorption of each solution.

b) Lifetime Measurements. The use of the TRW Model 31A nanosecond fluorometry system for measuring lifetimes of fluorescence is described in the TRW handbook (32). A deuterium lamp was used as the source because its light pulse had a shorter decay time (2ns) than did the nitrogen lamp. A 3600 Å broad pass filter was used between the source and the sample. For measuring NMA lifetimes a 425 nm interference filter was used between the sample and the photomultiplier. A 490 nm broad pass filter was used in measuring lifetimes for lucigenin and DBA.

Because many of the lifetimes measured were less than 10 ns. the internal photomultiplier was not used and only the external photomultiplier was employed. A suspension of aluminum hydroxide in water was used as a scatterer when the light pulse profile was measured. Care was taken to use the lowest possible photomultiplier voltage

to eliminate saturation of the tube. The apparatus was set up for each experiment so that the photomultiplier voltage and oscilloscope gain settings could be left unchanged during a series of measurements. Differences in intensities of fluorescence were compensated for by use of an iris diaphragm between the source and the sample. Round cells were employed to minimize differences in cell geometry between measurements.

Studies of singlet-singlet energy transfer between NMA* and both DBA and lucigenin were done on this instrument. The acceptor concentration was varied while the donor (NMA) concentration was kept constant at 10^{-5} M. Use of the 425 nm isolation filter allowed measurement of only NMA emission. Decreasing fluorescence intensity from NMA as the acceptor concentration was increased, was compensated for by opening the diaphragm until the fluorescence pulse was of the same height as that previously measured.

4. Non-Aqueous Chemiluminescence.

a) Qualitative observation of chemiluminescence. Solutions of lucigenin and potassium t-butoxide (KOtBu) were prepared in DMSO, DMF and AN. The solution containing lucigenin was saturated with oxygen and that containing KOtBu was purged with nitrogen by bubbling in a glove bag. The solutions were then mixed and light was visually observed.

b) Measurement of nonaqueous chemiluminescence spectra. The spectra of the non-aqueous CL generated by the reaction of oxygen, KOtBu and lucigenin were measured on the Image Intensifier Spectrograph. Small test tubes were filled with 2 cc of the lucigenin solution in the

appropriate solvent and were sealed with a serum cap. This solution was then saturated with oxygen by bubbling through a syringe needle. The solution containing KOtBu was purged with nitrogen and 1cc was admitted into the test tube by use of the syringe. Care had to be taken when DMSO was used as the solvent that the concentration of base was not excessive as decomposition of the solvent by reaction with base and oxygen was noted. The syringe drive was used to provide continuous mixing of the reagents. 100 ml syringes were used and the emission was viewed 1 cm below the mixing "T". At flow rates of 3.75 and 77.4 ml/min this distance corresponds to a time after mixing of 5×10^{-1} and 2.5×10^{-2} sec respectively. The preparation of the solutions to be mixed was the same as described above.

V. Results Electrochemistry

A. Cyclic-voltammetry

Electrochemical studies were done in both aqueous and non-aqueous media. Typcial current-voltage curves for lucigenin and oxygen in DMSO at a platinum electrode (curve A) and in water at a mercury electrode (curve B) are shown in Figure V-1. The solid line in curve A is the voltammogram obtained with only lucigenin present in the solution. The wave peaking at -0.30V (vs Ag/AgCl in 0.1 M KCl) corresponds to the reduction of lucigenin and that peaking at +0.45V corresponds to the oxidation of lucigenin's reduction product. The dotted line in curve A is obtained with only oxygen present. The wave peaking at -0.9 V is the reduction of O_2 to superoxide ($O_2^{-\cdot}$) and that peaking (anodic current) at -0.85 V is the reoxidation of superoxide to oxygen. The dotted line in curve B is the reduction of oxygen to OH^- and H_2O_2 in water at Hg and the solid line is lucigenin's reduction wave in H_2O at Hg.

The lucigenin reduction product is insoluble in water and plated out on a platinum electrode in aqueous solution. This product was isolated by washing the plated electrode with distilled water, drying, and dissolving the product in chloroform. A mass spectrum of the product was taken and a major M/e peak at 386 was observed. This mass corresponds to the molecular weight of the two-electron reduction product of lucigenin, dimethyl biacridene (DBA). A sample of DBA was prepared by the method of Decker and Petsch (22). The mass, IR and UV spectra of the synthesized DBA were identical to those obtained for the electrochemical product. Samples of the reduction product obtained

Figure V-1

Current-voltage curves for lucigenin and oxygen in DMSO at Pt(Tetrabutyl ammonium perchlorate supporting electrolyte, 0.1 M) and in H_2O at Hg (0.1 M KCL supporting electrolyte) both vs Ag/AgCL in 0.1 M KCL.

A —— lucigenin in DMSO

\- - - oxygen in DMSO

B ——— lucigenin in H_2O

\- - - oxygen in H_2O

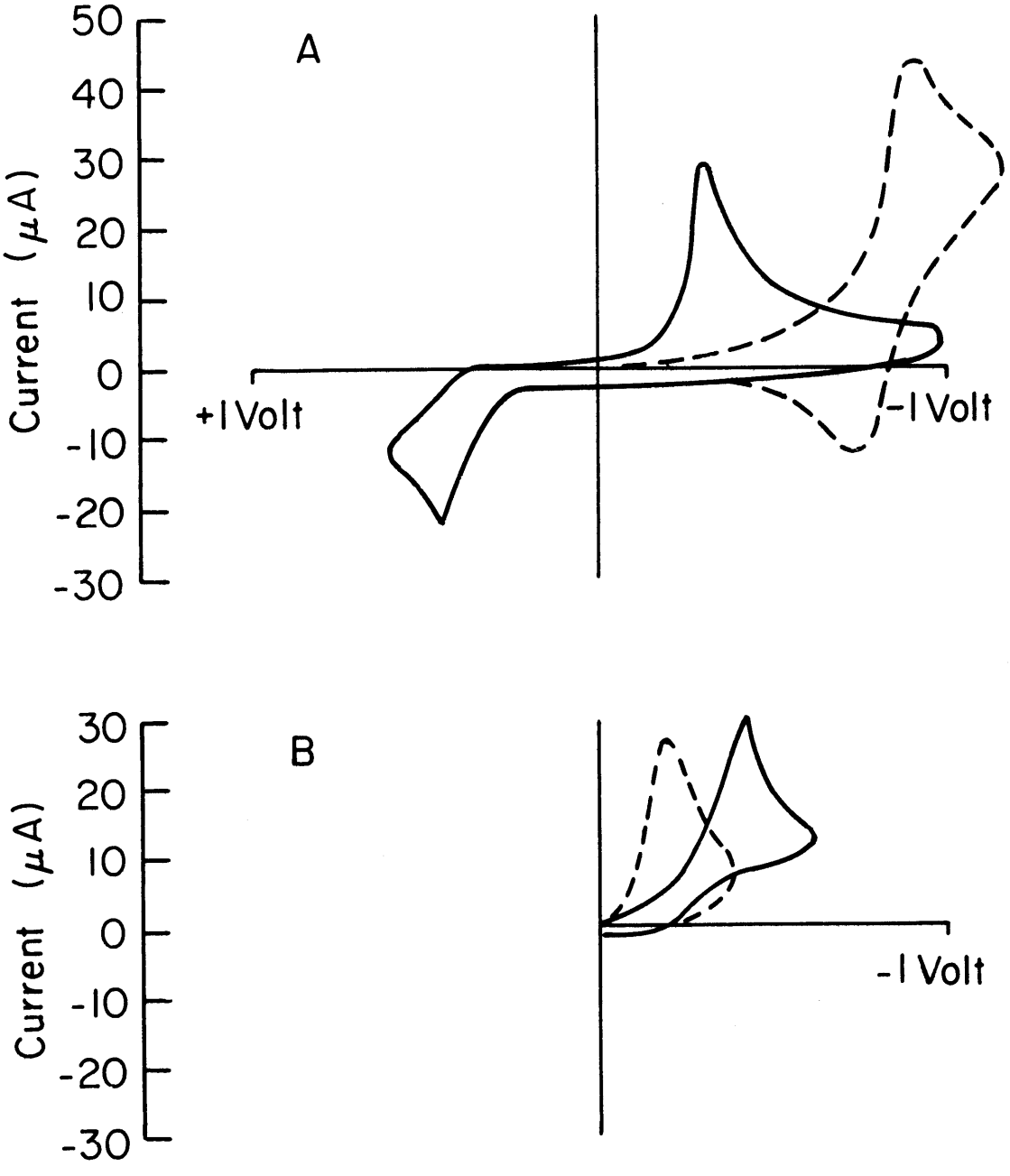
A
50
40
30
20
10
0
-10
-20
-30
Current (μA)
+1 Volt
-1 Volt
B
30
20
10
0
-10
-20
-30
Current (μA)
-1 Volt

by reduction in non-aqueous media gave the same spectral data. On this basis DBA was identified as the electrochemical reduction product of Lucigenin in both aqueous and non-aqueous solvents.

Referring back to Figure V-1A, if the potential was swept anodically with only lucigenin present no anodic peak was observed at +0.45V. If, however, after scanning cathodically over the lucigenin reduction wave the potential was scanned anodically, the peak at +0.45 V was observed. When DBA was present in solution no wave peaking at -0.30 V was observed until an anodic scan had been made over the DBA oxidation peak at +0.45 V.

The peak potential of the lucigenin reduction and DBA oxidation were found to be independent of pH over the range 4.7 - 10.0 in aqueous solution. In non-aqueous media these potentials were found to be unaffected by addition of either HCl (dissolved gas) or KOH.

B. Coulometry

Attempts to determine the value of n, the number of electrons involved in the electrochemical reduction of lucigenin, by use of a Hydrogen-Nitrogen gas coulometer (33) proved unsatisfactory. This was due to the low currents encountered and the subsequent small volumes of gas evolved. More satisfactory results were obtained when the current was electronically integrated. Coulometry of the lucigenin reduction in aqueous solution proved impossible due to rapid plating of the electrode by DBA, which inhibits further reduction of lucigenin. DMSO was chosen as the solvent because of its low volatility and consequent minor concentration changes due to evaporation of solvent while bubbling with nitrogen during electrolysis. The results of the coulometric measurements of n_c for lucigenin in DMSO are summarized in

Table V-1. The average of 8 determinations gave a value for n_c of 1.96.

Coulometry was also used to determine the value of n_a for the oxidation of DBA in DMSO. A saturated solution was prepared and its concentration determined by spectrophotometry using ε_{max} at 420 nm as 1.66×10^4. The results of the coulometric determinations for the DBA oxidation are summarized in Table V-2. The average value of n_a was found to be 2.06.

C. Scan Rate Studies

To determine what, if any, kinetic complications were involved in the electrochemistry of lucigenin, studies were made concerning the behavior of the reduction wave of lucigenin and the oxidation wave of DBA as a function of scan rate. A three electrode cell was used and at low scan rates care was taken to allow the solution to come to rest after bubbling (1 minute) before the scan was begun. The cell itself was jacketed to prevent thermal convection. For scan rates greater than 10 V/min an oscilloscope was used for recording the current-voltage curves.

The results of these studies on the lucigenin reduction wave in DMSO at various concentrations are shown in Tables V-3 - V-5 and the normalized peak current ($i_p/\nu^{1/2}$) corrected for concentration plotted vs. scan rate is shown in Figure V-2. Similar studies were made on the oxidation wave of DBA in DMSO and are presented in Table V-6. The current function ($i_p/\nu^{1/2}$) vs. scan rate plot is shown in Figure V-3. Scan rates greater than 2×10^{-1} V/sec gave ill defined values of i_p due to merging of the oxidation wave with the solvent oxidation.

Table V-1

Coulometry of Lucigenin Reduction in DMSO

$k = 8.3X10^{-6}$M/cm -0.325V vs Ag/AgCL Constant Potential Electrolysis

i_p	Δi	Moles Reduced	E_o(total)	Coulombs	Moles e^-	n_c
6.05						
5.30	0.75	$6.23 X 10^{-7}$	2.05 V	$1.03X10^{-1}$	$1.07X10^{-6}$	1.72
4.70	1.35	$1.12 X 10^{-6}$	4.02 V	$2.01X10^{-1}$	$2.08X10^{-6}$	1.86
4.25	1.80	$1.49 X 10^{-6}$	5.71 V	$2.86X10^{-1}$	$2.96X10^{-6}$	1.99
3.75	2.30	$1.91 X 10^{-6}$	7.36 V	$3.68X10^{-1}$	$3.81X10^{-6}$	1.99

$k = 9.35 X 10^{-6}$M/cm(a)

i_p	Δi	Moles Reduced	E_o(total)	Coulombs	Moles e^-	n_c
5.35						
5.00	0.35	$3.27 X 10^{-7}$	1.37 V	$6.85X10^{-2}$	$2.10X10^{-7}$	2.17
4.30	1.05	$9.82 X 10^{-7}$	3.87 V	$1.94X10^{-1}$	$2.01X10^{-6}$	2.05
3.75	1.60	$1.50 X 10^{-6}$	5.81 V	$2.91X10^{-1}$	$3.02X10^{-6}$	2.01
3.30	2.05	$1.92 X 10^{-6}$	7.24 V	$3.62X10^{-1}$	$3.75X10^{-6}$	1.92

average of 8 runs $n_c = 1.96$

(a) electrode area different from above

Table V-2

Coulometry of DBA Oxidation in DMSO

50 cc 1.11×10^{-5} M DBA $k = 2.47 \times 10^{-7}$ M/unit

i_p	i	Moles Oxidized	E_o	Moles e^-	n_a
2.25					
1.60	.65	1.61×10^{-7}	.64 V	3.32×10^{-7}	2.06

50 cc 1.21×10^{-5} M DBA $k = 3.90 \times 10^{-7}$

i_p	i	Moles Oxidized	E_o	Moles e^-	n_a
1.55					
1.30	.25	9.75×10^{-8}	.40 V	2.07×10^{-7}	2.12
0.95	.60	2.34×10^{-7}	.90 V	4.66×10^{-7}	1.99

average of three runs $n_a = 2.06$

Table V-3

Scan Rate Study of Lucigenin Reduction

(2.14×10^{-3} M Lucigenin in DMSO)

ν(V/sec)	$\sqrt{\nu}$	$i_p(\mu_a)$	$i_p/\sqrt{\nu} \times 10$	Ep-Ep/2 mv
1.67×10^{-3}	4.09×10^{-2}	0.93	2.26	40
3.33×10^{-3}	5.77×10^{-2}	1.28	2.24	40
8.34×10^{-3}	9.15×10^{-2}	1.94	2.12	40
1.67×10^{-2}	1.29×10^{-1}	2.61	202	45
3.33×10^{-2}	1.83×10^{-1}	3.52	1.92	40
8.34×10^{-2}	2.89×10^{-1}	5.20	1.80	40
1.67×10^{-1}	4.09×10^{-1}	6.95	1.70	40
3.33×10^{-1}	5.78×10^{-1}	9.25	1.60	45
4.64×10^{-1}	6.75×10^{-1}	10.4	1.54	50
1.17	1.08	14.6	1.36	60
2.32	1.53	18.4	1.20	60
4.64	2.15	24.1	1.12	60
17.7	4.21	41.2	0.98	65
28.0	5.30	50.8	0.96	70
56.0	7.50	72.0	0.96	70
140.0	11.8	113.0	0.96	80

Table V-4

Scan Rate Study of Lucigenin Reduction

(1.07×10^{-2} M Lucigenin in DMSO)

ν(v/sec)	$\sqrt{\nu}$	i_p(μA)	$i_p/\sqrt{\nu} \times 10^2$	$i_p/\sqrt{\nu}$ corr X 10
1.67×10^{-3}	4.09×10^{-2}	4.65	1.14	2.28
3.33×10^{-3}	5.77×10^{-2}	6.46	1.12	2.20
8.34×10^{-3}	9.15×10^{-2}	9.35	1.02	2.04
1.67×10^{-2}	1.29×10^{-1}	12.4	0.97	1.94
3.33×10^{-2}	1.83×10^{-1}	16.7	0.91	1.83
8.34×10^{-2}	2.89×10^{-1}	24.3	0.84	1.68
1.67×10^{-1}	4.09×10^{-1}	31.8	0.78	1.55
3.33×10^{-1}	5.78×10^{-1}	41.6	0.72	1.44
4.80×10^{-1}	6.94×10^{-1}	47.2	0.68	1.36
1.20	1.10	66.0	0.60	1.20
3.20	1.79	106	0.59	1.18
6.40	2.53	122	0.48	0.96
16.0	4.00	164	0.41	0.81
34.0	5.84	210	0.36	0.73
68.0	8.25	290	0.35	0.71
170	13.1	457	0.35	0.71

Table V-5

Scan Rate Study of Lucigenin Reduction

(2.14×10^{-2} M Lucigenin in DMSO)

ν(v/sec)	$\sqrt{\nu}$	i_p (μA)	$i_p/\sqrt{\nu} \times 10^2$	$i_p/\sqrt{\nu}$ corr X 10
1.67×10^{-3}	4.09×10^{-2}	9.3	2.28	2.28
3.33×10^{-3}	5.77×10^{-2}	12.6	2.22	2.22
8.34×10^{-3}	9.15×10^{-2}	19.0	2.08	2.08
1.67×10^{-2}	1.29×10^{-1}	25.5	1.97	1.97
3.33×10^{-2}	1.83×10^{-1}	31.5	1.72	1.72
8.34×10^{-2}	2.89×10^{-1}	48.0	1.67	1.67
1.67×10^{-1}	4.09×10^{-1}	61.5	1.50	1.50
3.33×10^{-1}	5.78×10^{-1}	78	1.35	1.35
6.40×10^{-1}	8.00×10^{-1}	105	1.30	1.30
1.6	1.27	149	1.18	1.18
3.2	1.79	200	1.12	1.12
6.4	2.53	233	0.92	0.92
16.0	4.0	335	0.84	0.84
38.0	6.16	460	0.75	0.75
72.0	8.48	575	0.68	0.68
190	13.8	830	0.60	0.60

Figure V-2

Current Function ($ip/\nu^{1/2}$) (Corrected for concentration)

vs. Scan Rate for Lucigenin Reduction in DMSO

o - o - o 2.44×10^{-3} M Lucigenin

Δ - Δ - Δ 1.07×10^{-2} M Lucigenin

□ - □ - □ 2.14×10^{-2} M Lucigenin

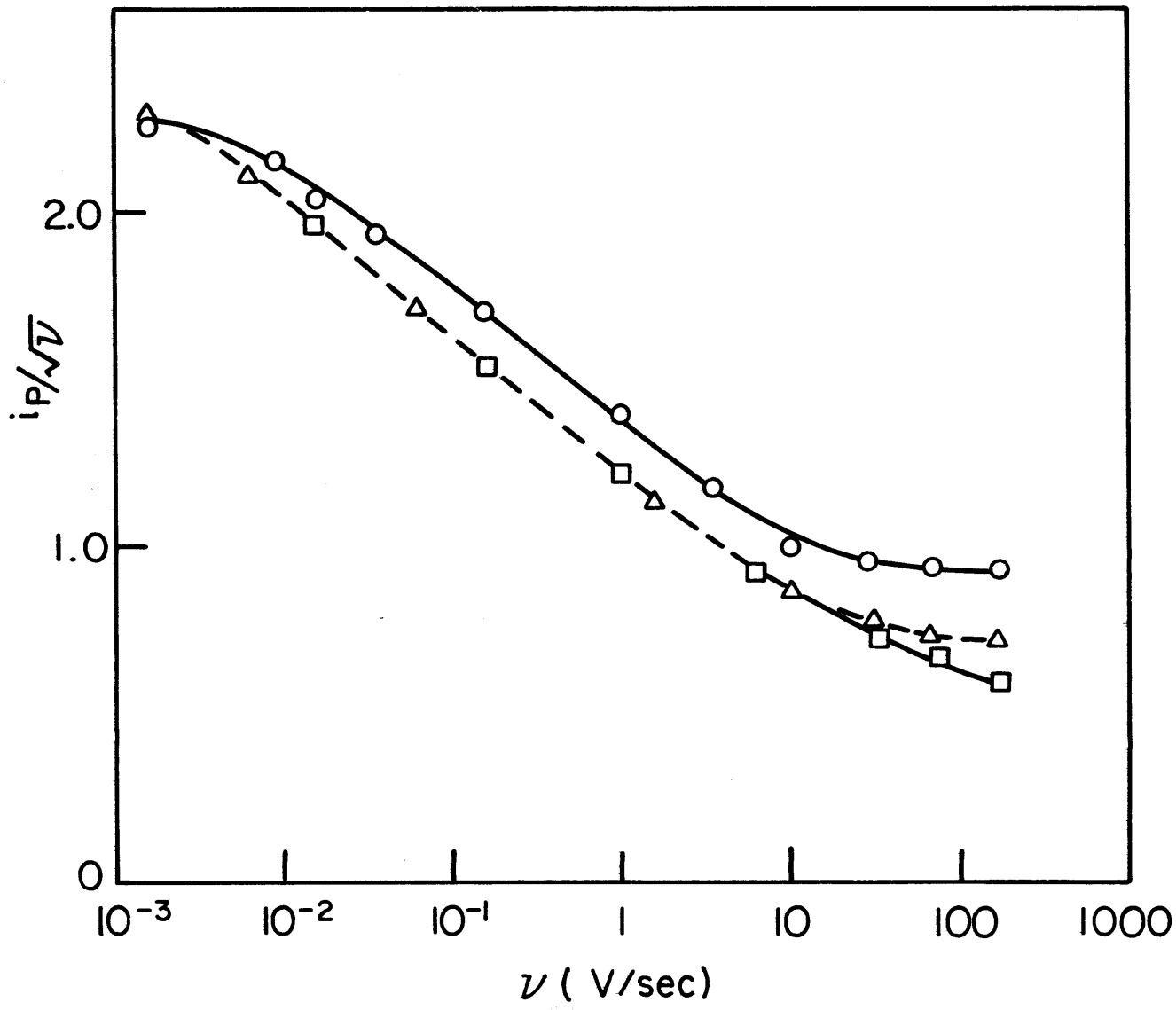
2.0
1.0
0
$i_p/\sqrt{\nu}$
10^{-3}
10^{-2}
10^{-1}
1
10
100
1000
ν (V/sec)

Table V-6

Scan Rate Study of DBA Oxidation in DMSO

ν V/sec	$\sqrt{\nu}$	i_{pa} (μA)	$i_{pa}/\sqrt{\nu}$ X 10^{-1}
1.67 X 10^{-1}	3.28 X 10^{-1}	10.3	3.15
8.33 X 10^{-2}	2.88 X 10^{-1}	8.8	3.05
3.33 X 10^{-2}	1.83 X 10^{-1}	5.6	3.06
1.43 X 10^{-2}	1.19 X 10^{-1}	3.8	3.2
6.67 X 10^{-3}	8.16 X 10^{-2}	2.5	3.07
2.33 X 10^{-3}	4.84 X 10^{-2}	1.5	3.1

Figure V-3

Current function ($ip/\nu^{1/2}$) vs. scan rate for DBA Oxidation in DMSO

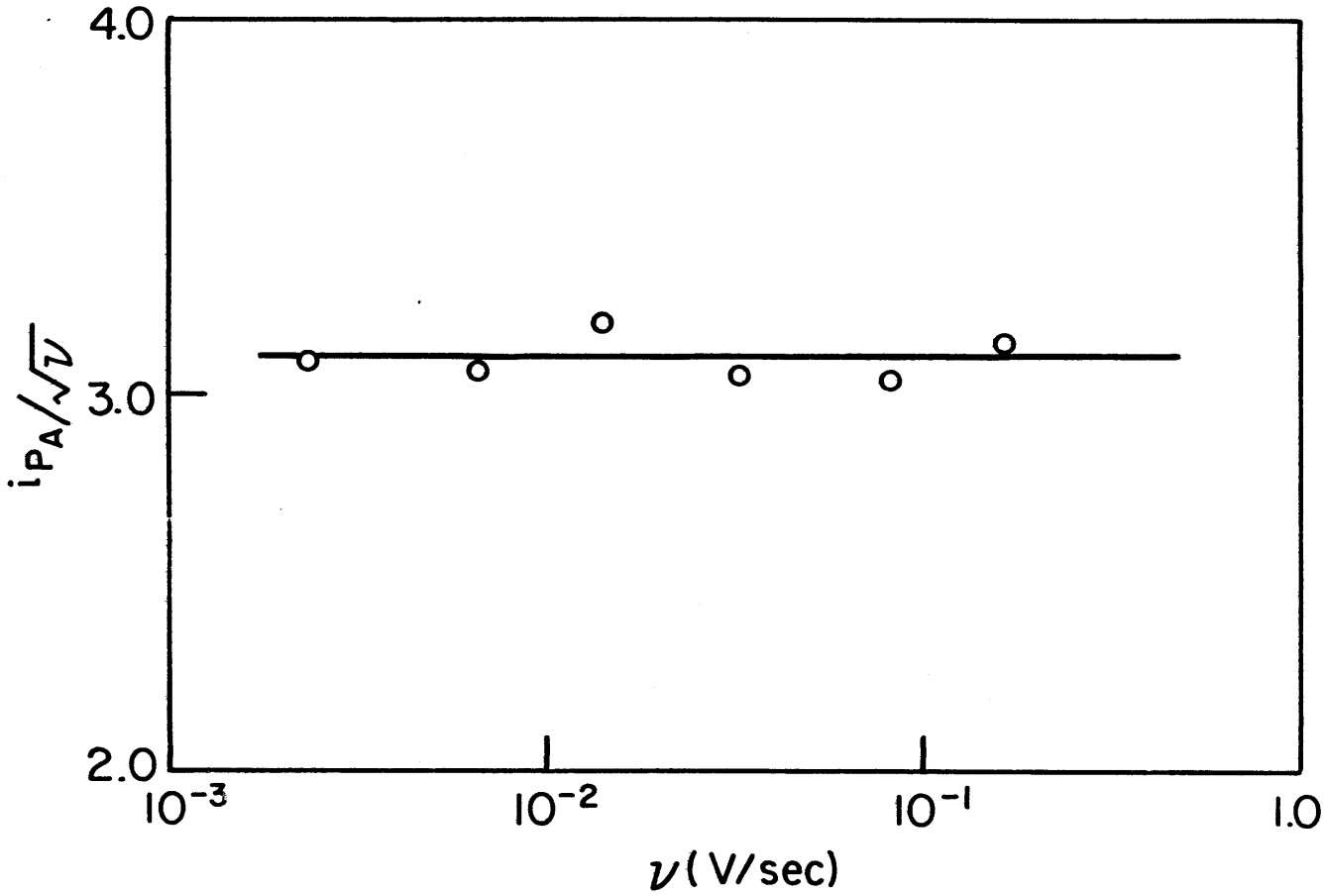
4.0
3.0
2.0
$i_{PA}/\sqrt{\nu}$
10^{-3}
10^{-2}
10^{-1}
1.0
ν (V/sec)

Studies at fast scansin solutions of lucigenin more dilute than 10^{-3} M were difficult to interpret due to the large capacitative currents encountered in relation to the peak currents found. At about the limit of usefulness of high scan rates and lucigenin concentration (50-100 V/sec with 10^{-3} M lucigenin) an anodic peak was observed approximately 0.3 volts anodic from the lucigenin reduction peak. A typical cyclic voltammogram showing this anodic peak is shown in Figure V-4.

The cell resistance of DMSO with 0.1 M tetrabutyl amnonium perchlorate as supporting electrolyte was measured to be 1000 ohms.

D. ESR

A two electrode cell consisting of a mercury reference and platinum wire indicator in a thin glass tube was used in an ESR cavity to attempt to detect the presence of radicals during the reduction of lucigenin in DMSO. A steady state potential of -0.40V was applied. A highly unresolved ESR signal was detected indicating low concentrations of some radical but the nature of this radical could not be determined because of the unresolved spectrum.

Figure V-4

Current Voltage Curve Obtained of 10^{-3} M

Lucigenin in DMSO at a Scan Rate of 80 V/sec

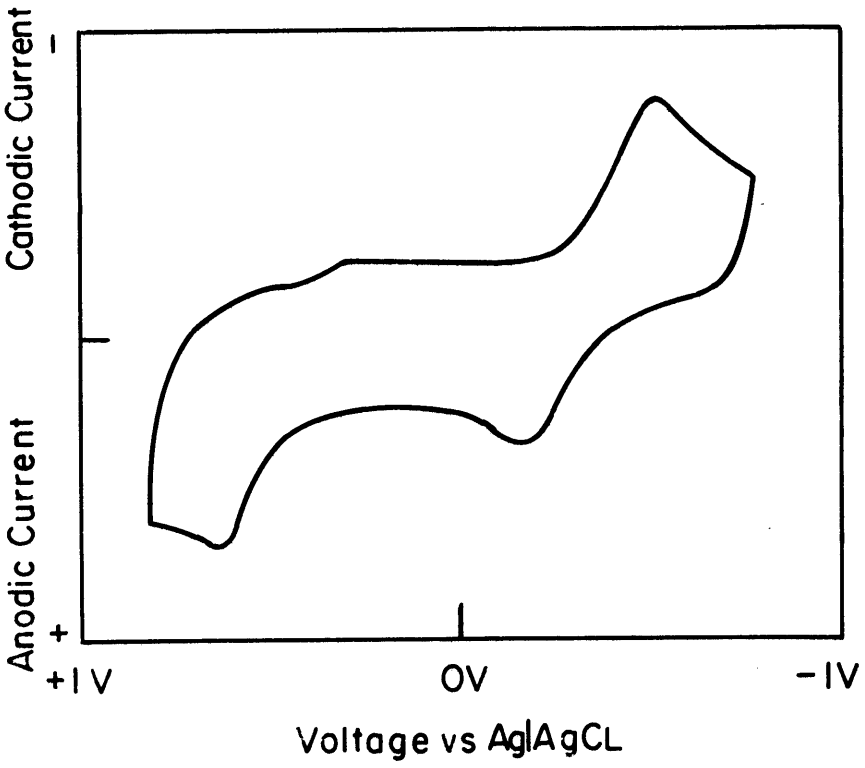
Cathodic Current
-
Anodic Current
+
+1V
0V
-1V
Voltage vs AgIAgCL

VI Discussion Electrochemistry

Several characteristics of the electrochemistry of lucigenin have been measured and appear in the results section above. These may be summarized as follows:

1. Lucigenin is reduced to DBA.
2. The overall value of n_c for the reduction is 2.
3. Neither the reduction of lucigenin nor the oxidation of DBA is pH dependent.
4. DBA is oxidized to lucigenin with an overall n_a of 2.
5. Radicals are observed during reduction of lucigenin.
6. There appear to be kinetic complications in the reduction of lucigenin indicative of a coupled chemical reaction.

Nicholson and Shain (34) have presented a theoretical discussion of electrochemical behaviour at a stationary electrode, as applied to cyclic scan methods. Since the peak current varies with the square root of the scan rate (ν) peak current can be normalized for scan rate by dividing them by $\nu^{1/2}$. A plot of normalized peak current (current function) vs scan rate gives a horizontal straight line for either a reversible or irreversible charge transfer step, the reversible line being lower than that of the irreversible case (39). If however, there are any coupled chemical reactions which affect the electrochemistry a plot of normalized peak current vs scan rate will deviate from the horizontal straight lines. Referring to Figure V-2 one sees a decreasing current function for the reduction of lucigenin as the scan rate is increased. This indicates chemical reaction coupled with the electrochemical reaction in this region of scan rates. Figure V-3 shows a

horizontal straight line dependence for the oxidation of DBA indicating no coupled chemical reactions.

Since no pH dependence was observed for the lucigenin reduction, a preceding or succeeding reaction of lucigenin or its reduction intermediates or products with either protons or hydroxyl ions is unlikely. Lucigenin is stable in the solutions studied showing no detectable equilibrium forms. Thus the possibility of any chemical reaction preceding the charge transfer step is highly unlikely. The possiblility of a chemical reaction after the charge transfer step to account for the observed behaviour is the only alternative.

As shown above, evidence of radicals was observed during the reduction of lucigenin. Janzen et. al. (35) have reported a radical produced during the reduction of lucigenin and identified it as being the mono-cation radical of lucigenin, $L^{+\cdot}$. This radical was observed when a constant potential was applied corresponding to the reduction potential of lucigenin. The radicals observed were on the very limit of detectability and it was estimated that their steady-state concentration was no greater than 10^{-6} M (36).

This evidence for $L^{+\cdot}$ radicals being involved in the reduction, coupled with their instability as seen by the difficulty of detection provides a route for a post charge-transfer reaction. Two such reactions seem possible. If lucigenin is designated L^{++}, the mono-cation radical $L^{+\cdot}$ and dimethyl biacridene as DBA these reactions are:

1. $L^{++} + e^- \rightleftarrows L^{+\cdot}$ (charge transfer)

   $L^{+\cdot} + S \xrightarrow{k_f} DBA + S^{+\cdot}$

   where S is either solvent or supporting electrolyte

$$2.\quad L^{++} + ie^- \leftrightarrows L^{+\cdot} \qquad \text{(charge transfer)}$$

$$2L^{+\cdot} \xrightarrow{k_f} L^{++} + DBA \qquad \text{(Disproportionation)}$$

Both reactions involve a one-electron charge transfer, followed by a chemical reaction of the mono-cation radical yielding DBA as the product. Reaction 1. has an overall n of 1 while reaction 2. has an n value of 2. Since the measured value of n is 2 for the reduction reaction 2. is the favored possibility.

The nature of the effect of following chemical reaction on the observed electrochemical behaviour depends on the time scale of the electrochemical measurements and the value of the rate constant of the chemical reaction (34, 37). In the case of reaction 2. one may observe two extremes. First, at slow scan rates the time scale of the electrochemical measurement is large compared with that of the chemical reaction, i.e. the chemical reaction is complete. For reaction 2. then one should observe behaviour corresponding to a two-electron, irreversible reduction. Second, at fast scan rates the time of the electrochemical measurement is small compared to that of the chemical reaction. In this case no chemical reaction occurs during the time of measurement. For reaction 2. in this instance one should observe behaviour corresponding to a one electron reduction with no kinetic complications. Nicholson and Shain (34) show that the current function for a two-electron irreversible reaction is 2.2 times the current function for a one electron reversible reaction. Referring to the data of Table V-3 and Figure V-2 it may be seen that the current function in the irreversible part of the curve (low scan rates) is 2.52 times the current function in the reversible region. Since the current function at low scan rates may be high due

to convection in solution this value corresponds well with the theory of Nicholson and Shain.

Studies at scan rates between the first and second cases will be greatly influenced by the following chemical step. The value of the scan rate such that the following reaction is negligible is dependent on the value of the rate constant of the following reaction. The larger the rate constant the higher the scan rate must be to negate the effect of the chemical reaction.

The results of scan rate studies on the reduction of lucigenin are shown in Figure V-2. The decrease in normalized peak current with increasing scan rate is indicative of a following chemical reaction. Several aspects of the curves in Figure V-2 are important. The curve obtained with 2.14×10^{-3} M lucigenin shows indications of becoming horizontal at scan rates greater than 20 V/sec. As the concentration of lucigenin was increased (1.07×10^{-2} M and 2.14×10^{-2} M) this leveling out of the curve becomes less apparent. It was also noted that at scan rates of greater than 20 V/sec in the 2.14×10^{-3} M lucigenin solution a new anodic wave appeared (see Figure V-4). It may also be seen from Figure V-2 that at low scan rates the normalized peak current is tending to level off.

The data shown in Table V-3-V-5 and in Figure V-2 may be interpreted only after some rather stringent qualifications. The measured cell resistance was 1000 ohms. Such a high cell resistance proves a source of large error in the values of the scan rates employed in the calculations. Assuming the lucigenin reduction to occur at an average potential of -0.4 V vs Ag/AgCl at moderate scan rates, a current of 100 μA will produce a 0.1 V IR drop across the cell, or 25% of the peak potential. The net effect

of this IR drop is a reduction of the scan rate. Thus, the portions of the curves greater than 50 V/sec for 2.14×10^{-3} M lucigenin, 1 V/sec for 1.07×10^{-2} M lucigenin and 0.5 V/sec for 2.14×10^{-2} M lucigenin are doubtless in error.

The effect of the net lowering of the scan rate due to IR drop may be seen in Figure V-2. At scan rates greater than 10 V/sec the normalized peak currents are lower as the lucigenin concentration is increased. Thus the values of $\nu^{1/2}$ employed in normalizing the peak currents are higher than those encountered in reality. The overall effect of the IR drop on the scan rate dependence is to broaden out the curve. Unfortunately, solutions of lucigenin more dilute than 10^{-3} M had such a large capacity background at the current scales required that measurements of peak currents on these solutions were rendered impossible.

The leveling of the current function at high scan rates, as explained above, is indicative of approaching the pure charge-transfer step of the reduction, with the following chemical reaction not affecting the measurement. The appearance of an anodic wave at the scan rates where this leveling occurs supports this premise. This anodic wave corresponds to the oxidation of the intermediate which is involved in the chemical reaction.

The results obtained at very low scan rates are also suspect. At scan rates less than 10 mV/sec convection in the solution may introduce serious error (37). Thus, the current functions at low scan rates may, in reality, be lower than those shown in Figure V-2.

The net result of the effects of convection and IR drop on

the scan rate dependence result in the distorted curve shown in Figure V-2. In reality the falling portion of the curve should be steeper, level out at lower scan rates as the chemical reaction dominates and should also level out at higher scan rates in the reversible region.

The value of $E_p - E_{p/2}$ is a measure of the peak shape of the reduction process (34, 37). At low scan rates (see Table V-3) the value of $E_p - E_{p/2}$ for the lucigenin reduction is 40 mV. At high scan rates this approaches a value of 65 mV. A completely reversible electrochemical reaction shows an $E_p - E_{p/2}$ of 57 mV (34, 37). At high scan rates, where one approaches the condition of a charge transfer step with no kinetic complications, the difference of 65 mV indicates that true reversibility has not been reached. This is also borne out by the large (0.3V) separation of the lucigenin reduction peak potential and that of the anodic peak appearing at high scan rates. The separation of 40 mV seen at low scan rates fits only the rising portion of a catlytic reaction (34).

From the above interpretation of the scan rate studies, coupled with the measured value of n and chemically feasible reactions, conclusions may be drawn concerning the electrochemical reduction of lucigenin. It is evident that there is a chemical reaction following charge transfer. The most probable reaction is that shown in reaction (2) above, an initial one electron reduction to the mono-cation radical ($L^{+\cdot}$) disproportionation of $L^{+\cdot}$ to lucigenin (L^{++}) and DBA. The current function plots indicate a one electron charge transfer followed by a chemical reaction producing a net two-electron, irreversible reduction

which is in agreement with the measured value of 2 for n. At moderate scan rates the rising portion of the wave fits only the case of a catalytic process and an analogy can be drawn between the disproportionation of $L^{+\cdot}$ regenerating L^{++} and a catalytic reaction. The cathodic shift of peak potential with increasing scan rate is also indicative of a following reaction.

The appearance of an anodic peak at fast scan rates, where the following chemical step has a negligible effect, corresponds to the oxidation of $L^{+\cdot}$. The exact region of scan rates at which the charge transfer step only is observed is questionable due to the effect of IR drop across the cell on the scan rate.

Nicholson and Shain (34) have treated only first order or pseudo-first order following chemical reactions. Booman (38) has treated disproportionation reactions but only applied to potential step methods. However, an analogy may be drawn between an irreversible following chemical step (Nicholson and Shain, case VI) and the proposed disproportionation. Nicholson and Shain (34) give a value of $k_{f/a}$ of 0.1 for the onset of seeing the anodic peak, corresponding to the oxidation of the electrochemical intermediate, where k_f is the rate constant of the following reaction and $a = nF\nu/RT$, where n is the number of electrons involved in the charge transfer step and ν is the scan rate in volts/sec. If one assumes, from the data of Table V-3 and Figure V-2, for the most dilute lucigenin solution (2.14×10^{-3} M), that the onset of the anodic wave occurs at an actual scan rate of 10 V/sec, a is then calculated to be 1.7×10^{2}. Assuming k_f/a to be 0.1 at this scan rate, then $k_f = 1.7 \times 10^{1}$ sec^{-1}. However, the following reaction is second order rather than first order. If one assumes a concentration of $L^{+\cdot}$ at the

surface of the electrode equal to the bulk concentration of lucigenin the rate of reaction of $L^{+\cdot}$ for the first order process may be calculated:

$$1^{st} \text{ order rate} = k_f(L^{+\cdot}) = 1.7 \times 10^{1} \text{ sec}^{-1}(2.14 \times 10^{-3} \text{ M/1})$$
$$= 3.64 \times 10^{-2} \text{ M-1}^{-1} \text{-sec}^{-1}.$$

If the actual following chemical step is second order this rate must equal that of the first order reaction. Calling the second-order rate constant k_f' one calculates:

$$k_f(L^{+\cdot}) = k_f' (L^{+\cdot})^2$$

$$\text{or } 3.64 \times 10^{-2} \text{ M-1 -sec}^{-1} = k_f' (2.14 \times 10^{-3} \text{ M/1})^2$$

$$\text{and } k_f' = 8 \times 10^{3} \text{ 1/M-sec.}$$

This calculated value of k_f' is only an approximation but is likely to be a good order of magnitude estimate of the second-order rate constant for the disproportionation.

The scan rate data of Table V-6 for DBA oxidation and plot of current function ($i_p/\nu^{1/2}$) vs scan rate of Figure V-3 shows no dependence of normalized peak current on scan rate. This is indicative of an electrochemical oxidation uncomplicated by chemical reactions. The experimental value of n_a being 2 indicates a net two-electron oxidation. Figure V-1 and V-4 show no reversible cathodic wave in conjunction with the anodic DBA wave, showing the two electron oxidation of DBA to be a net irreversible process.

Since true two-electron oxidations in organic systems are unlikely it is more probable that the oxidation passes through a one-electron oxidation intermediate. The one-electron oxidation product of DBA is $L^{+\cdot}$. By reference to Figure V-4 it may be seen that $L^{+\cdot}$ itself will be oxidized to lucigenin at the anodic potential necessary to oxidize

DBA to $L^{+\cdot}$. Thus, the oxidation of DBA appears to fit the scheme:

$$DBA - 1e^- \rightarrow L^{+\cdot} \; -1e^- \rightarrow L^{+\cdot}$$

or two, consecutive one-electron oxidations occurring at the same potential.

In summary, the electrochemical behaviour of lucigenin appears to best fit the following scheme:

$L^{++} + 1e^- \rightleftarrows L^{+\cdot}$

$2L^{+\cdot} \xrightarrow{k_f'} L^{++} + DBA$ for the reduction of lucigenin

$DBA - 1e^- \rightarrow L^{+\cdot} \; -1e^- \rightarrow L^{++}$ for the oxidation of DBA

The value of k_f' has been estimated as 8×10^3 1/M-sec. Further work is necessary to evaluate conclusively the electrochemistry of this system. Perhaps potential step methods may prove fruitful as these have been treated by Booman (38) for following disproportionation reactions.

VII. Results ECL

A. Production of Lucigenin ECL

All attempts to generate ECL under the conditions described by Tammanmushi and Akiyama (19) failed. However, when a mercury pool was substituted for the platimum cathode and the solution was unbuffered at pH 7, light could be observed. Oxygen was found necessary for the production of light. Furthermore, no light was observed until the potential was sufficiently negative (-0.15 V vs. Ag/AgCL in 0.1 M KCl) to reduce the oxygen. The oxygen wave is anodic relative to lucigenin in this system as can be seen in Figure V-1, curve B. When a steady potential of -0.15 V was applied, the electrochemical reduction of lucigenin was not a significant process.

It was possible to produce lucigenin ECL in four non-aqueous solvents: EtOH, DMF,DMSO and AN. One is limited to polar solvents due to the insolubility of both lucigenin and the supporting electrolyte (t-butyl ammonium perchlorate) in non-polar media. Once again it was necessary to reduce oxygen, in this case to superoxide ($O_2^{\cdot -}$) (39, 40) before light was observed. In the case of non-aqueous solvents the potential necessary for oxygen reduction is more cathodic than for the lucigenin reduction as shown in Figure V-1, curve A. Therefore, two processes are ocurring at the electrode: lucigenin $\overset{e^-}{\rightarrow}$ DBA and $O_2 \overset{e^-}{\rightarrow} O_2^{\cdot -}$

To ascertain which species were reacting, three experiments were run. First, a solution containing lucigenin in DMSO was bubbled with N_2 to exclude oxygen and the lucigenin was totally reduced to DBA. Then oxygen was bubbled through the solution. No light was observed. Second, a solution was used containing only DBA and oxygen.

The oxygen was reduced to superoxide while the DBA was unaffected at this potential. Once again no light was observed. Third, a solution containing only oxygen was used. The oxygen was electrolyzed to superoxide and a solution of lucigenin (oxygen free) was admitted only after the electrolysis had been stopped. In this case light was observed. These observations support the thesis that superoxide formed by the reduction of oxygen reacts only with lucigenin to cause light emission.

B. Spectral Study of Lucigenin ECL.

The ECL spectra were obtained using the cell shown in Figure IV-1. It should be noted that due to size limitations in the cell holder a platinum reference electrode was used in this cell and thus the potentials employed during the spectral studies do not necessarily correspond to those used when an Ag/AgCl reference was used. At first these spectra were obtained on the Aminco-Bowman spectrofluorometer, but better results were found when the Image Intensifier Spectrograph (IIS) was used.

1. Non-aqueous ECL Spectra.

Figure VII-1 shows the spectra obtained on the IIS for the ECL of lucigenin in DMSO at various concentrations and extents of reaction. Figure VII-2 presents similar spectra obtained for the ECL of lucigenin in DMF. Figure VII-3 shows the relationship between the ECL spectra of Figure VII-2 and the fluorescence spectra of lucigenin, DBA and NMA in DMF (all spectra were obtained using the IIS and are uncorrected). It can be seen that the short wavelength component of the ECL corresponds to NMA emission whereas the long wavelength component corre-

Figure VII-1

ECL SPECTRA IN DMSO

A ———— 1 X 10^{-4} M Lucigenin, initial

B - — — - 1 X 10^{-4} M Lucigenin, final

C — — — 5 X 10^{-4} M Lucigenin, initial

D — - - — 5 X 10^{-4} M Lucigenin, final

E — - — - 1 X 10^{-3} M Lucigenin, initial

F - - - - - 1 X 10^{-3} M Lucigenin, final

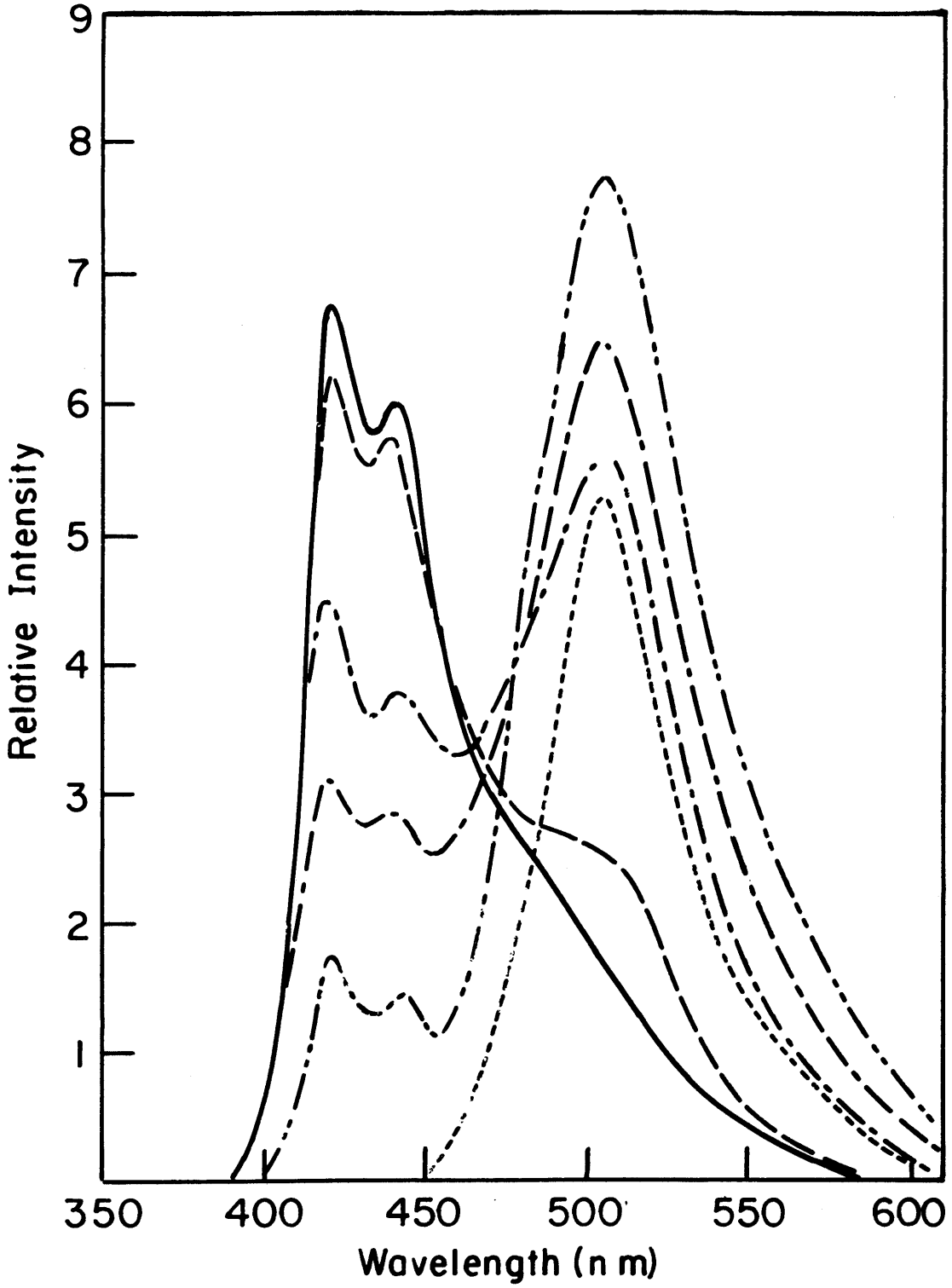
9
8
7
6
5
4
3
2
1
Relative Intensity
350
400
450
500
550
600
Wavelength (n m)

Figure VII-2

ECL Spectra in DMF

A ———— 1×10^{-4} M Lucigenin, initial

B — — — 1×10^{-4} M Lucigenin, final

C — -- — 5×10^{-4} M Lucigenin, initial

D - — — - 5×10^{-4} M Lucigenin, final

E — - — 1×10^{-3} M Lucigenin, initial

F - - - - - 1×10^{-3} M Lucigenin, final

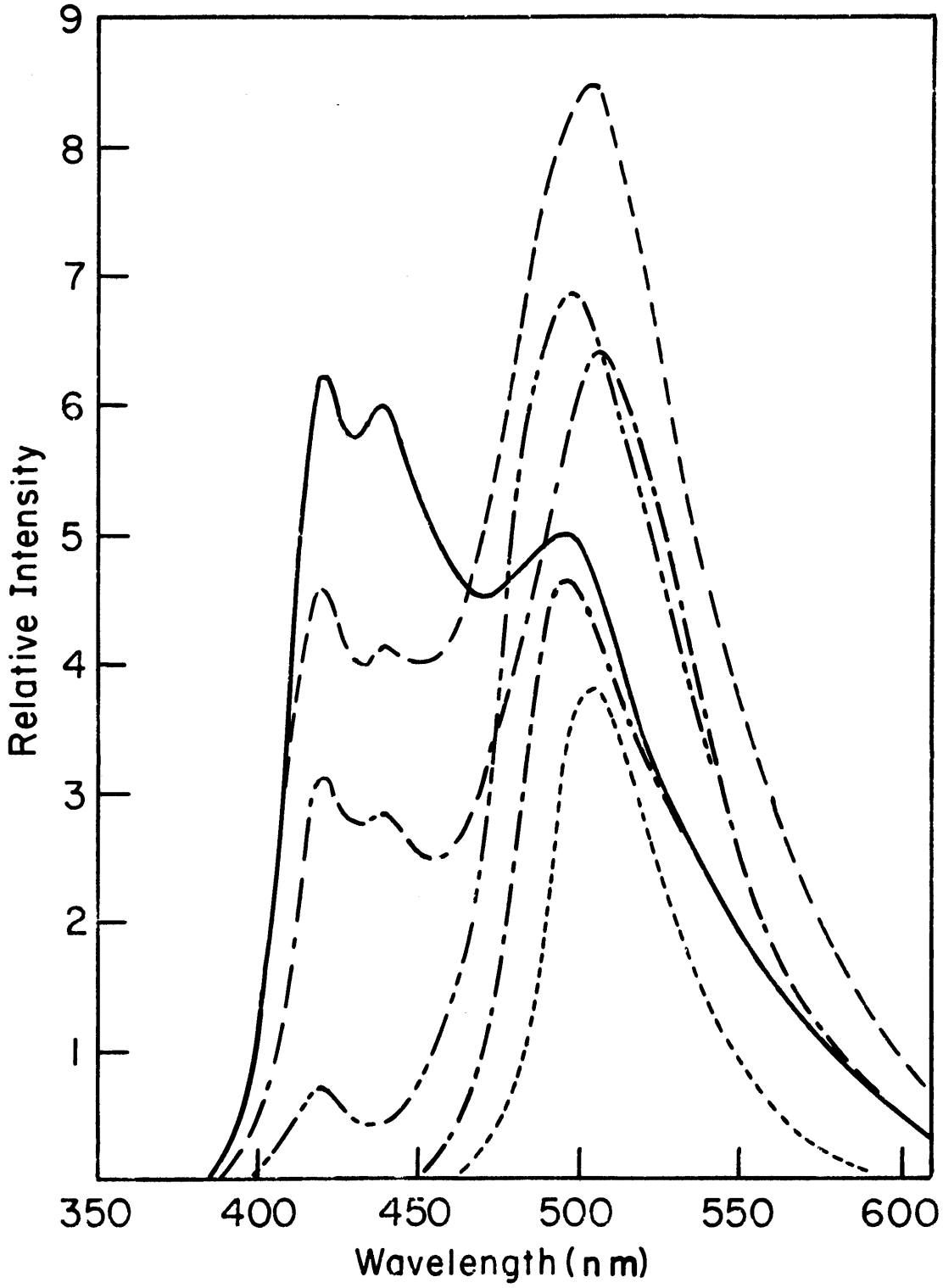
9
8
7
6
5
4
3
2
1
Relative Intensity
350
400
450
500
550
600
Wavelength (nm)

Figure VII-3

ECL and Fluorescence Spectra in DMF

A — - - — Fluorescence of NMA

B - — — - Fluorescence of Lucigenin

C — - — - Fluorescence of DBA

D ———— initial 1 X 10^{-4} M Lucigenin

E — — — Initial 1 X 10^{-3} M Lucigenin

F - - - - - Final 1 X 10^{-3} M Lucigenin

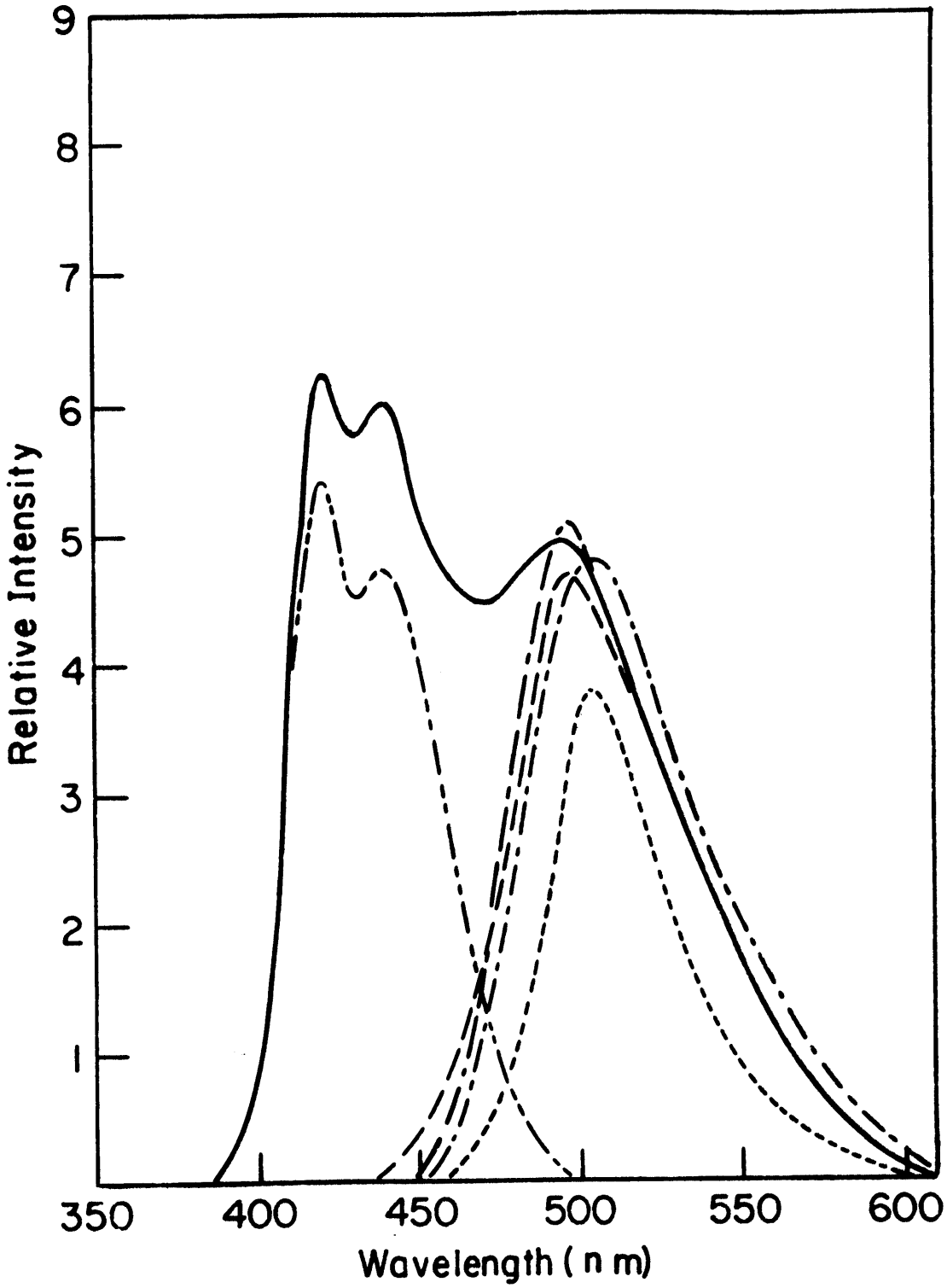
9
8
7
6
5
4
3
2
1
Relative Intensity
350
400
450
500
550
600
Wavelength (n m)

sponds to either emission from DBA or lucigenin. Figure VII-4 shows the spectra of the ECL of lucigenin in AN obtained on the IIS. The spectral changes as a function of extent of reaction for various lucigenin concentrations in AN are shown in Figure VII-5. Figure VII-6 shows the ECL and fluorescence spectra obtained in ETOH. It can be seen that in this case the ECL at all times matches NMA emission.

The spectral response curve of the total IIS system (spectrograph, Image Intensifier tube and Polaroid film) was obtained using an N.B.S.6201 tungsten lamp of known spectral distribution operating at a color temperature of 2854°K. This response curve is shown in Figure VII-7 and has a peak sensitivity at 500 nm.

2. Aqueous ECL Spectra

Several studies were made on the electrochemical generation of lucigenin CL in aqueous solution. As reported above, a mercury pool cathode was used in unbuffered pH 7 solutions. Figure VII-8 shows the ECL spectra obtained in aqueous solution on the IIS. Figure VII-9 presents the spectra of the "classical" CL of lucigenin in H_2O_2. The ECL spectra in H_2O are compared with the fluorescence spectra of NMA and lucigenin in water in Figure VII-10 (taken on the IIS, all spectra are uncorrected).

C. Summary of ECL Results.

In all cases (except for the ECL in ethanol in which only NMA emission was present) a two component spectrum was observed. The short wavelength component corresponds to emission from NMA, the primary emitter in the "classical" CL reaction (11). Changes in the intensity of the long wave length band with time of electrolysis were noted.

Figure VII-4

ECL Spectra in AN

A — - — - 1.1×10^{-4} M Lucigenin, initial

B — - - — 1.1×10^{-4} M Lucigenin, final

C - - - - - 5.5×10^{-4} M Lucigenin, initial

D — — — 5.5×10^{-4} M Lucigenin, final

E - — — - 1.1×10^{-3} M Lucigenin, initial

F ——— 1.1×10^{-3} M Lucigenin, final

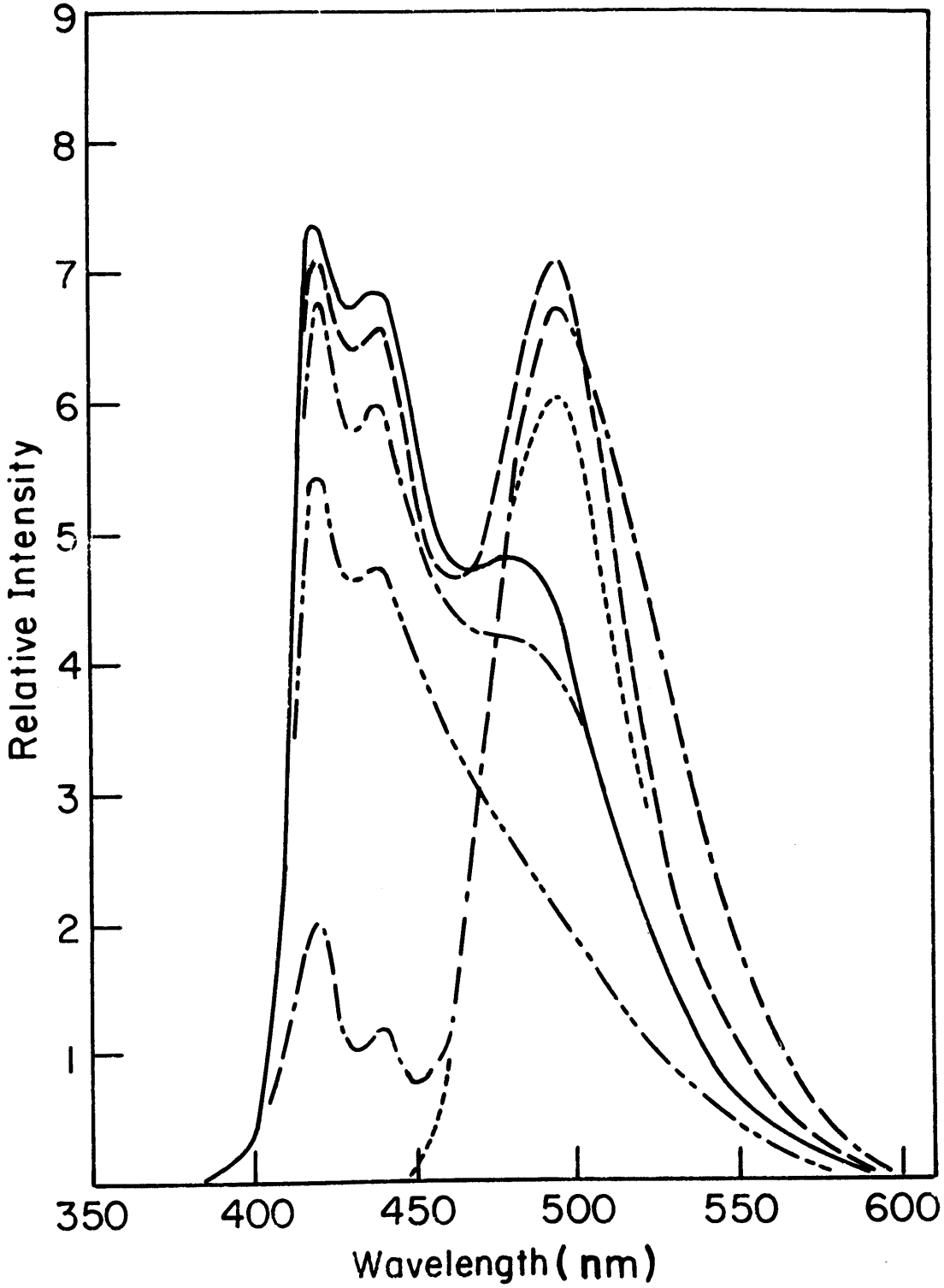
9
8
7
6
5
4
3
2
1
Relative Intensity
350
400
450
500
550
600
Wavelength (nm)

Figure VII-5

ECL Spectra in AN at Various Times of Reaction

- - - - Initial

— — — Middle

_____ Final

A 1.1 X 10^{-4} M Lucigenin

B 5.5 X 10^{-4} M Lucigenin

C 1.1 X 10^{-3} M Lucigenin

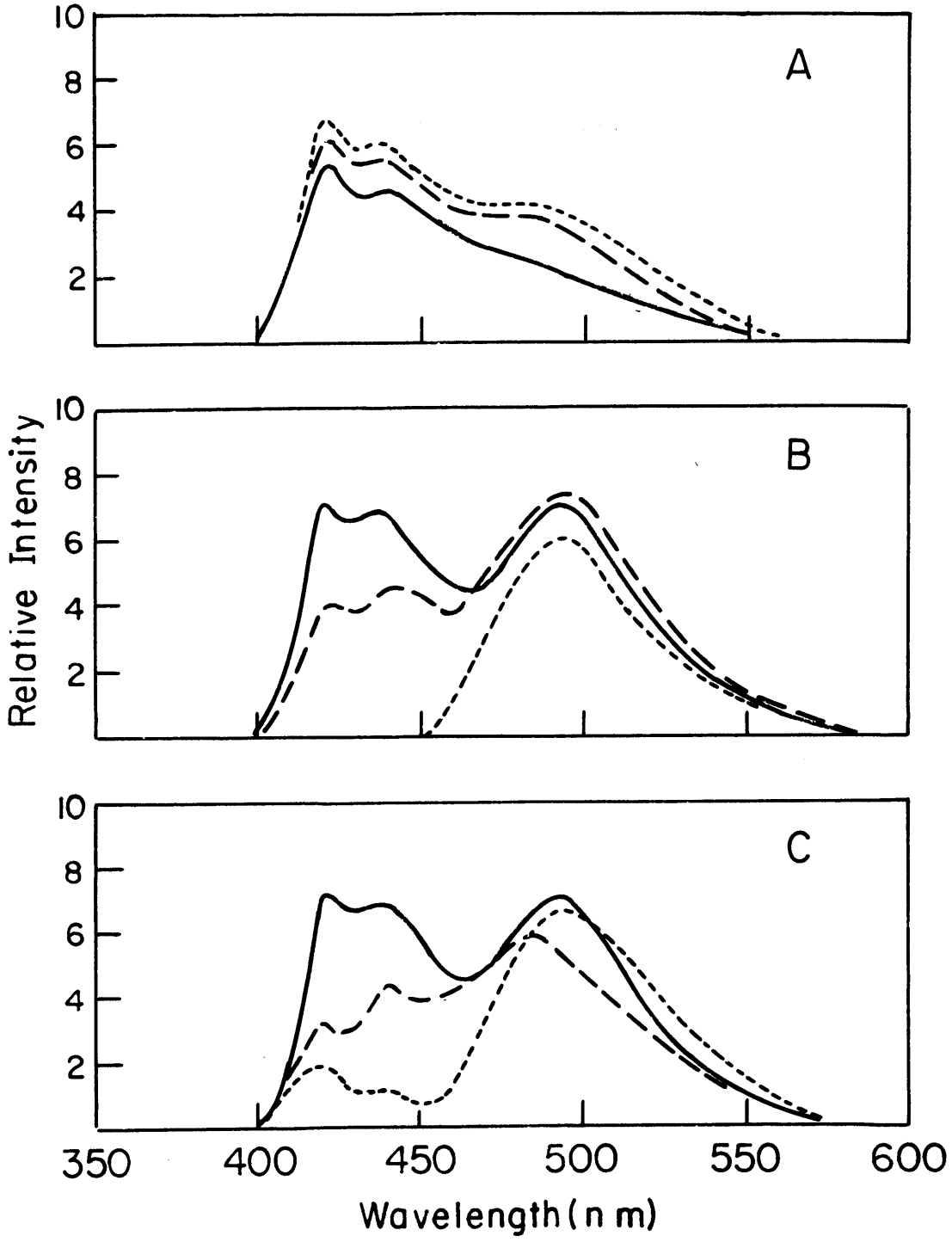
A
B
C
10
8
6
4
2
Relative Intensity
350
400
450
500
550
600
Wavelength (nm)

Figure VII-6

ECL and Fluorescence Spectra in Ethanol

A ——— ECL initial and final of 1 X 10^{-3} M Lucigenin

B - - - Fluorescence of NMA

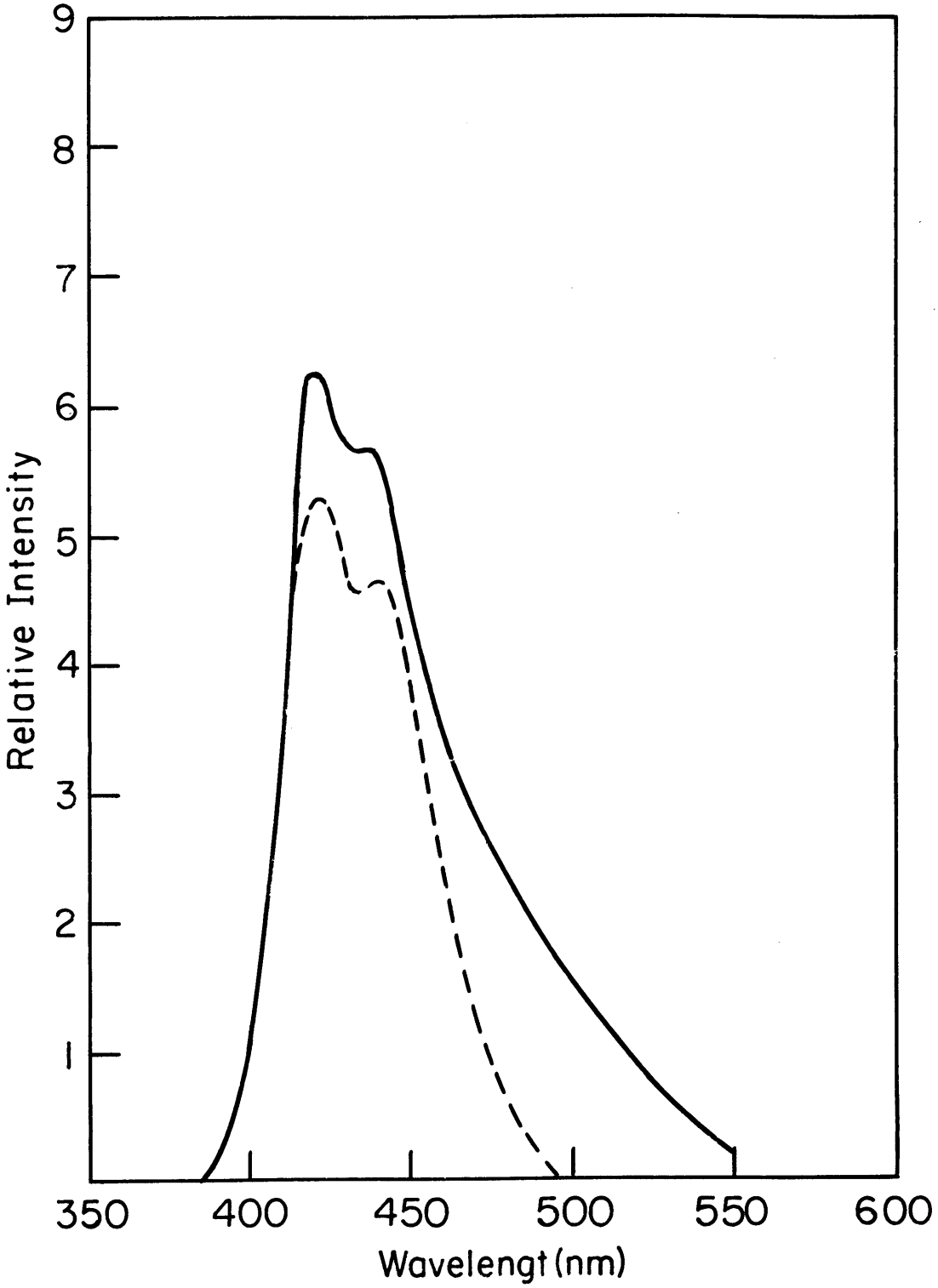
9
8
7
6
5
4
3
2
1
Relative Intensity
350
400
450
500
550
600
Wavelengt (nm)

Figure VII-7

Sensitivity Curve for the Image Intensifier Spectrograph

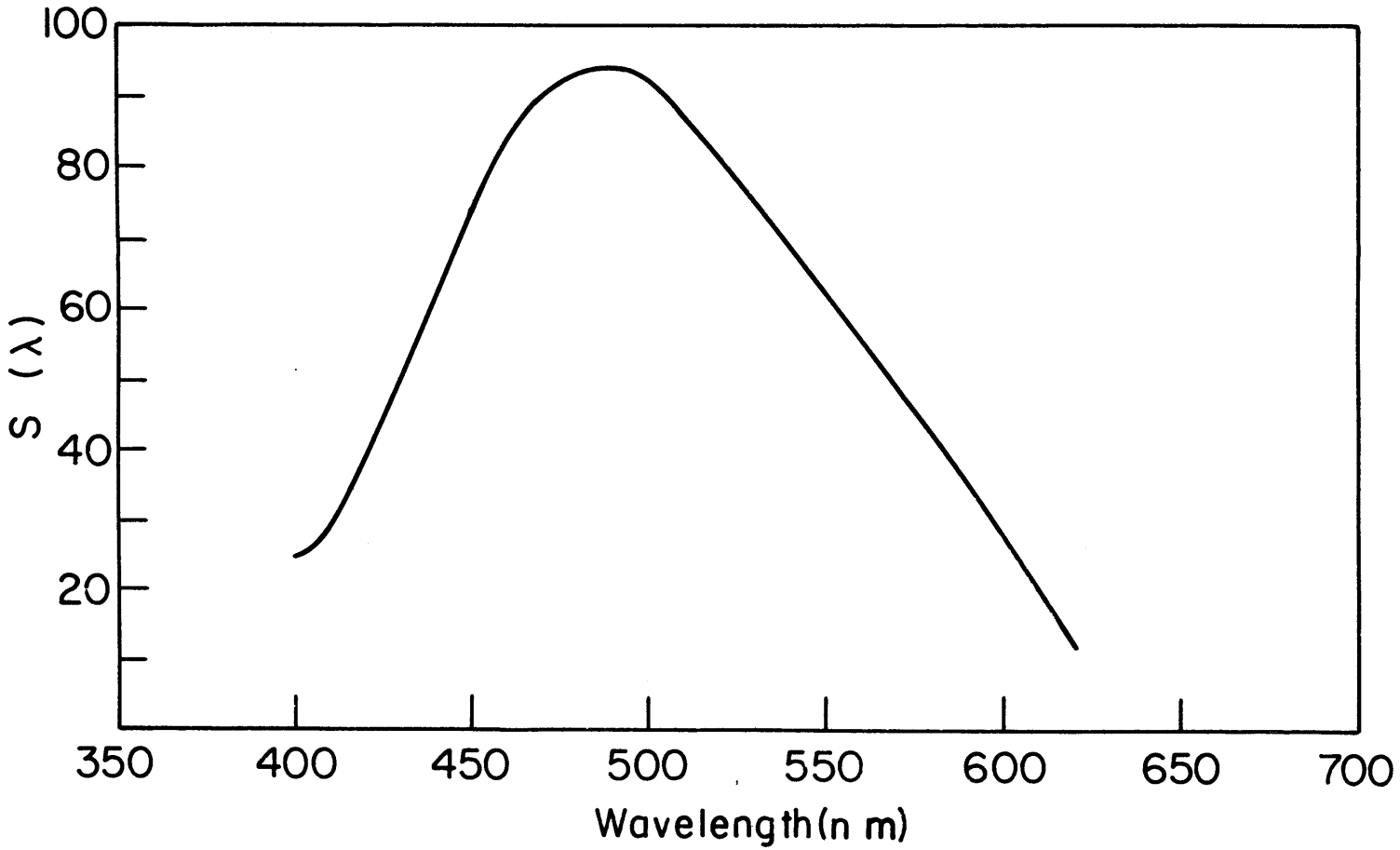
100
80
60
40
20
S (λ)
350
400
450
500
550
600
650
700
Wavelength(n m)

Figure VII-8

ECL Spectra in Water

A — - — 1×10^{-4} M Lucigenin, initial

B ——— 1×10^{-4} M Lucigenin, final

C — — — 1×10^{-3} M Lucigenin, initial

D - - - - 1×10^{-3} M Lucigenin, final

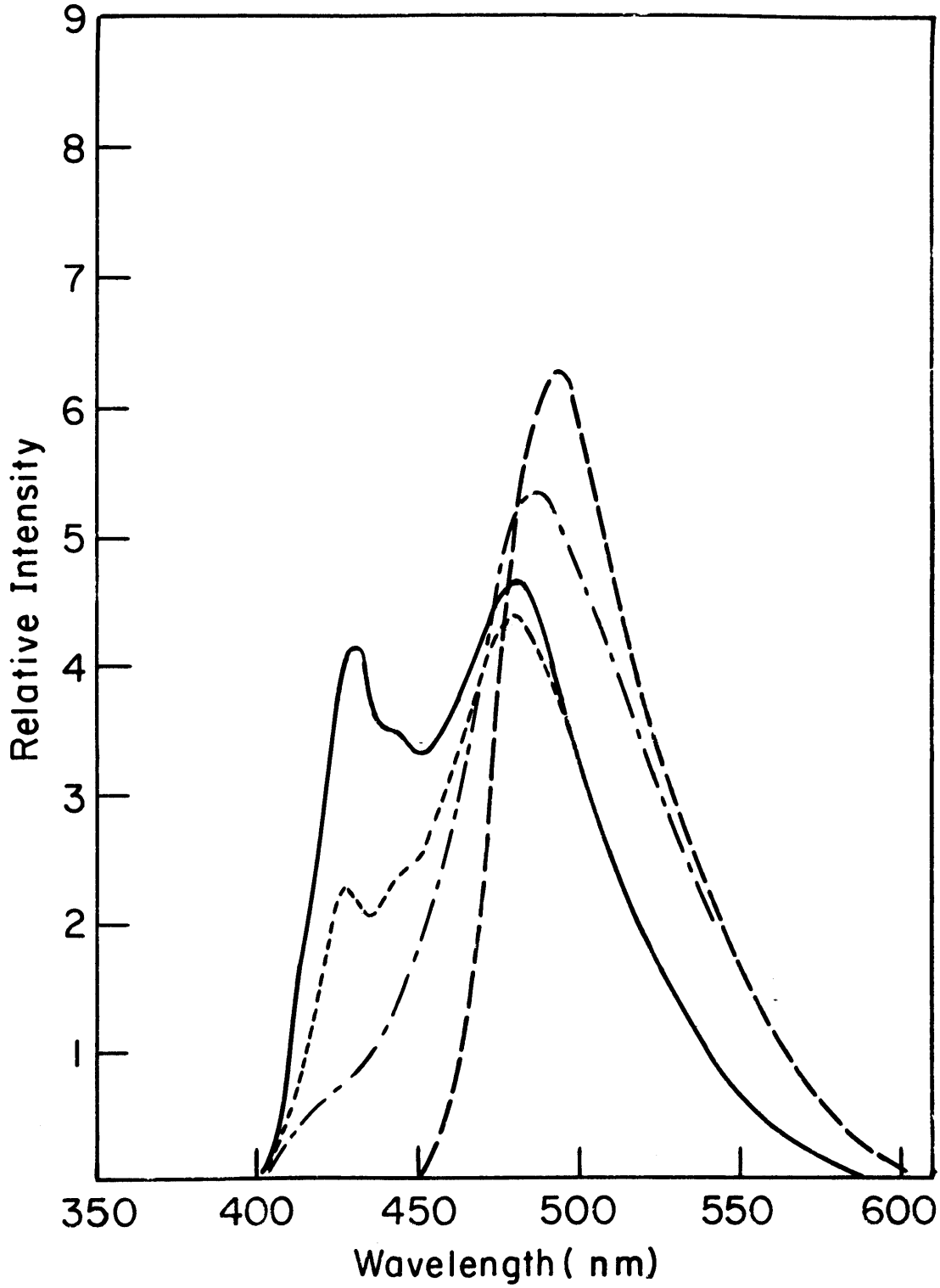
9
8
7
6
5
4
3
2
1
Relative Intensity
350
400
450
500
550
600
Wavelength (nm)

Figure VII-9

"Classical" CL Spectra in Water

A - — — - 9×10^{-5} M Lucigenin, initial

B ———— 9×10^{-5} M Lucigenin, final

C — - - — 4.5×10^{-5} M Lucigenin, initial

D — — — 4.5×10^{-5} M Lucigenin, final

E - - - - - 9×10^{-4} M Lucigenin, initial

F — - — - 9×10^{-4} M Lucigenin, final

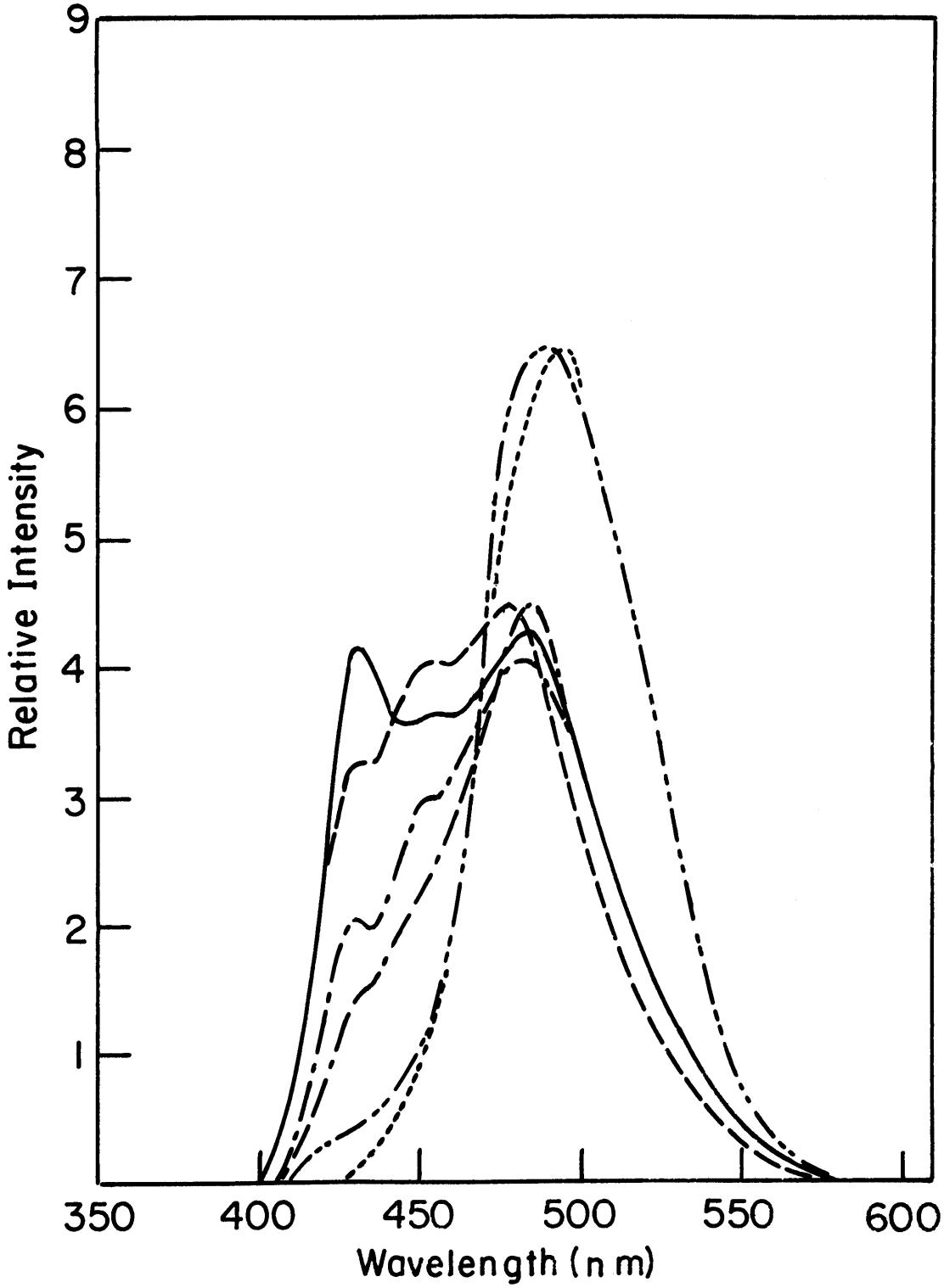
9
8
7
6
5
4
3
2
1
Relative Intensity
350
400
450
500
550
600
Wavelength (nm)

Figure VII-10

Fluorescence and ECL Spectra in Water

A — — — Fluorescence of NMA

B — - — Fluorescence of Lucigenin

C - - - - 1×10^{-3} M Lucigenin, initial

D ——— 1×10^{-4} M Lucigenin, final

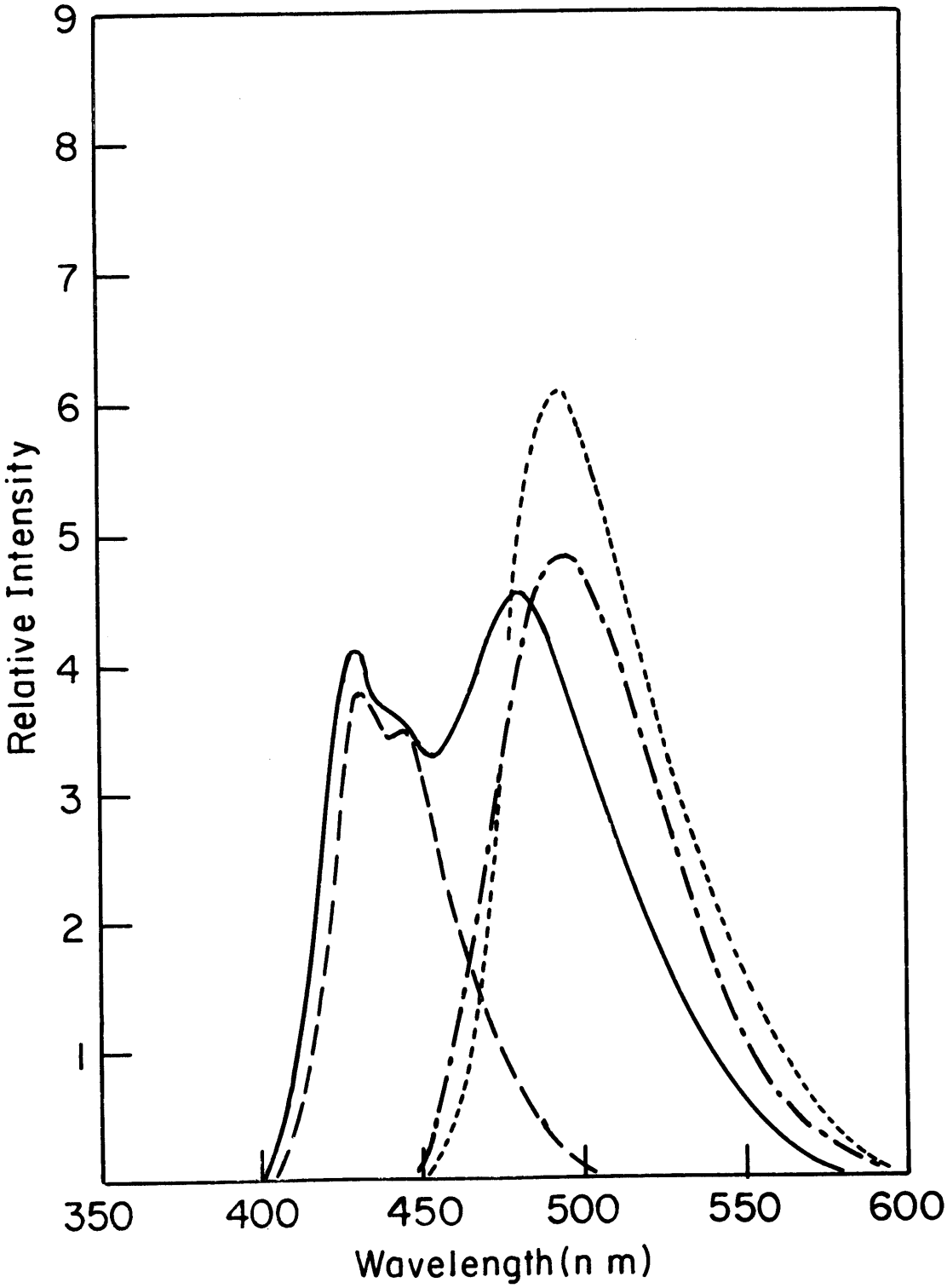
9
8
7
6
5
4
3
2
1
Relative Intensity
350
400
450
500
550
600
Wavelength (n m)

The direction of this change was solvent-dependent. Also, in DMSO the long wavelength band corresponded to the fluorescence of DBA, while in AN it corresponded to that of lucigenin. These observations support the thesis that NMA is the molecule initially formed in the excited state by the reaction of superoxide (or H_2O_2 in aqueous systems) with lucigenin, and thus is the primary emitter. It appears from the above observations that the long wavelength bands are due to secondary emission from either lucigenin or DBA, the extent of which depends on several parameters. To investigate the nature of this secondary emission, studies were made on the possibility of energy transfer occurring in these systems.

D. Energy Transfer Studies.

To ascertain the possibility of energy transfer causing the long wavelength bands observed in the ECL systems, fluorescence spectra were obtained for given concentrations of NMA and DBA in DMSO separately and together. These spectra are shown in Figure VII-11. These results indicate energy transfer from excited NMA, but it is not possible by this method to distinguish between "trivial" re-absorption of NMA fluorescence and singlet-singlet energy transfer to the acceptor.

To further study energy transfer, it was necessary to obtain data on the lifetimes of fluorescence (τ_f) and the quantum efficiencies of fluorescence (ϕ_f) for NMA, DBA and lucigenin in the various solvents. The lifetimes were measured on the TRW lifetime apparatus described above. The quantum efficiencies were taken on the Turner Model 210 Spectrofluorometer, using quinine sulfate as the standard. These results appear in Table VII-1.

Figure VII-11

Fluorescence Quenching of NMA By DBA in DMSO

$\lambda_{excitation}$ = 375 nm

A ———— Fluorescence of 5 X 10^{-5} M NMA

B - - - - Fluorescence of 9.9 X 10^{-5} M DBA

C — — — Fluorescence of 5 X 10^{-5} M NMA + 9.9 X 10^{-5} M DBA

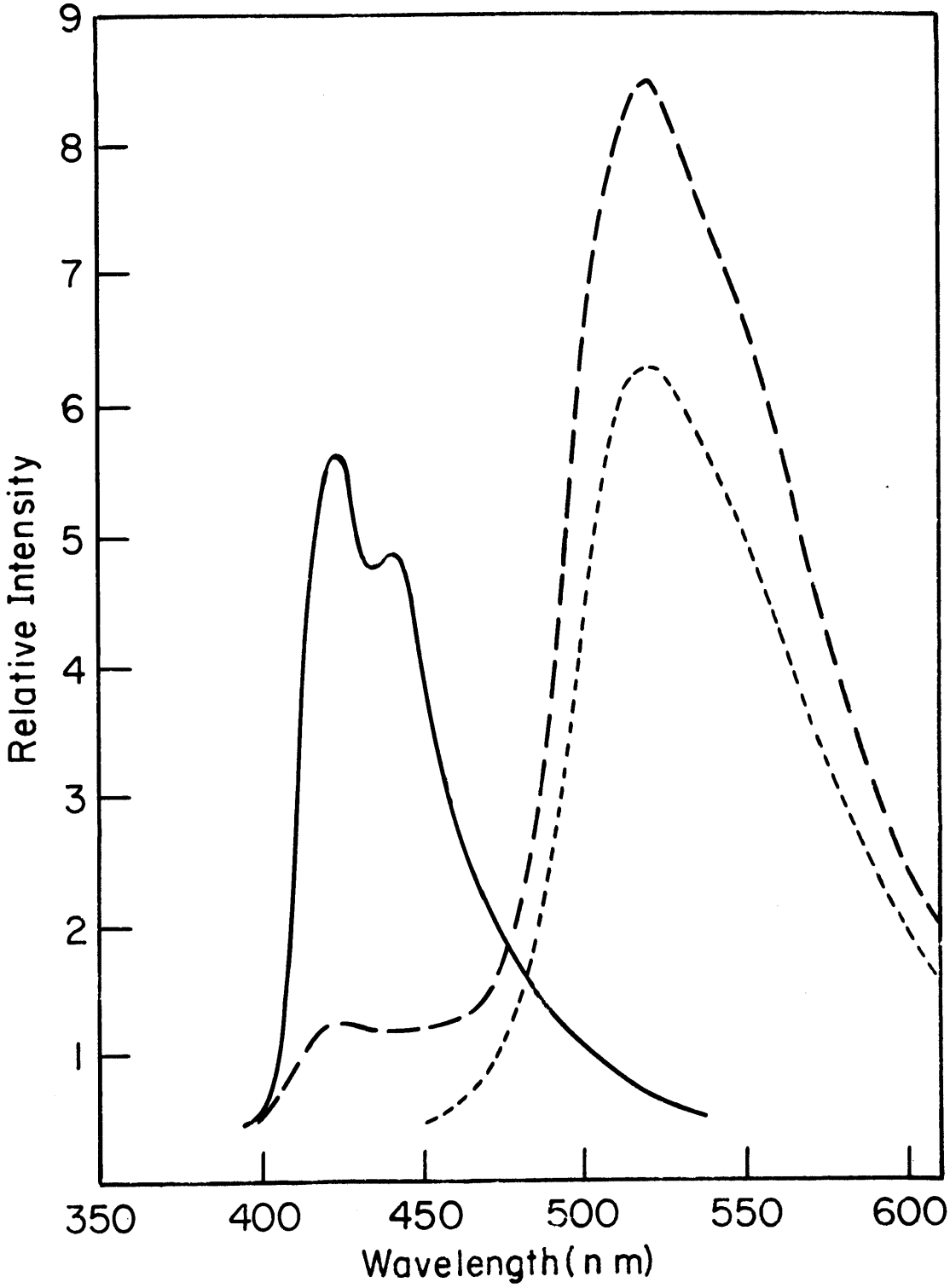
9
8
7
6
5
4
3
2
1
Relative Intensity
350
400
450
500
550
600
Wavelength (n m)

Table VII-1

Fluorescent Lifetimes and Quantum Efficiencies

Solvent	NMA τ (ns)	NMA ϕ	DBA τ (ns)	DBA ϕ	Lucigenin τ (ns)	Lucigenin ϕ
H_2O	18.5	0.82	-----	-----	18.8	0.43
EtOH	14.1	0.61	4.0	0.45	<1	0.09
DMSO	9.0	0.49	4.9	0.58	<1	0.08
DMF	7.6	0.42	5.3	0.60	3.1	0.24
AN	7.2	0.35	3.2	0.40	24.7	0.72

τ = Fluorescence lifetime

ϕ = Fluorescence Quantum Efficiency

If singlet-singlet energy transfer occurs in the NMA-DBA or NMA-lucigenin systems then, as the acceptor concentration is increased, the observed lifetime of the donor should be shortened (41) (42). A plot of the recriprocal of the donor lifetime, $1/\tau$, vs acceptor concentration should give a straight line with slope equal to the rate constant for singlet-singlet energy transfer (41). A series of such measurements was made and the plots of $1/\tau_D$ vs acceptor concentration were found to be linear. Figure VII-12 shows such a plot for transfer from NMA to lucigenin in DMSO. The rate constants derived from these plots appear in Table VII-2 and are ca. 1.5×10^{11} 1/M-sec, an order of magnitude faster than diffusion controlled rate constants. This respresents good evidence for singlet-singlet energy transfer via the resonance mechanism of dipole-dipole interaction.

Forster (43) has derived a theoretical relationship for dipole-dipole interaction resulting in energy transfer in which the "critical distance", R_o, for equal probability of transfer and other modes of deactivation of the excited state is given by:

$$R_o^6 = \frac{9000\ (\ln 10)\ (2/3)\ \phi_D}{128\pi^5\ n^4\ N}\ J(\bar{\nu}) \quad (1)$$

where

$$J(\bar{\nu}) = \int F_D(\nu)\,\epsilon_A(\nu)\,\frac{d\nu}{\nu^4} \quad (2)$$

and R_o is related to the rate constant for energy transfer by:

$$k_{ET} = \frac{R_o^3}{(7.35 \times 10^{-8})^3\ \tau_D([A] = 0)}$$

Figure VII-12

Stern-Volmer Plot for Energy

Transfer from NMA to Lucigenin DMSO

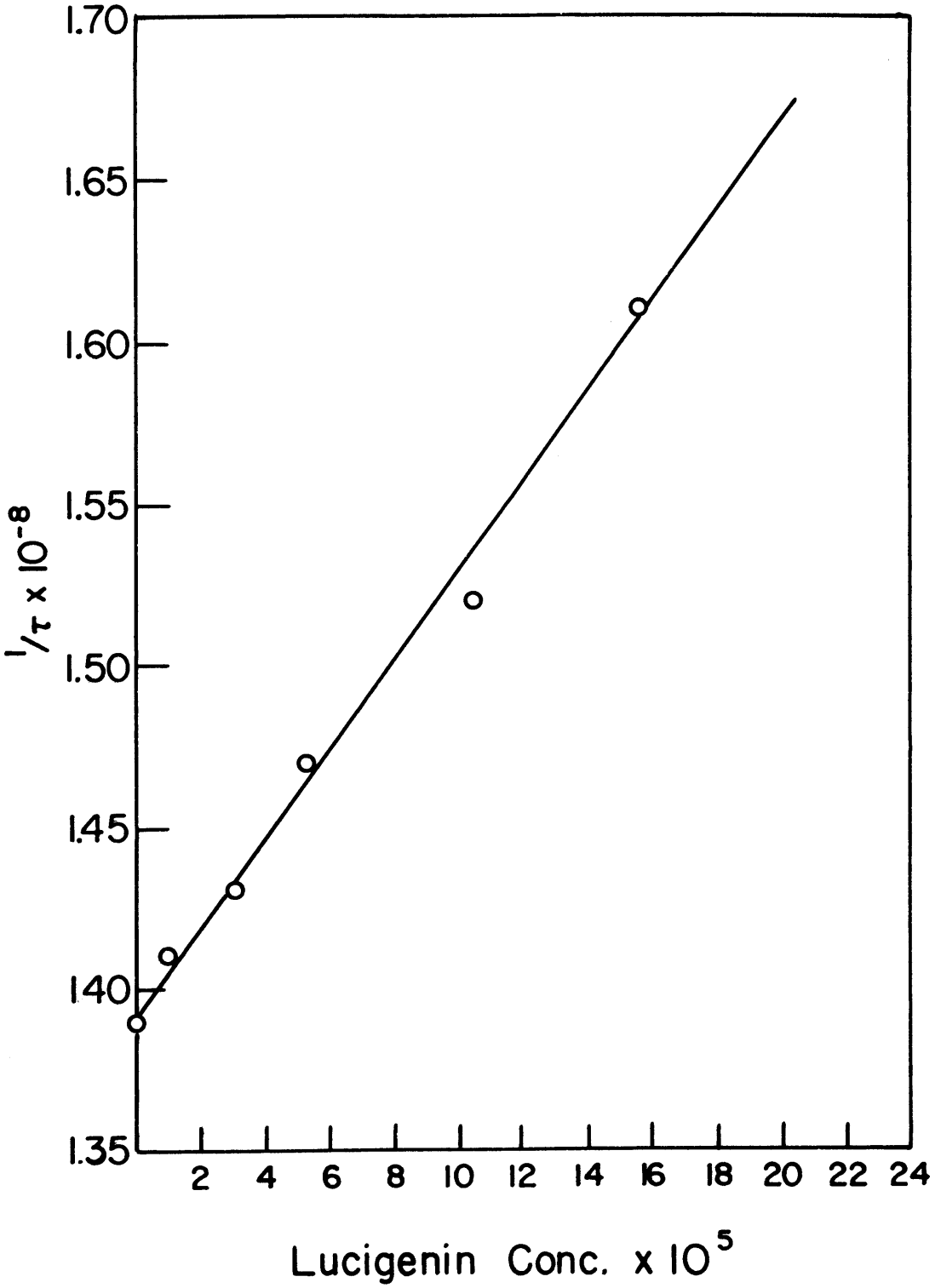
1.70
1.65
1.60
1.55
1.50
1.45
140
1.35
1/τ x 10-8
2
4
6
8
10
12
14
16
18
20
22
24
Lucigenin Conc. x 10^5

Table VII-2

Experimental and Theoretical Rate Constants

For Energy Transfer and Critical Radius

Solvent	Lucigenin			
	(a) k_{ET}(exp)	k_{ET}(theor)	(b) R_o(exp)	R_o(theor)
DMSO	9×10^{10}	1.1×10^{10}	69 Å	34 Å
DMF	2×10^{11}	1.3×10^{10}	86 Å	34 Å
AN	1.4×10^{11}	1.4×10^{10}	74 Å	34 Å

Solvent	DBA			
	k_{ET}(exp)	k_{ET}(theor)	R_o(exp)	R_o(theor)
DMSO	1.7×10^{11}	1.1×10^{10}	86 Å	34 Å
DMF	1.8×10^{11}	1.3×10^{10}	83 Å	35 Å
AN	1.5×10^{11}	1.5×10^{10}	76 Å	34 Å

(a) Rate constant for energy transfer

(b) Critical radius

where n is the refractive index of the solvent, N is Avagadro's number, ϕ_D is the fluorescence efficiency of the donor in the absence of acceptor, $f_D(\nu)$ the donor fluorescence distribution in quanta normalized unity on a wavenumber scale, $\varepsilon_A(\nu)$ is the molar decadic extinction coefficient of the acceptor and ν is the wavenumber.

The fluorescence spectrum of NMA and the absorption spectra of DBA and lucigenin in DMSO are shown in Figure VII-13, indicating the overlap favorable for energy transfer in these systems. Theoretical values of R_o were calculated from these data along with those of Table VII-1. The overlap integral $J(\bar{\nu})$ was evaluated graphically. These theoretical values of R_o along with the rate constants for energy transfer calculated from equation (3) appear in Table VII-2. The calculated values of R_o of ca. 34 Å also give strong evidence for singlet-singlet transfer occurring in these systems.

Figure VII-14 shows the results of calculations on the probability of energy transfer and trivial re-absorption from NMA to DBA (top) and to lucigenin (bottom) in AN as a function of acceptor concentration. Curve A is the probability of energy being transferred via the resonance mechanism (using the experimental value of k_{ET}). Curve B is the resultant probability that excited NMA will behave normally, i.e. either fluoresce or undergo radiationless de-activation. Curve C is the probability of the acceptor absorbing a photon emitted by NMA. When curve B is multiplied by the quantum efficiency of NMA's fluorescence in AN and this product multiplied by curve C, curve D results, namely the probability of the "trivial" process occurring. Curve E is the sum of curves A and D and indicates the total probability of energy being transferred by either process. It should be noted that

Figure VII-13

Overlap of NMA Fluorescence with DBA and Lucigenin Absorption

A ———— Fluorescence of NMA

B - - - - Absorption of DBA

C — — — Absorption of Lucigenin

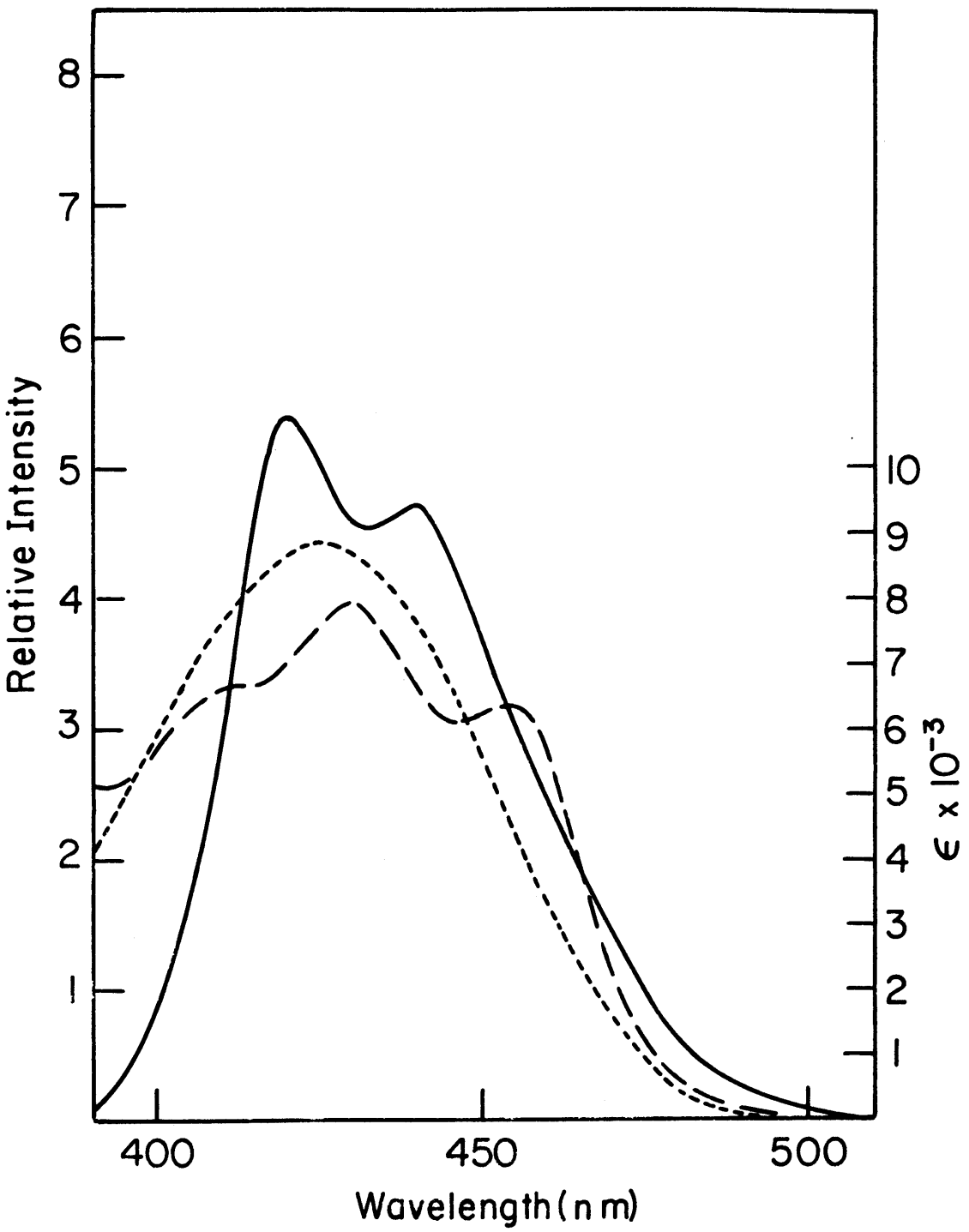
Relative Intensity
8
7
6
5
4
3
2
1
10
9
8
7
6
5
4
3
2
1
ε x 10⁻³
400
450
500
Wavelength (nm)

Figure VII-14

Probability Plots for Energy Transfer from

NMA to DBA and Lucigenin in AN

A — - — - — Probability of energy transfer

B — - - - — Probability of NMA remaining in the excited state after energy transfer

C - - - - - - Probability of absorption of NMA emission

D — — — — Probability of trivial re-absorption

E ———— Total probability of energy gained by acceptor

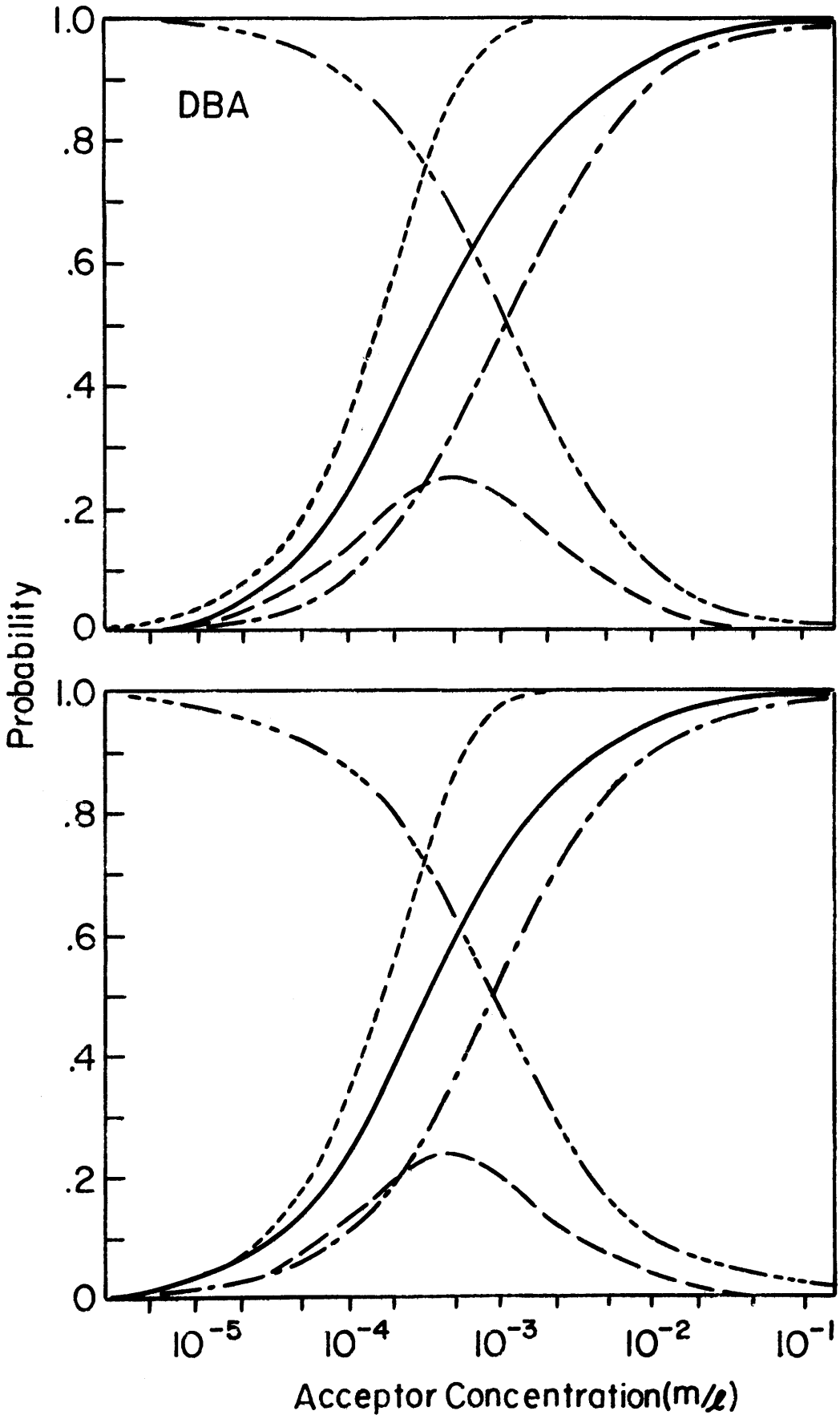
DBA
1.0
.8
.6
.4
.2
0
Probability
10^{-5}
10^{-4}
10^{-3}
10^{-2}
10^{-1}
Acceptor Concentration(m/ℓ)

at acceptor concentrations greater than 5×10^{-4} M the probability of energy transfer via the resonance mechanism is greater than for the trivial process.

Similar calculations were made for lucigenin and DBA in the various solvents studied. All showed 50% probability for total transfer at approximately the same acceptor concentrations. This arises because the extinction coefficients and k_{ET}'s of lucigenin and DBA are approximately the same. Table VII-3 shows the concentrations for all systems where the total probability of transfer equals 50 percent.

TABLE VII-3

Concentration of Acceptor where Total Probability of Energy Transfer and the "Trivial Process" from NMA = 0.5

Solvent	Acceptor	C at P = .5
DMSO	Luc	2.7×10^{-4} M
	DBA	2.4×10^{-4} M
DMF	Luc	2.3×10^{-4} M
	DBA	2.5×10^{-4} M
AN	Luc	4.0×10^{-4} M
	DBA	3.8×10^{-4} M

VIII. Discussion ECL

A. Qualitative Observations.

The explanation as to why light was observed when a mercury pool cathode was used in place of a platinum cathode in the generation of CL in aqueous media seems straight forward. It is known that in basic solutions at a platinum electrode, oxygen is reduced to OH^- via a multi-step process, all steps occurring at the same potential (44), whereas in neutral solutions at mercury there are two, well-separated waves, the first of which is:

$$O_2 + 2H_2O + 2e^- \rightarrow H_2O_2 + 2\ OH^-.$$

Thus, when the reaction was run in basic solution at platinum, only OH^- was produced in the bulk of the solution, while under neutral conditions, at mercury, hydrogen peroxide and OH^- were produced. The latter are the same reagents necessary for the "classical" production of lucigenin CL with two of the reagents supplied by the electrochemical reduction of oxygen. Figures VII-8 and VII-9 bear this out as the ECL and "classical" CL spectra are identical. It should be noted that at the potentials employed to produce the aqueous ECL the electrochemical reduction of lucigenin is not a factor (see Figure V-1). In view of these facts it is difficult to understand how Tammamushi and Akiyama (19) were able to observe light under the conditions which they reported.

It is also clear from the results in non-aqueous media that the reaction leading to light emission is that of superoxide, generated by the electrochemical reduction of oxygen, with lucigenin. It is important to note in non-aqueous ECL that lucigenin is being electrochemically reduced to DBA at the same time that O_2 is being reduced to

O_2^- (although DBA does not react with O_2^- to give light). The importance of this fact will become evident in the discussion below.

The spectra presented earlier give excellent evidence for identification of the primary emitter of the CL reaction. This has been shown to be NMA and its emission is common to all systems. When sufficiently dilute solutions ($< 10^{-4}$ M) are used, the predominant emission is that of NMA. Thus the primary chemiluminescent process is the reaction of electrogenerated superoxide with lucigenin to form NMA in the excited state.

The long wavelength component of the ECL spectra may be attributed to secondary emission from lucigenin or DBA which are excited by energy transfer from the excited NMA. The feasibility of this process has been demonstrated in the section on energy transfer and the data presented there will be correlated with the observed ECL spectra below.

B. ECL Spectra.

The spectra shown in Figures VII-1-6 may be misleading as they are uncorrected. A more realistic set of spectra is shown in Figure VIII-1. These are some of the spectra of Figure VII-4 (ECL in AN) which have been corrected by applying the sensitivity curve of the IIS (Figure VII-7). It can be seen that the short wavelength components of the spectra are, in reality, more intense than the uncorrected spectra would indicate.

The initial studies of the ECL spectra were made on an Aminco-Bowman spectrofluorometer. Although this instrument had sufficient sensitivity for these measurements, it has one drawback over the IIS. This drawback is that the spectrofluorometer has a scanning readout. Over the time of a scan of a spectrum, the CL reaction may be decaying

Figure VIII-1

Corrected ECL Spectra in AN

A ———— 5.5×10^{-4} M Lucigenin, final

B - - - - 1.1×10^{-4} M Lucigenin, initial

C — — — 1.1×10^{-4} M Lucigenin, final

D — - — 1.1×10^{-3} M Lucigenin, initial

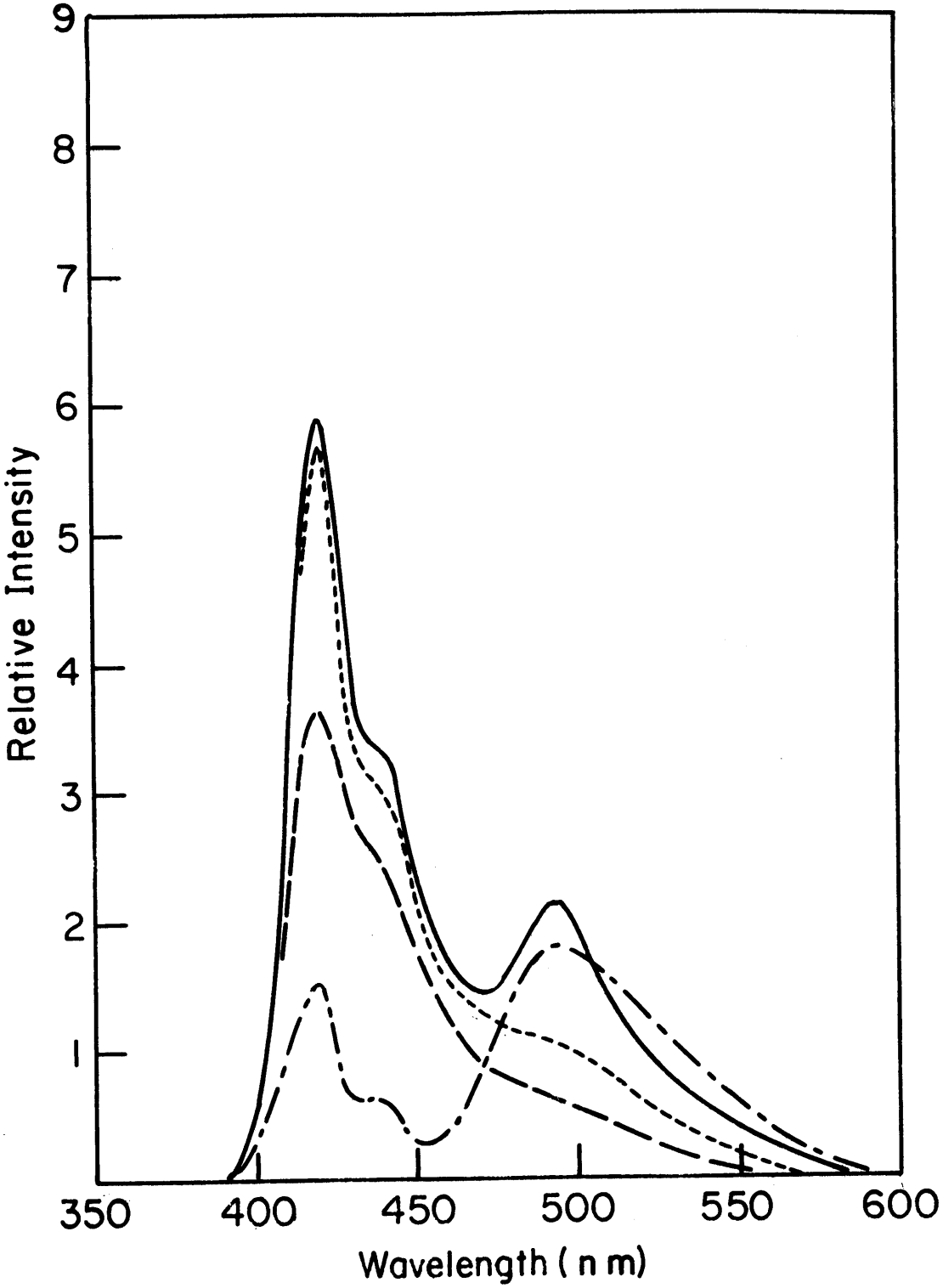
9
8
7
6
5
4
3
2
1
Relative Intensity
350
400
450
500
550
600
Wavelength (n m)

and the resultant decrease in intensity of emission over the time of a scan may result in a distorted spectrum. The IIS circumvents this difficulty in that it records the whole spectrum continuously over the time of measurement (which is small, being, on the average 10 sec.). Thus even the small changes in intensity occurring in this time are "integrated" and the resulting spectrum shows no distortion.

The effect of using a scanning fluorometer is shown in Figure VIII-2. It is evident from this figure that the spectra obtained on the Aminco-Bowman are distorted and the peaks appear shifted towards shorter wavelengths. This effect is most marked at the beginning of the reaction (curve C) where the light intensity is changing most rapidly. Near the end of the reaction the emission is fairly constant over the time of a scan and little distortion is seen (curve D).

Figure VIII-2

Comparison of ECL spectra in AN taken on Aminco -Bowman Spectrofluorometer and IIS

Lucigenin ~5 X 10^{-4} M

A ———— Initial on IIS

B — - — Final on IIS

C — — — Initial on Aminco

D -------- Final on Aminco

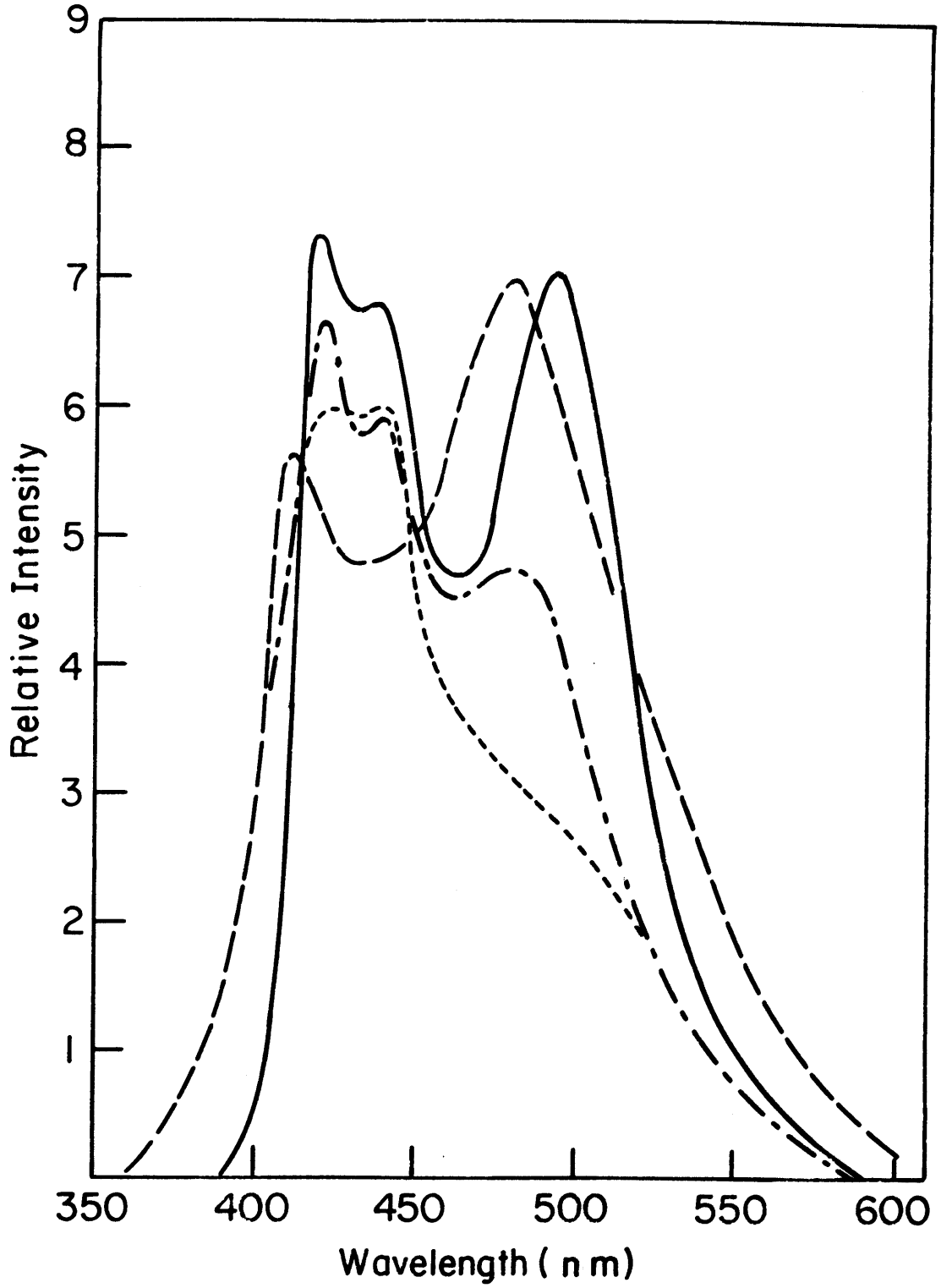
9
8
7
6
5
4
3
2
1
Relative Intensity
350
400
450
500
550
600
Wavelength (n m)

C. Singlet-Singlet Energy Transfer.

The existence of singlet-singlet energy transfer, via dipole-dipole resonance interactions, in the NMA*--DBA and NMA*--lucigenin systems has been proven by the results from the energy transfer studies. The fluorescence enhancement results depicted in Figure VII-10 qualitatively show some form of transfer from NMA* to DBA in DMSO, but as described earlier, such an experiment does not distinguish between true energy transfer and "trivial" reabsorption of NMA fluorescence. Figure VII-13 gives an indication of the excellent overlap between the emission of NMA and the absorption of DBA and lucigenin. This overlap is extremely important as the overlap integral ($J(\bar{\nu})$ (equation 2) is a direct function of the overlap, expressed as $f_D(\nu)\ \varepsilon_A(\nu)$. However this overlap is necessary for the "trivial" process also.

Studies of the effect of acceptor concentration on the donor lifetime provide a convenient method of distinguishing between true singlet-singlet energy transfer and "trivial" reabsorption of NMA's fluorescence. The following scheme can be presented for the interaction of exciting light with a donor molecule (D) and the resultant interaction of D* with an acceptor(A):

		Rate
1.	$D + h\nu \rightarrow D^*$	I_A
2.	$D^* \rightarrow D$	$K_{ic}(D^*)$
3.	$D^* \rightarrow {}^3D$	$k_{ix}(D^*)$
4.	$D^* \rightarrow D + h\nu_f$	$k_f(D^*)$
5.	$A + h\nu_f \rightarrow A^*$	I_f
6.	$D^* + A \rightarrow D + A^*$	$k_{ET}(D^*)(A)$

The lifetime of the donor fluorescence in the absence of acceptor is given by:

$$\tau_D^{\circ} = \frac{1}{k_{IC} + k_{IX} + k_f} \qquad (7)$$

while the lifetime of the donor fluorescence with acceptor present is:

$$\tau_D^{A} = \frac{1}{k_{IC} + k_{IX} + k_f + k_{ET}(A)} \qquad (8)$$

or $$1/\tau_D^{A} = 1/\tau_D^{\circ} + k_{ET}(A) \qquad (9)$$

Thus, while the "trivial" process does not affect the lifetime of the excited donor, singlet-singlet energy transfer does. A plot of $1/\tau_D^{A}$ vs acceptor concentration should give a straight line with a slope equal to the rate constant for energy transfer (equation 9 above).

The lifetime of the donor fluorescence was found to decrease with increasing acceptor concentration and Stern-Volmer plots gave a straight line from which the value of the energy transfer rate constant was measured by determining the slope of these lines (see Figure VII-12).

The experimentally derived values of R_o for energy transfer (Table VII-2) are seen to be over twice as large as those calculated from Forster's theoretical equations (75Å as compared with 34Å). This disagreement between theory and the measured value may be easily explained. Forster's equations consider the donor and acceptor molecules to be stationary, whereas in fact they are in motion during the lifetime of the excited donor molecule. At room temperature in a solvent of 10 millipoise, a molecule may move as much as 40 Å when the donor lifetime is 10 ns. The net result of this motion during the donor lifetime is an increase in the measured value of R_o. Since the value of k_{ET}

is proportional to R_o^3, the observed values of k_{ET} are approximately an order of magnitude greater than those predicted from the Forster equations. This disparity between measured and predicted values arises from the fact that the theory inadequately describes the system. All references to k_{ET} for the systems studies should be to the experimentally derived values.

The probability plots shown in Figure VII-14 give an indication of the effect of energy transfer on the ECL spectra. From these curves and the data of Table VII-3 one can see that at concentrations of greater than 10^{-4} M acceptor a significant amount of energy may be transferred from the donor molecule. At acceptor concentrations greater than 5×10^{-4} M 50 percent or more of the excited state energy of the donor is transferred and if the acceptor is fluorescent in this solution, one could expect to see large contributions due to secondary, long wavelength emission at these acceptor concentration levels. Such effects were observed and are discussed below.

D. Correlation of ECL spectra with quantum efficiencies of acceptor fluorescence, extent of reaction and energy transfer.

Since the data in Table VII-2 indicate that excited NMA transfers energy at about the same rate to either DBA or lucigenin in all of the solvents studied, the origin and intensity of the long wavelength band in the ECL is dependent only on the fluorescence efficiency of the acceptor and the acceptor concentration. Thus, if the acceptor (either lucigenin or DBA or both) is present at high enough concentrations ($> 10^{-4}$ M) and has a relatively high quantum efficiency of fluorescence, a long wavelength band will be present. When the acceptor concentration

is low, no long wavelength band will be observed. In addition, when the quantum efficiency of the acceptor is low and its concentration is high, energy will be transferred to the acceptor, but, because of radiationless deactivation, no long wavelength band will be present. These arguments correlate well with the observed ECL spectra and the data of Table VII-1.

In DMSO (Figure VII-1) the long wavelength emission corresponds to DBA fluorescence. In this solvent lucigenin has a very low quantum efficiency of fluorescence (ϕ_f) of 0.08 (see Table VII-1) whereas DBA has a ϕ_f of 0.58. When lucigenin is present at a low initial concentration and DBA has not yet been built up in solution (Figure VII-1, curve A) little energy is tranferred to lucigenin and very little, if any long wavelength emission is present, and the observed spectrum correponds to emission from NMA. When the initial concentration of lucigenin is high, at the beginning of the reaction when small amounts of DBA have been built up in solution (Figure VII-1, curve E) one observes emission from both NMA and DBA. In this case energy is being transferred from NMA to both DBA and lucigenin but, since the ϕ_f of lucigenin is so low, the long wavelength emission observed is solely due to DBA fluorescence. At the other extreme, when the initial concentration of lucigenin is high and the reaction has proceeded for some time(Figure VII-1, curve F) only the long wavelength component is observed. Under these conditions the concentration of lucigenin is relatively low, whereas the DBA concentration is high (having been produced by the electrochemical reduction of lucigenin). In this case, because of the high concentration of DBA in solution all of the energy from excited NMA is transferred to DBA and the

emission observed is that of DBA fluorescence (λ_{max}, 505 nm). The other spectra presented in Figure VII-1 show the behavior observed for intermediate concentrations and extents of reaction.

The trends observed when AN was used as the solvent are the opposite of those discussed above for DMSO. In acetonitrile lucigenin has a high ϕ_f of 0.72 while the ϕ_f of DBA is much lower (0.40). Once again, two extremes will illustrate the point. In the first case, when lucigenin is at a reatively low initial concentration (1.1×10^{-4} M) the initial spectrum (Figure VII-4, curve A) shows a predominance of NMA emission, but with some long wavelength contribution due to lucigenin. Near the end of the reaction, the lucigenin concentration has been greatly reduced and only NMA emission is observed (curve B). In the second case, when lucigenin is present at a high initial concentration (1.1×10^{-3} M), the initial spectrum (curve E) shows a predominance of long wavelength emission corresponding to lucigenin fluorescence (λ_{max}, 495 nm). Near the end of the reaction, little lucigenin is present and the DBA built up during the electrolysis, while it does act as an energy acceptor, has a low ϕ_f and the spectrum (curve F) shows a predominance of NMA emission. This latter case should be, and is, similar to the initial spectrum obtained when lucigenin is present at a low initial concentration (curve A). It should be remembered that the spectra shown in Figure 4 are uncorrected and that the corrected spectra would show an even greater contribution due to NMA emission (see Figure VIII-1).

It is interesting to observe the behaviour of the ECL in AN at various concentrations and for different extents of reaction. These

spectra are shown in Figure VII -5. When lucigenin is present initially at a low concentration (1.1×10^{-4} M) one sees a decrease in the long wavelength band (secondary emission from lucigenin) as the reaction proceeds. However, at no time does the long wavelength emission predominate that of NMA. When lucigenin is initially present at a high concentration (1.1×10^{-3} M) the secondary, long wave length emission is seen to be dominant until the end of the reaction. At an initial lucigenin concentration of 5.5×10^{-4} M the spectra do not appear to change as rapidly as is observed at the higher concentration. This is a result of the chemiluminescent reaction being a bi-molecular process. Since a steady state potential was employed and all solutions were saturated with oxygen, the production of O_2 should be relatively constant in all cases. However, when lucigenin is present at a high concentration, the bi-molecular chemiluminescence reaction proceeds much faster than when lucigenin is present at a lower initial concentration. As a consequence one observes a more intense emission at higher lucigenin concentrations and a more rapid change in the spectrum.

The ECL spectra encountered when DMF was used as the solvent are shown in Figure VII-2 and appear to be a combination of those seen in AN and DMSO. In DMF lucigenin has a ϕ_f of 0.24 while DBA has a ϕ_f of 0.60. Since lucigenin has a moderate ϕ_f in this solvent, secondary emission from lucigenin is seen when it is present at high enough concentrations (curves A,C and E). It can be seen that the intensity of the lucigenin emission (λ_{max}, 495 nm) at the beginning of the reaction is a direct function of the initial lucigenin concentration, which correlates well with the energy transfer results. As the reaction proceeds, the lucigenin concentration decreases, while the DBA

concentration is increased due to electrochemical reduction of lucigenin and a shift in the long wavelength emission to that of DBA (λ_{max}, 505 nm) is observed. In the extreme, at the end of the reaction when lucigenin was present at a high initial concentration only DBA emission is observed (curve F).

Figure VII-3 gives a comparison of the ECL spectra in DMF with the fluorescence spectra of NMA, DBA and lucigenin, all uncorrected and taken on the IIS. From these spectra the identification of the species causing the various emissions is easily done and this complements the discussion above.

The only emission observed in E_tOH was that of NMA, (Figure VII-6). In this solvent lucigenin has a ϕ_f of 0.09 while that of DBA is 0.45. Even though DBA has a moderate ϕ_f in this solvent, it is quite insoluble and thus no contribution due to either DBA or lucigenin is present and only NMA emission is observed.

The ECL spectra taken in aqueous solution are presented in Figure VII-8. These may be compared with the spectra of the "classical" CL of lucigenin in H_2O shown in Figure VII-9. Figure VII-10 compares the ECL spectra in aqueous solution with the fluorescence spectra of lucigenin and NMA. Once again NMA is seen to be the primary emitter and a long wavelength component of emission is also observed which in some cases can be assigned to secondary emission from lucigenin (Figure VII-8, curves A and C). The similarity of the ECL spectra to those of the "classical" reaction are not surprising and the reason for this has been discussed above.

The nature of the long wavelength component peaking at 480 nm (Figure VII-8, curves B and D; Figure VII-9, curves A, B and F) is

not yet understood. This peak is observed in solutions of lucigenin where the fluorescence of lucigenin is totally quenched by chloride ion, and thus is not due to lucigenin emission. All attempts to monitor intermediate species which could give rise to this emission have failed. Since this emission cannot be ascribed to any of the starting materials or known products of the reaction, one must assume that it is a result of some unknown intermediate. Since such an intermediate is not easily observed, it must be present at a very low concentration, too low for energy transfer from excited NMA to be significant. Thus, one must assume that the species giving rise to this emssion at 480 nm must itself be formed in the excited state by a chemiluminescent mechanism different from that which forms NMA in the excited state.

IX Preliminary Investiations of the Non-Aqueous Chemiluminescence of Lucigenin

A. Results

1. Qualitative observation of Chemiluminescence.

When the oxygen saturated lucigenin solution was mixed with the KOtBu solution light was observed. The emission was long-lived at a very low level of intensity. The intensity of the emission was a direct function of the lucigenin concentration. At a constant lucigenin concentration a dependance of intensity on the KOtBu concentration was observed. The intensity of the CL increased as KOtBu was increased. However, if the lucigenin concentration exceeded 5×10^{-4} M when the KOtBu concentration was greater than 10^{-3} M the intensity of the CL was seen to decrease. Addition of water tended to quench the CL.

2. Spectral study of Non-Aqueous chemiluminescence.

The spectra of the CL of lucigenin in DMSO are shown in Figure IX-1. Figure IX-2 shows the CL spectra in DMF and Figure IX-3 compares the CL and fluorescence spectra obtained on the IIS in DMF. Figure IX-4 shows the CL spectra in acetonitrile. Figure IX-5 presents the CL spectra obtained when the reagents were mixed in the "T" mixer by use of the syringe drive unit. Flow rates were 77.4 and 3.75 cc/min at speed setting 1 and 10 respectively. Incomplete mixing was observed at speed settings greater than 15 (Slower flow rates).

B. Discussion

1. Qualitative observation of chemiluminescence

When dry solvents were used it was comparatively easy to produce

Figure IX-1

Chemiluminescence Spectra in DMSO

5×10^{-4} M KOtBu

A ———— 3×10^{-5} M Lucigenin, initial

B - - - - - 3×10^{-5} M Lucigenin, final

C — - - — 3×10^{-4} M Lucigenin, initial

D — - — - 3×10^{-4} M Lucigenin, final

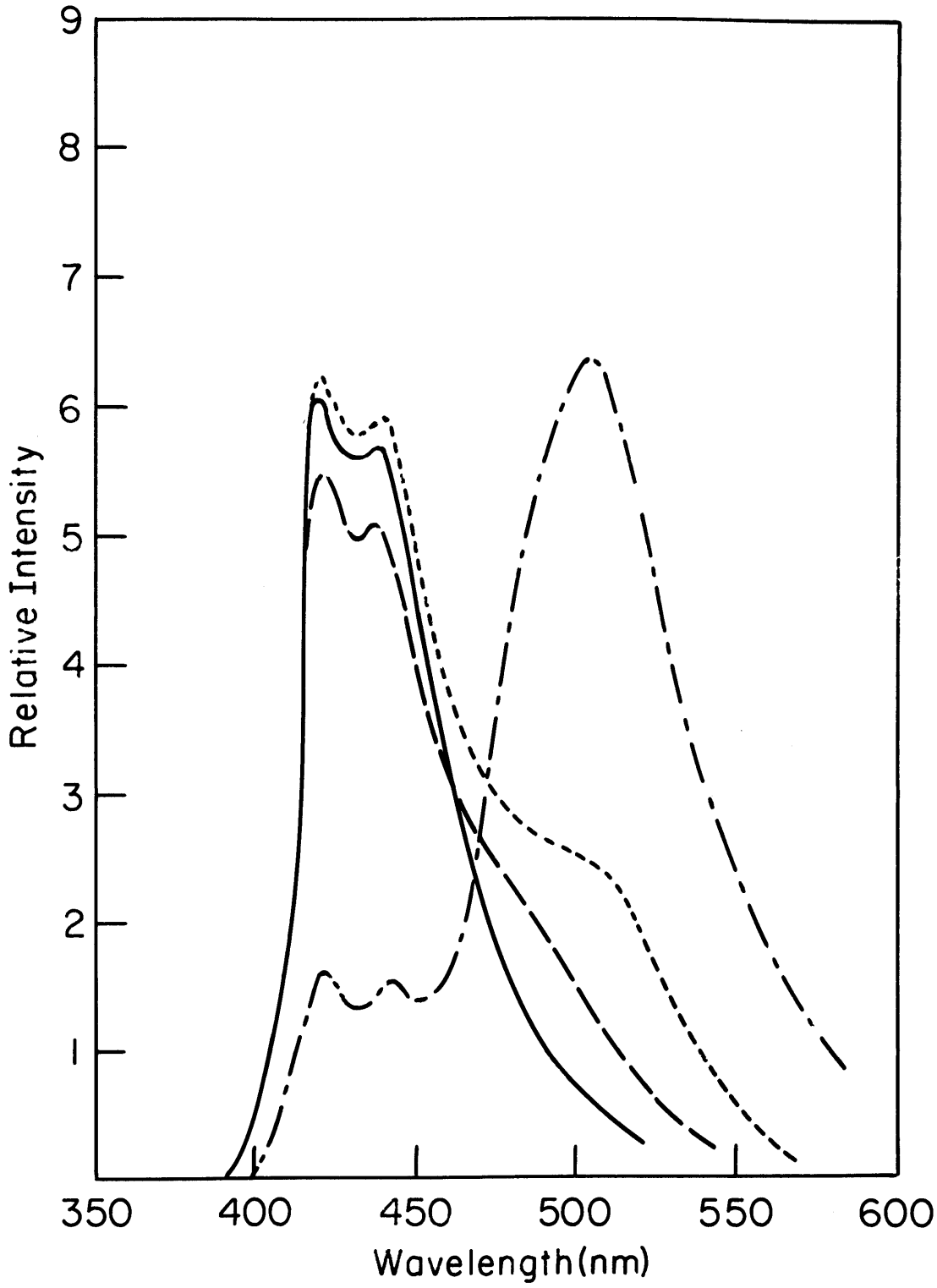
9
8
7
6
5
4
3
2
1
Relative Intensity
350
400
450
500
550
600
Wavelength(nm)

Figure IX-2

Chemiluminescence Spectra in DMF

5×10^{-4} M KOtBu

A ———— 3×10^{-5} M Lucigenin, initial

B - - - - - 3×10^{-5} M Lucigenin, final

C — - - — 3×10^{-4} M Lucigenin, initial

D — - — - 3×10^{-4} M Lucigenin, final

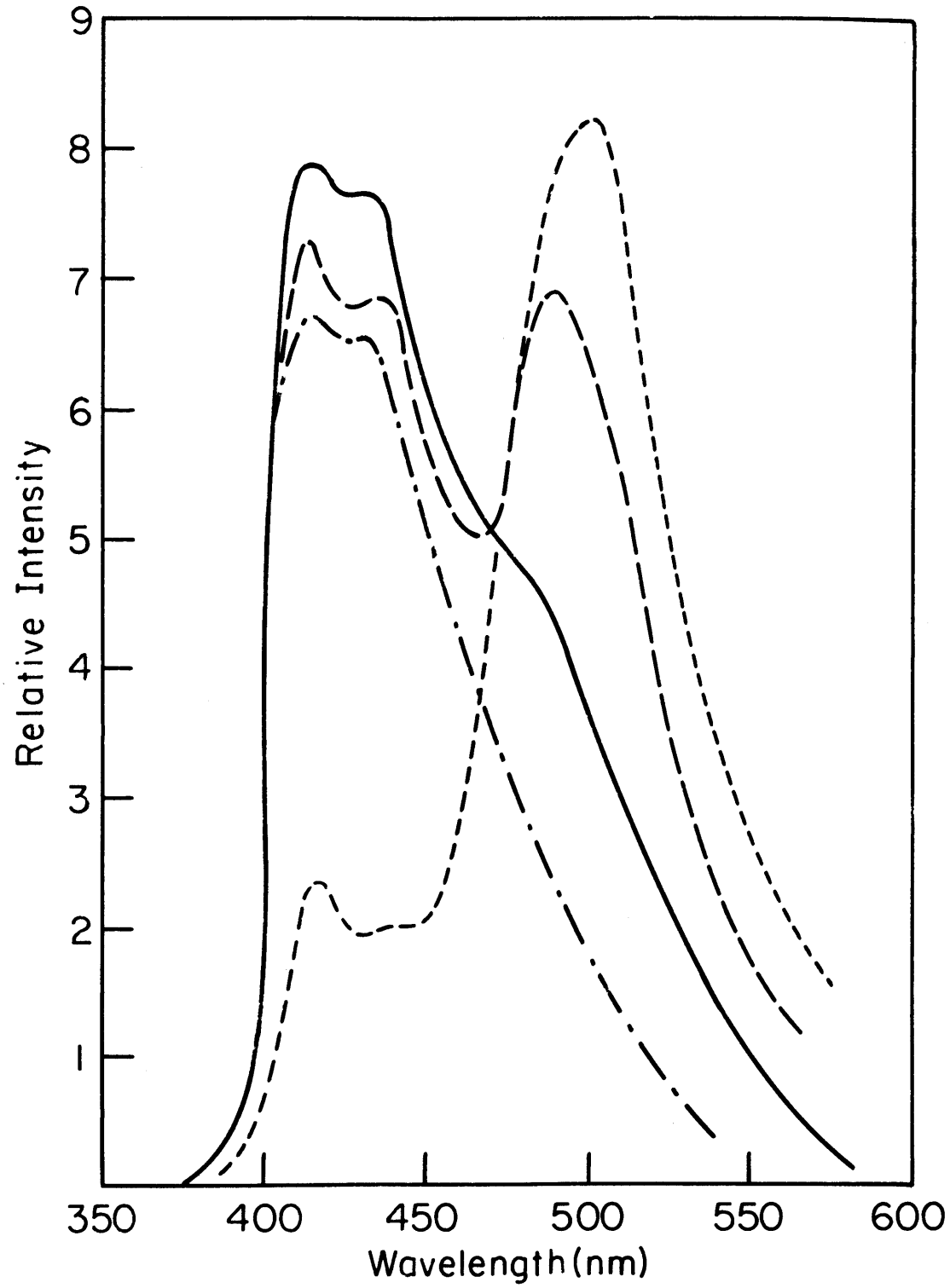
9
8
7
6
5
4
3
2
1
Relative Intensity
350
400
450
500
550
600
Wavelength (nm)

Figure IX-3

Chemiluminescence and Fluorescence Spectra in DMF

A — - — Fluorescence of NMA

B — — - Fluorescence of Lucigenin

C - - - - Fluorescence of DBA

D — — — 3×10^{-5} M Lucigenin, final

E ———— 3×10^{-4} M Lucigenin, initial

F — - - — 3×10^{-4} M Lucigenin, final

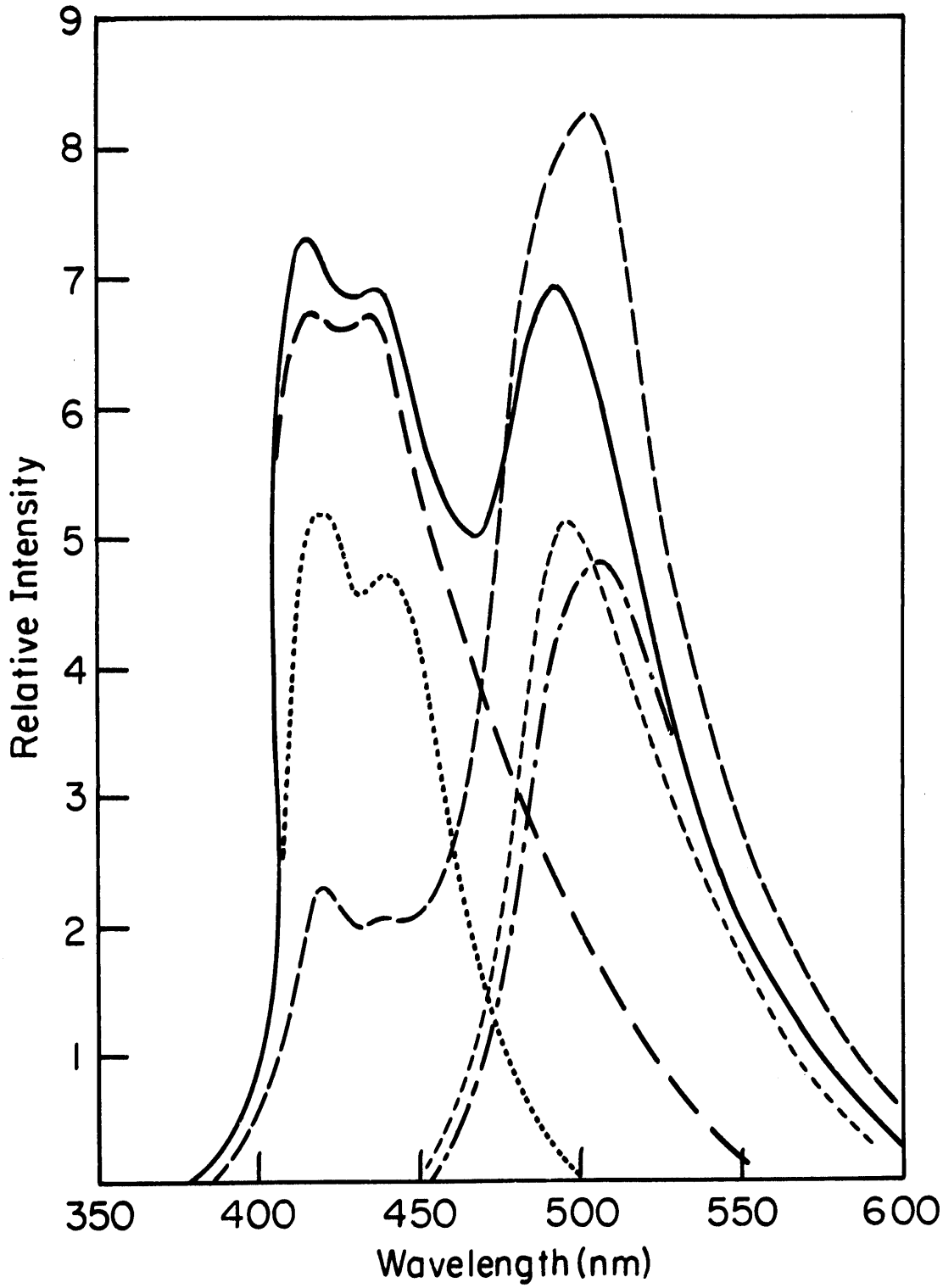
9
8
7
6
5
4
3
2
1
Relative Intensity
350
400
450
500
550
600
Wavelength (nm)

Figure IX-4

Chemiluminescence Spectra in AN

5×10^{-4} M KOtBu

A - - - - - - 3×10^{-5} M Lucigenin, initial

B —— - - —— 3×10^{-5} M Lucigenin, final

C —— - —— - 3×10^{-4} M Lucigenin, initial

D ———————— 3×10^{-4} M Lucigenin, final

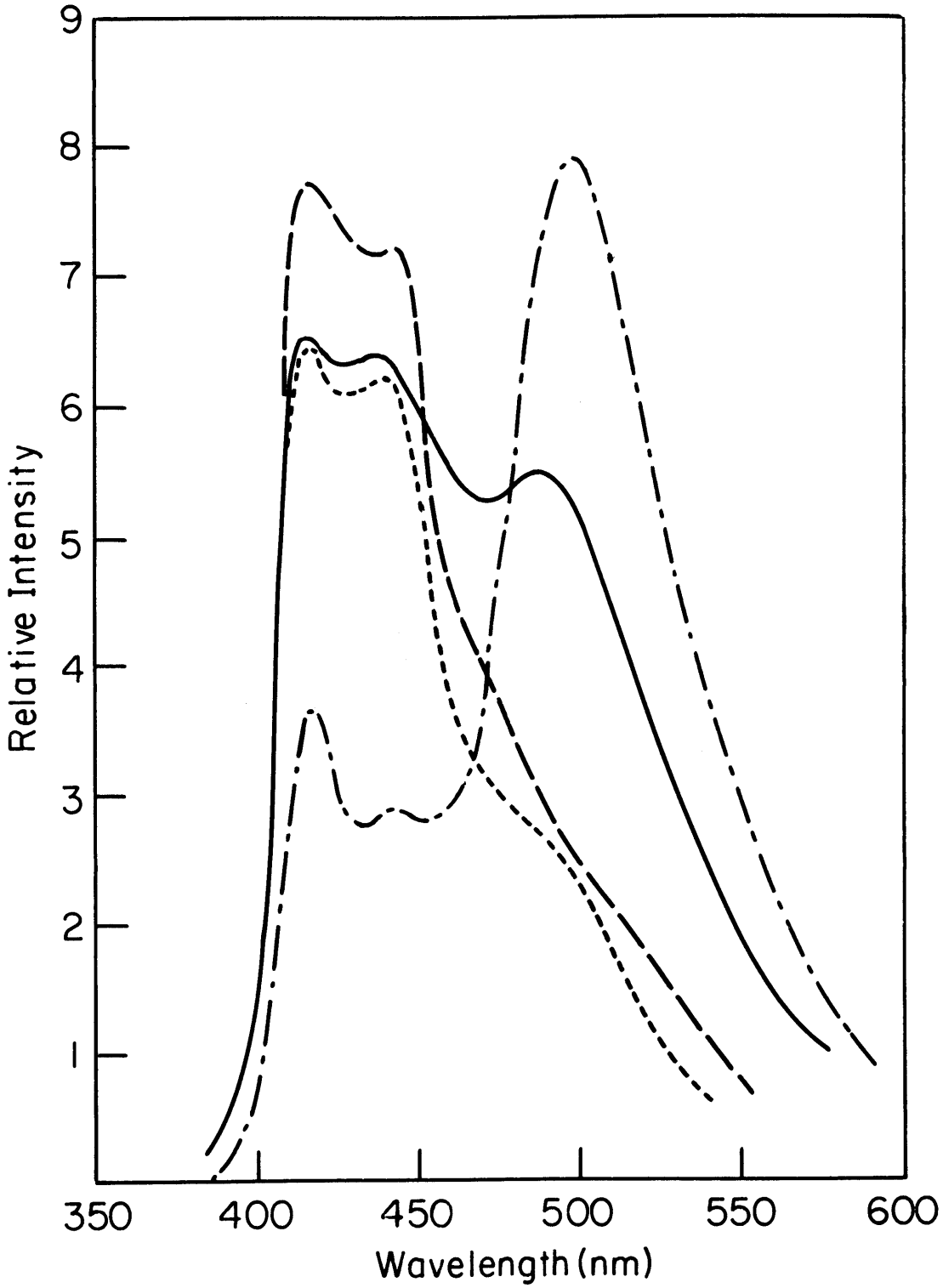
9
8
7
6
5
4
3
2
1
Relative Intensity
350
400
450
500
550
600
Wavelength (nm)

Figure IX-5

Chemiluminescence Spectra in AN at Various Flow Rates

10^{-4} M Lucigenin, 5 X 10^{-4} M KOtBu

A - - - speed 1, 2.5 X 10^{-2} sec after mixing

B ——— speed 10, 5 X 10^{-1} sec after mixing

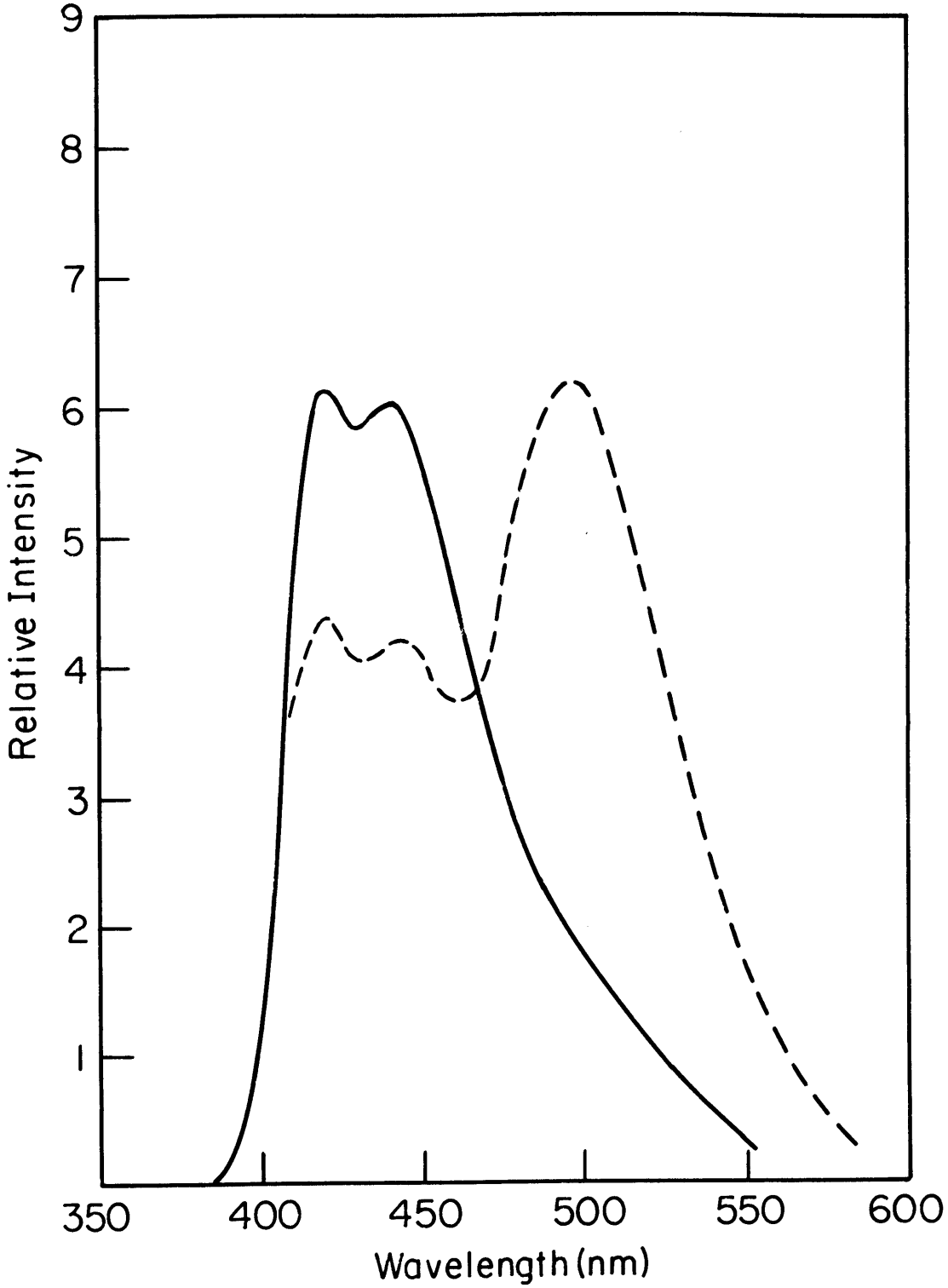
9
8
7
6
5
4
3
2
1
Relative Intensity
350
400
450
500
550
600
Wavelength (nm)

light in DMSO, DMF and AN by reaction of KOtBu with oxygen and lucigenin. Driscoll et. al. (20) have reported the observation of weak CL by reaction of KOtBu and oxygen with lucigenin in methanol but no work has been reported in other non-aqueous solvents. Addition of small amounts of water quenched the luminescence and this may be due to a reaction of KOtBu with water forming KOH and t-butyl alcohol which do not produce CL in these solvents. At high lucigenin concentrations (greater than 5×10^{-4} M) and high KOtBu concentrations (greater than 10^{-3} M). The intensity of the emission decreased. It was also noted that at these concentrations the solution, after reaction, fluoresced green, even when the solvent was AN. At the end of the reaction there is little lucigenin present and in AN DBA fluoresces poorly. A saturated solution of DBA in AN yields only 10% of the fluorescence intensity measured for the green fluorescing product. Thus it appears that a third, yet unidentified product is formed at these concentrations. Its effect on the spectra observed is discussed below. This product has not been characterized. Its absorption and fluorescence spectra in basic media and its absorption spectra after acidification with HCl gas are shown in Figure IX-6. (Compound formed from reaction of 10^{-3} M lucigenin with 10^{-3} M KOtBu,) It may well be that this compound is the product of a direct reaction of lucigenin with strong base much like the reaction in water at pH 12 forming DBA. Totter (45) has seen such a reaction in ethanol forming a product with similar absorption and fluorescence spectra to those obtained for this compound. Further work is necessary to identify this compound and fit its role into the gross kinetic scheme.

Figure IX-6

Absorption and Fluorescence Spectra of Compound

Formed by Reaction of Lucigenin with KOtBu in AN

A ——— Absorption Spectrum of solution after addition of KOtBu to 10^{-3} M Lucigenin and diluting 10:1

B — - — Fluorescence spectrum of A excited at 400 nm

C - - - - Absorption spectrum of A after acidification with HCL gas

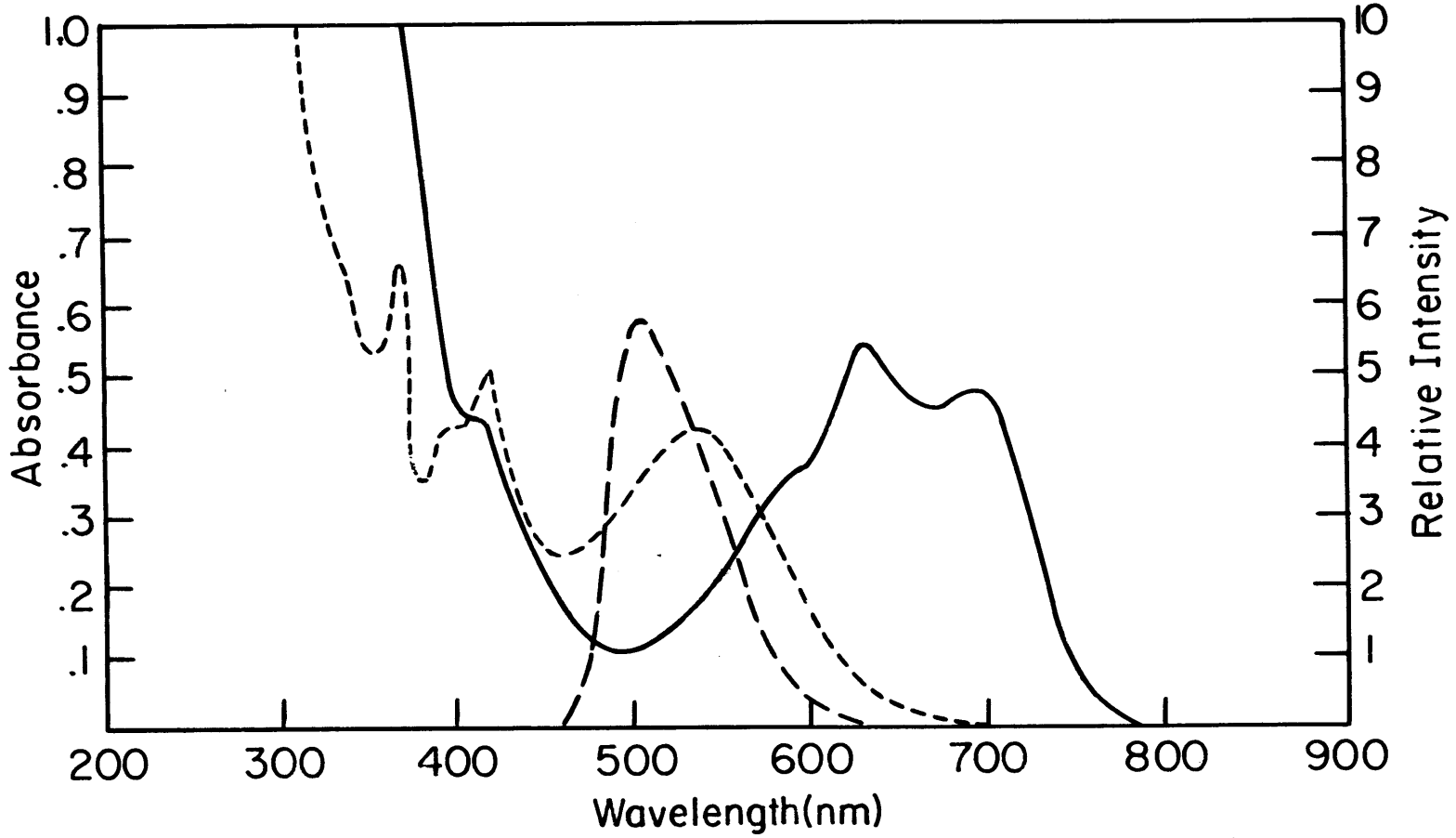
Absorbance
1.0
.9
.8
.7
.6
.5
.4
.3
.2
.1
Relative Intensity
10
9
8
7
6
5
4
3
2
1
200
300
400
500
600
700
800
900
Wavelength(nm)

In the course of studies of the green-fluorescent product of the reaction of KOtBu with lucigenin the NMR spectrum of lucigenin was obtained. This appears in Figure IX-7 along with the assignments for the various protons of lucigenin. Trifluoro acetic acid (TFA) was used as the solvent because lucigenin was not soluble enough in any other solvent to obtain a spectrum. When this solvent was used to obtain the NMR spectrum of DBA another interesting reaction was seen to occur. The NMR spectrum obtained was identical to that of lucigenin. This suggested an oxidation of DBA back to lucigenin in this system. When DBA was dissolved in vacuum degassed TFA and sealed off it was seen to be stable for a period of several days. However, when the cell was opened to the atmosphere the absorption spectrum obtained showed a rapid change from that of DBA to that of lucigenin. This indicates a rapid, acid catalyzed air oxidation of DBA to lucigenin:

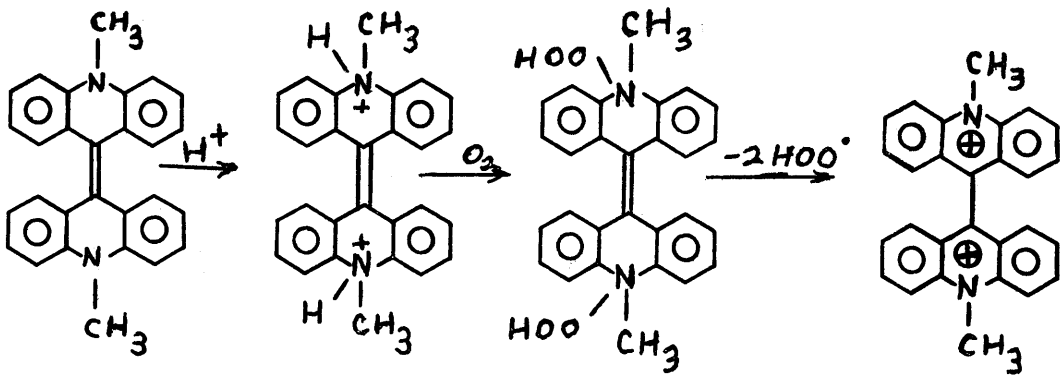

As indicated above, the structure of the green-fluorescing product is unknown. It has been shown to exist in different forms in acid and basic media (see Figure IX-6) which are interconvertable. Since each form has a very long wavelength absorption the reaction must involve ring closure between the primary acridene rings of lucigenin to provide the necessary conjugation for this long-wavelength absorption.

Figure IX-7

NMR Spectrum of Lucigenin in Trifluoroacetic Acid

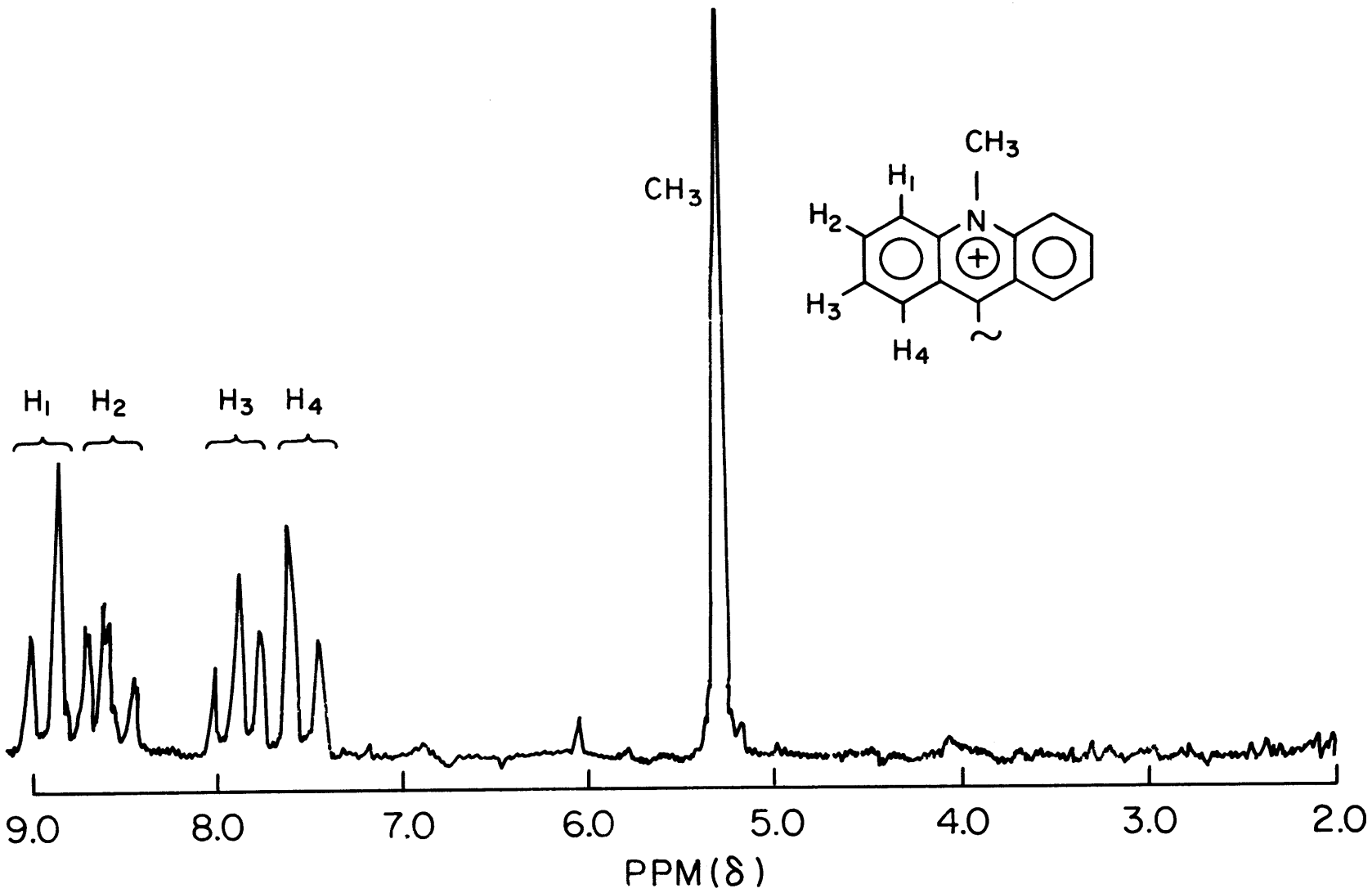
CH3
H1
H2
H3
H4
N
CH3
H1
H2
H3
H4
9.0
8.0
7.0
6.0
5.0
4.0
3.0
2.0
PPM(δ)

Further work is necessary before any definitive structural assignment may be made.

2. Non-Aqueous Chemiluminescence Spectra

Ideally one should use a flow apparatus to observe CL spectra. However, as observed in Figure IX-5, in this system the spectrum obtained is highly dependent on the flow rate employed. To obtain spectra which reflect the gross properties of the emission from this reaction non-flow conditions were necessary. The IIS proved invaluable in taking these spectra as it was able to record a spectrum in ca 10 sec. This spectrum is integrated over the time interval of measurement and shows no distortion due to intensity decay during the time of measurement. The spectra presented in Figure IX-1-4 are very similar to those obtained in these solvents for the ECL (see section VII). The same arguments presented above may be used to explain these spectra and it would be redundant to reiterate them here. Thus, at lucigenin concentrations up to 3×10^{-4} M when the KOtBu concentration was 5×10^{-4} M the characteristics of the spectra are easily explained by correlation of the extent of reaction with energy transfer and the quantum efficiencies of the acceptors.

Spectral studies at concentrations of lucigenin greater than 5×10^{-4} M when KOtBu was greater than 10^{-3} M were extremely difficult and no reliable spectra were obtained. This was due to the great decrease in intensity of the emission at these concentrations. A probable cause of this effort is the rapid reaction of lucigenin with KOtBu forming the green-fluorescing product which is non-chemiluminescent. Visual observation of the spectra (in AN at 6×10^{-4} M lucigenin) projected

on the phosphor screen of the IIS showed a persistent long wavelength emission, probably a result of energy transfer to the third product.

The results of the spectra obtained when flow-type mixing was employed are extremely interesting. Figure IX-5 shows these results in AN. At very slow flow rates (looking at the emission a longer time after mixing) only NMA emission was observed, indicating that lucigenin had been greatly reduced in concentration during the time interval before observation. At very fast flow rates (looking at the emission a shorter time after mixing) both short and long wavelength emission was observed and the spectrum matches that seen initially under stationary conditions. These spectral dependencies on flow rate (which is a direct measure of the time of reaction) should provide an extremely useful handle for studying the reaction kinetics for this system.

The work of Matheson and Lee(46) indicates that KOtBu reacts with oxygen in DMSO to form superoxide. This is important since the striking similarity between the CL spectra, obtained from reaction of dilute KOtBu with lucigenin and oxygen, to the ECL spectra in the same solvents indicates similar reactions. This has been shown to be the case when comparing the ECL and CL spectra in water where both involve reaction of lucigenin with OH^- and H_2O_2. In non-aqueous solvents the chemiluminescence would then appear to arise from the reaction of lucigenin with superoxide. Superoxide is formed by direct electrochemical reduction of oxygen in the ECL whereas in the non-aqueous CL it is formed by the reaction of KOtBu with oxygen. At higher KOtBu concentrations the parallel reaction of base with lucigenin forming the green-fluorescent compound effectively competes with the CL reaction.

Appendix A

Quenching of Lucigenin Fluorescence

Weber (47) has reported the quenching of lucigenin fluorescence by chloride, bromide, iodide and thiocyanate ions. He noted that the quenching by iodide and bromide appearted to be due to the "heavy-atom" effect (48), while quenching by chloride and thiocyanate appeared to be related to their oxidation potentials. Leonhardt and Weller (49) observed charge-transfer quenching of perylene fluorescence by certain electron donors (notably amines). They confirmed what others (50, 57) surmised, namely that quenching proceeds through a charge-transfer intermediate:

$$F^* + Q \rightarrow (F^- Q^+) \rightarrow F + Q.$$

In the case of perylene quenching by amines, they were able to observe the mono-anion radical of perylene in polar solvents. They were also able to show a relationship between the ionization potential of the amine and its quenching efficiency. These observations were in accord with the following mechanism:

$$1.\quad P^* + Q \rightarrow (P^{-\cdot} Q^{+\cdot})$$

$$2.\quad (P^{-\cdot} Q^{+\cdot}) \rightarrow P^{-\cdot} \text{ solv } Q^{+\cdot} \text{ solv}$$

$$3.\quad (P^{-\cdot} Q^{+\cdot}) \rightarrow P + Q.$$

They were not able to observe the charge-transfer complex $(P^{-\cdot} Q^{+\cdot})$ due to its short lifetime ($<10^{-7}$ sec).

Since Weber (47) has shown a relationship between oxidation potential and the efficiency of quenching of lucigenin fluorescence by chloride and thiocyanate it was thought that further investigation,

similar to the work of Leonhardt and Weller (49) would provide a better understanding of this quenching mechanism.

Results and Discussion

The TRW lifetime apparatus was used to determine the rate constant for chloride quenching of lucigenin fluorescence in water. A straight line was obtained in the Stern-Volmer plot with a slope of 4.4×10^{10} 1/M-sec, a diffusion-controlled rate.

The effect of a series of anions on the fluorescence of lucigenin was studied. These results are shown in Table A-1. Iodide and bromide were not included because they quench primarily by the "heavy-atom" effect. The rate constant for quenching (k_q) was calculated from:

$$k_q (Q) = I_o/I_q - 1.$$

These rate constants give a good indication of the relative quenching efficiency of the various ions. Although only a partial list of the ionization potentials (I_q) of the ions was available, it appears that the quenching efficiency is related to the ionization potential. Some discrepancies are noted but these occur when a reaction between lucigenin and the salt appeared to take place.

Since amines have been shown to be efficient charge-transfer quenchers (49), and because the ionization potentials of these compounds are well-known, (52, 53), a study was made of the quenching of lucigenin fluorescence by various amines. The results of this study appear in Table A-2. A plot of the fluorescence intensities with quencher present vs. ionization potential of the quencher is shown in

Table A-1

Anion Quenching of Lucigenin Fluorescence

Quencher Concentration 5 X 10^{-2} M

Quencher	I_f	k_q (1)	I_p (2)
	92 (I_o)	-	
KF	92	-	17.4
$NaClO_4$	92	-	
Na_2SO_4	55	7.1 X 10^8	
$NaC_2H_3O_2$	29	2.3 X 10^9	10.35
$NaHSO_3$	7.8	1.1 X 10^{10}	
NaOH (3)		1.1 X 10^{10}	13.2
KCN	5.1	1.8 X 10^{10}	13.7
KCL	4.7	1.9 X 10^{10}	13.0
Na_2SO_3	3.1	3.0 X 10^{10}	
NaCNS	1.3	7.4 X 10^{10}	
Na_2S	0.3	(4)	10.5

(1) From $I_o/I_f = 1 + k_q(Q)$

(2) R.W. Kiser, U.S. Atomic Energy Comm. Report TID-6142 (1960)

(3) From Lifetime Measurements

(4) appeared to react, k_q calcualated to be 3.2 X 10^{11}

Table A-2

Quenching of Lucigenin Fluorescence by Amines[a]

Quencher	I_f[b]	I_P[c]
	10.0[d]	
CH_3NH_2	1.0	8.97
$i\text{-}C_3H_7NH_2$	0.9	8.72
$n\text{-}C_4H_9NH_2$	0.8	8.71
$(CH_3)_2NH$	0.6	8.24
$(CH_3)_3N$	0.5	7.82
$(C_2H_5)_3N$	0.4	7.56

(a) aqueous solutions 2 X 10^{-2} M in quencher, 10^{-4} M Lucigenin

(b) Fluorescence intensity

(c) ionization potential from Watanabe (52,53)

(d) 10^{-4} M Lucigenin

Figure A-1. The linear dependence of quenching efficiency is good evidence for charge transfer quenching of lucigenin by these amines. Quenching by chloride at the same concentrations gives an I_f of 1.2. The ionization potential of chloride is 1.30 ev (54), and it may be seen from Figure A-1 that this will not fall on the same straight line observed for amine quenching. In fact, chloride is a more efficient quencher than are the amines studied.

Leonhardt and Weller (49) were able to observe an effect of solvent polarity on the quenching efficiency of amines on perylene. This has been ascribed to solvent stabilization of the radical ions formed during charge-transfer. Analogous experiments were run for the chloride quenching of lucigenin. These results are shown in Table A-3. The quenching efficiency showed no effect due to solvent polarity.

During the course of flash photolysis studies of the quenching by chloride, it was noted that lucigenin photoreacts in water, but that when chloride was present no photoreaction was observed. Figure A-2 shows the absorption spectra before and after 10 flashes (500 joules per flash). When chloride was present at 10^{-1} M, no absorption change was noted.

Three experiments were run to further study the nature of the photoreaction. A solution of lucigenin in water was vacuum degassed by six freeze-pump-thaw cycles, and irradiated in a photoreactor for one hour using 365 nm lamps. Significant photoreaction occurred. Next, a solution of lucigenin in water was saturated with oxygen and irradiated under the same conditions. Photoreaction was also observed amounting to 90% of that when oxygen was absent. Third, a solution

Figure A-1

Relationship between Ionization Potential and Curves and their Efficiency of Quenching Lucigenin Fluorescence

aqueous solutions 2 X 10^{-2} M in quencher, 10^{-4} M in Lucigenin

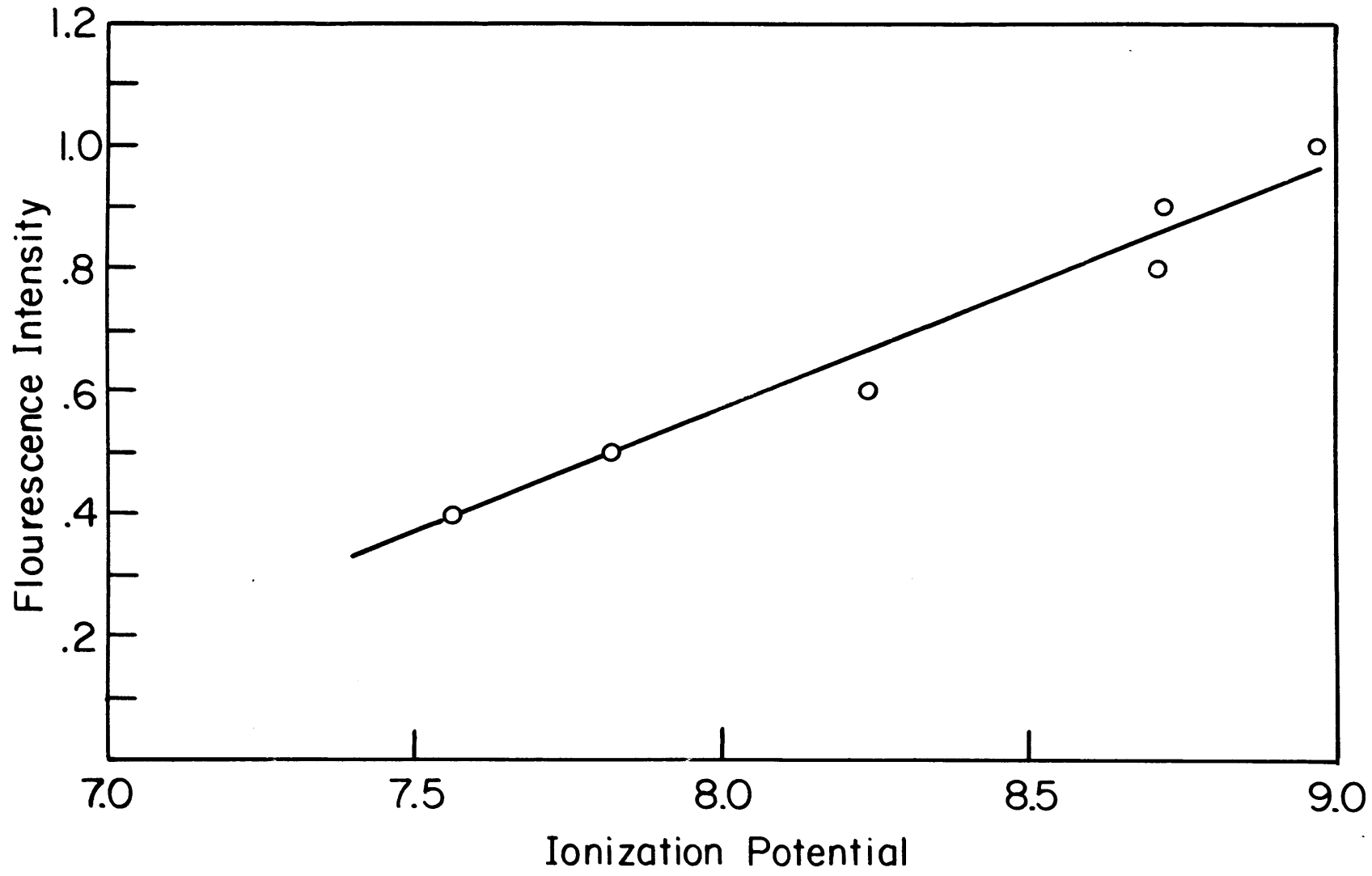
1.2
1.0
.8
.6
.4
.2
Flourescence Intensity
7.0
7.5
8.0
8.5
9.0
Ionization Potential

Table A-3

Chloride Quenching of Lucigenin in Fluorescence in Various Solvents

	H_2O	EtOH	DMSO	AN
I_o[(a)]	25.2	7.6	2.2	24.4
I[(b)]	4.7	1.4	0.4	4.6
I_o/I	5.4	5.1	5.5	5.3

a) Fluorescence intensity without Tetramethyl Ammonium Chloride (TMAC)

b) Fluorescence intensity with 10^{-2} M TMAC

Figure A-2

Absorption Spectra of Lucigenin in Water before and after Photoreaction

_____ Absorption spectrum of Lucigenin solution before flashing

— — — Absorption spectrum of Solution after 10 flashes (500 joules per flash)

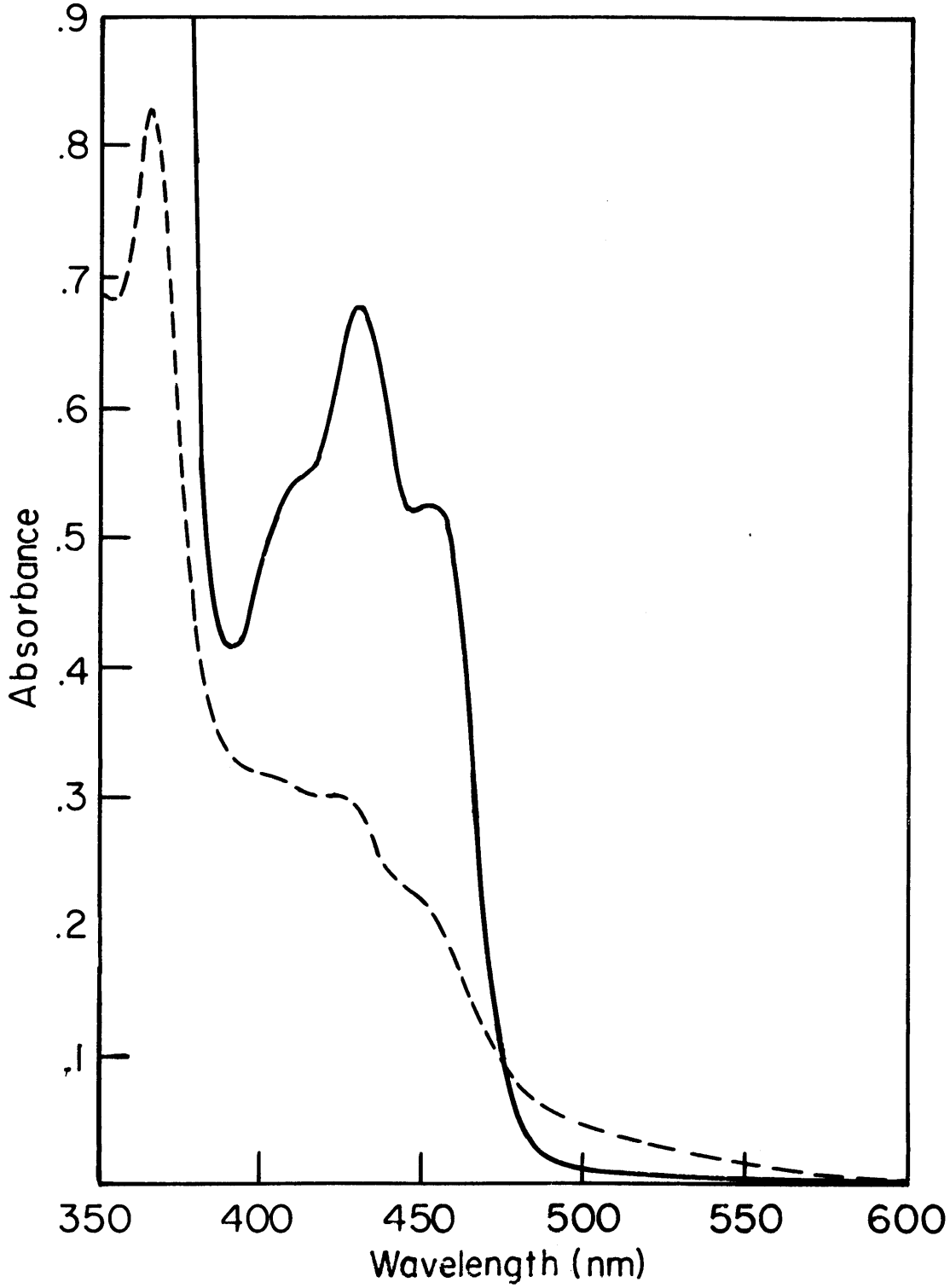
.9
.8
.7
.6
.5
.4
.3
.2
.1
Absorbance
350
400
450
500
550
600
Wavelength (nm)

of lucigenin in water with 10^{-1} M KCL was irradiated under the same conditions after being vacuum degassed. No evidence of photoreaction was seen. These three experiments indicate that the photoreaction involves the excited singlet state of lucigenin. Since a significant amount of photoreaction was observed when oxygen was both present and absent it is unlikely that the triplet state is involved due to the rapid quenching of triplets by oxygen (48). The slight decrease in photoreactivity when oxygen was present is probably a result of enhancement of the intersystem crossing rate by oxygen perturbation (48).

To further identify the reactive state responsible for the photoreaction the following experiment was run. Solutions of lucigenin were prepared with varying chloride concentrations. This provided a series of solutions of lucigenin with varying quantum efficiencies of fluorescence. The lifetime of the lucigenin fluorescence (directly related to the quantum efficiency) and the absorbance of each solution were measured. The 450 nm wavelength was chosen because there is little overlap between lucigenin and the photoproduct absorption at this wavelength (see Figure A-2). The solutions were placed in a caroussel photoreactor to ensure identical exposure and were irradiated for one hour. The absorbance of each solution was again measured. These results are presented in Table A-4.

The change in absorbance (ΔA, at 450 nm) is a measure of the amount of photoreaction. When the lifetime is plotted vs. ΔA a straight line should result if the reaction proceeds from the singlet state, since chloride affects only the singlet state of lucigenin. Figure A-3 shows the plot of ΔA vs. the lifetime for the data of

Table A-4

Photolysis of Lucigenin as a Function of Chloride Concentration

Solution	τ (ns)	A (450 nm) Initial	After 1 hr Photo	ΔA
1	20.4	1.26	1.09	.17
2	13.6	1.27	1.09	.13
3	10.0	1.26	1.18	.08
4	9.2	1.24	1.19	.05
5	5.4	1.195	1.18	.015
6	3.2	1.245	1.24	.005

Table A-4. This plot provides proof that the photoreaction proceeds through the first excited singlet state of lucigenin. Long term photolysis of lucigenin has yielded a product of yet undetermined structure. Traces of NMA are present, and it has been shown that the product is not DBA.

The results of the flash photolysis studies were of dubious value. Due to the photoreaction of lucigenin, it was hard to distinguish between the various absorption changes, although it did appear that no absorption due to $L^{+\cdot}$ or $L^{+\cdot}CL^{+\cdot}$ were present. The effect of chloride on the amount of triplet lucigenin could not be determined.

The above mentioned studies indicate that the quenching of lucigenin fluorescence by anions is due to a charge-transfer mechanism similar to that proposed by Leonhardt and Weller (49) for quenching of perylene by amines. The mechanism for chloride quenching of lucigenin fluorescence is as follows:

$$(L^{++})^{*} + Cl^{-} \rightarrow (L^{+\cdot}\ Cl^{\cdot}) \rightarrow L^{++} + Cl^{-}.$$

This mechanism is consistent with the observations and is reasonable by analogy to similar system. Since, for chloride quenching of lucigenin, a chlorene atom is formed in the charge-transfer complex, one would not expect to see solvent stabilization of the complex. This was seen to be the case. When an amine is used to quench lucigenin fluorescence the charge-transfer complex is $(L^{+\cdot}A^{+\cdot})$ and one would expect to see a large effect due to solvent polarity. However, these amines stimulate the photoreaction of lucigenin and thus studies of the charge-transfer complex or the solvated radical ions are virtually impossible.

Figure A-3

Amount of Photoreaction (ΔA) vs. the Lifetime of Lucigenin Fluorescence at Various Chloride Concentrations

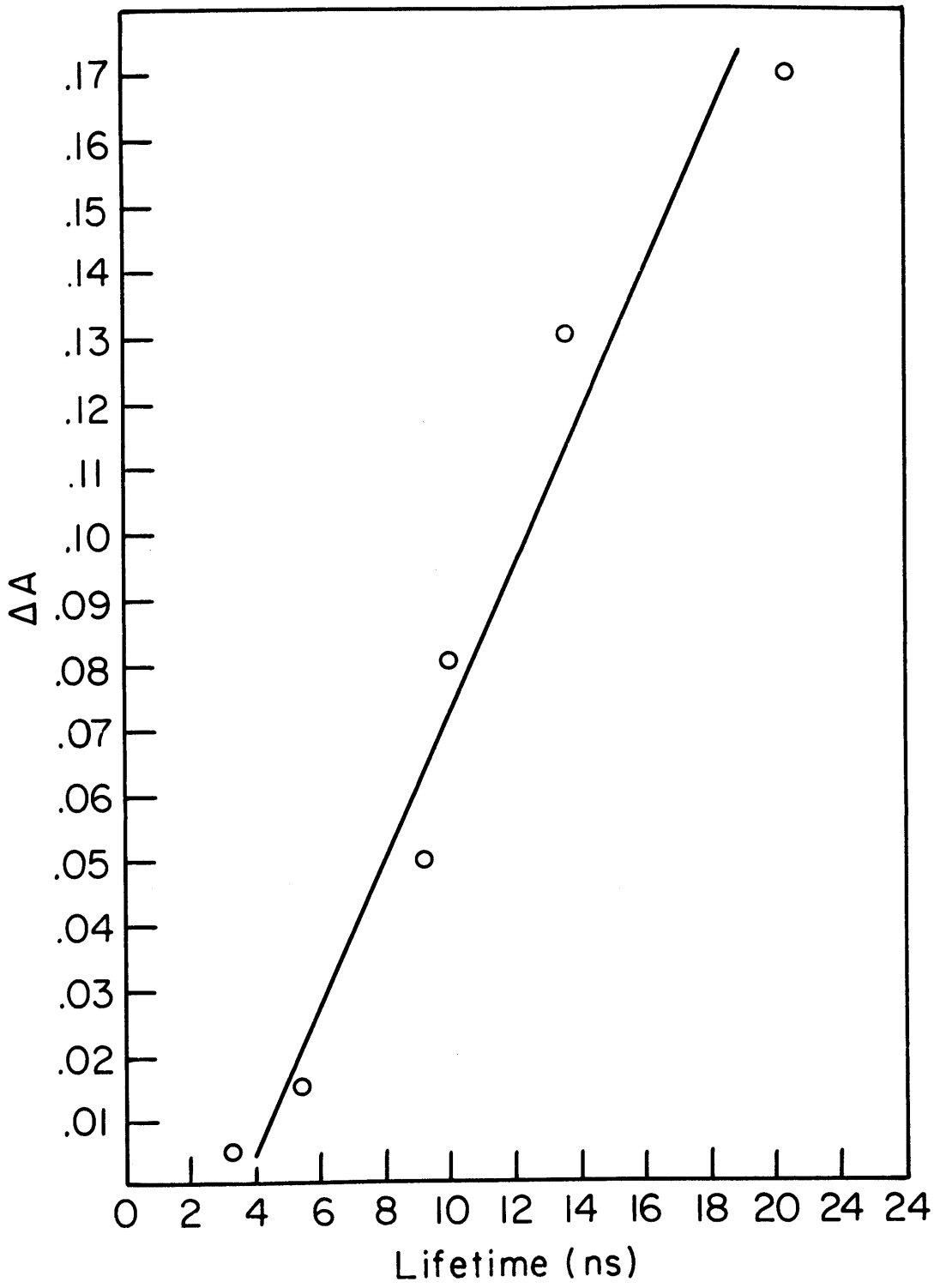
.17
.16
.15
.14
.13
.12
.11
.10
.09
.08
.07
.06
.05
.04
.03
.02
.01
ΔA
0 2 4 6 8 10 12 14 16 18 20 24 24
Lifetime (ns)

When amines are used to quench the fluorescence a straight line dependence between quenching efficiency and ionization potential of the amine is seen. Thus, the lower the ionization potential of the quencher, the greater is its quenching efficiency. This trend is also seen when anions are used as quenchers. It appears that these anions are more efficient quenchers than are the amines studied. This is not unreasonable since lucigenin is a doubly charged cation and would have a stronger attraction for an anion than for an amine. The net result of this attraction would be a lower energy of activation for formation of the charge-transfer complex and an overall increase in the quenching efficiency.

The mode of dissipation of energy from excited singlet state lucigenin is shown in Figure A-4. Although the absolute relationship between the ground and excited states energies of L^{++}, $L^{+\cdot}$ and Cl^{-} are not known, a reasonable relationship may be surmised. Since chloride does not reduce lucigenin its highest ground state level must lie below the lowest excited singlet level of lucigenin. It is also known that chloride does not oxidize lucigenin. Thus the ground level of chloride must lie between the ground and lowest excited singlet levels of lucigenin. Figure A-4, (1) is the state diagram for excited singlet state lucigenin $(L^{++})^{*}$ and for ground state chloride. When the charge transfer complex with chloride is formed the situation depicted in Figure A-4, (2) results. Energetically the electron from chloride will preferably go into the lowest possible level in lucigenin as shown by the arrow in (1). When the charge-transfer complex breaks up, the electron transferred back to the chlorine atom will be that from the highest energy level of $L^{+\cdot}$ which then leaves lucigenin and chloride both in the ground state (Figure A-4, (3)).

Figure A-4

State Diagrams Showing Mode of Energy Dissipation

in Fluorescence Quenching by Chloride Ion

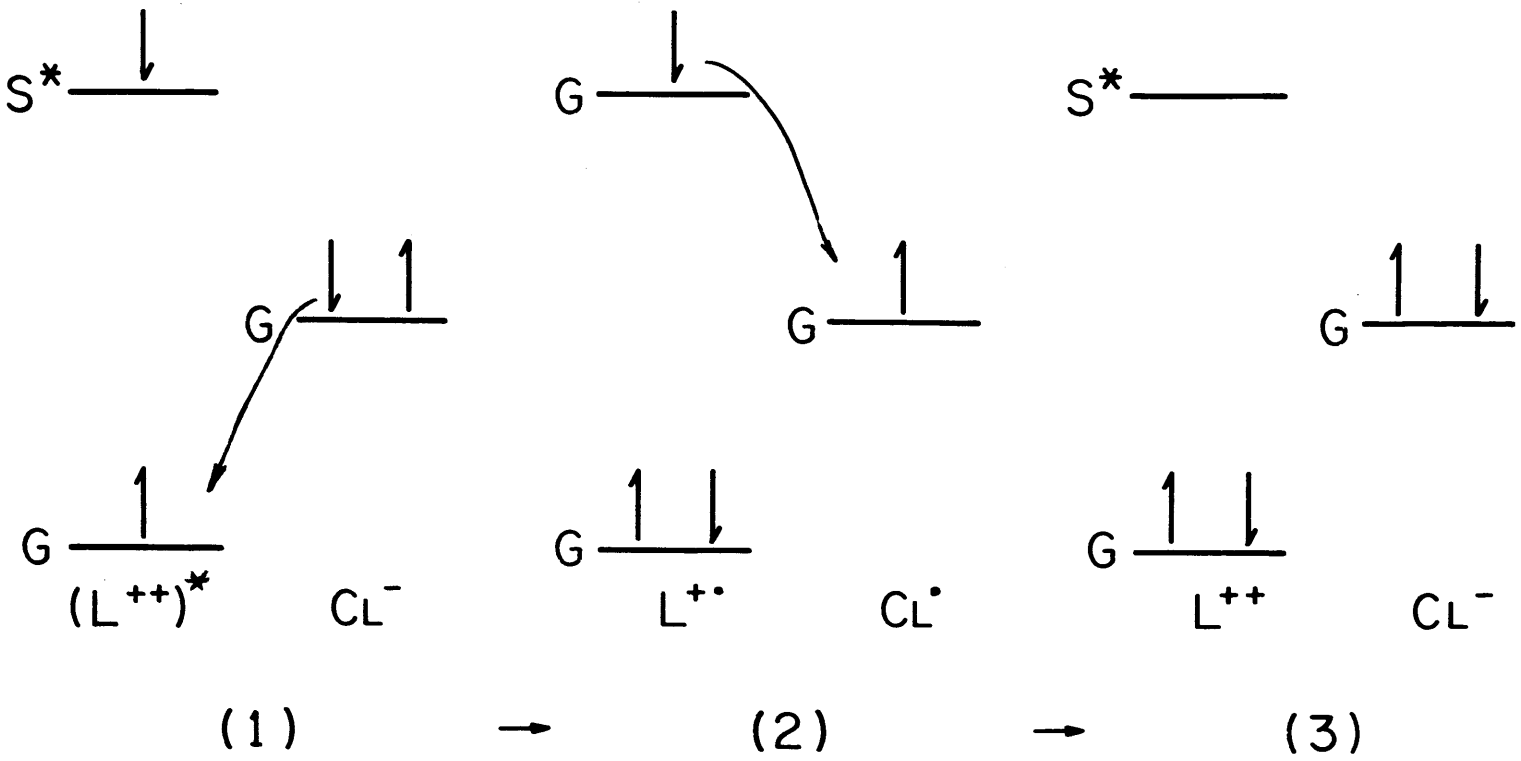
S*
G
S*
G
G
G
G
G
(L++)*
CL−
L+•
CL•
L++
CL−
(1)
(2)
(3)

References

1. B. Radzisewaki, Ber., 10, 70, 321 (1877)
2. H. O. Albrecht, Z. Phys. Chem., 136, 321 (1928)
3. K. Gleu and W. Petsch, Angew. Chem., 48, 57 (1935)
4. K. D. Gundermann, Angew. Chem. Inter. Ed., 4, 566 (1965)
5. E. A. Chandross and F. I. Sontag, J. Amer.Chem. Soc., 86, 3179 (1964)
6. D. M. Hercules, Science, 145, 808 (1964)
7. R. E. Visco and E. A. Chandross, J. Amer. Chem. Soc., 86, 5350 (1964)
8. F. E. Lytle, Ph.D. Thesis, Mass. Inst. of Tech., Cambridge, Mass (1968)
9. H. Kautsky and K. H. Kaiser, Naturwiss, 31, 505 (1943)
10. A. Spruit-van der Berg, Recueil, 69, 1525 (1950)
11. J. R. Totter, Photochem. Photobiol., 5, 177 (1966)
12. K. Weber and W. Oschenfeld, Z. Physik. Chim., B51, 63 (1942)
13. B. D. Ryzhikov, Bull. Akad. Sci. USSR, Phys. Ser., 20, 487 (1956)
14. B. J. Sveshinkov, Dokl. Akad. Nauk USSR, 35, 278 (1956)
15. F. McCapra and D. G. Richardson, Tetrahedron Letters, 43, 3167 (1964)
16. L. Greenlee, I. Fridovich and P. Handler, Biochemistry I, 779 (1962)
17. F. Mc Capra, Quar. Rev., 485 (1966)
18. J. R. Totter, Photochem. Photobiol., 3, 231 (1964)
19. B. Tammamushi and H. Akiyama, Trans. Faraday Soc., 35, 491 (1939)
20. J. S. Driscoll, et al, Monsanto Research Technical Report No. AD-643-132 (1966)
21. We wish to thank Dr. D. Kemp for this sample
22. H. Decker and W. Petsch, J. Prakt. Chem., 43, 211 (1935)
23. D. W. Shive, Ph.D. Thesis, MIT, Cambridge, Mass. (1969)
24. "Electronics for Scientists", H. Malmstadt, C. Enke and E. Toren Jr., W. A. Benjamin, Inc., New York, 1963

25. Model 210 Operating Manual, G. K. Turner Associates, Palo Alto, Calif.

26. G. K. Turner, Science, 146, 183 (1964)

27. A. M. Bass and K. G. Kessler, J. Opt. Soc. Am., 49, 1223 (1959)

28. S. Ness and D. M. Hercules, submitted to Anal. Chem., (1969)

29. Leeds and Northrup Manual DB-1325

30. K. D. Legg and D. M. Hercules, J. Am. Chem. Soc., 91, 1902 (1969)

31 C. A. Parker and W. T. Rees, Analyst, 85, 587 (1960)

32. "TRW Fluorometry Handbook", TRW Instruments, El Segundo, Calif.

33. J. A. Page and J. J. Lingane, Anal. Chem. Acta, 16, 175 (1957)

34. R. S. Nicholson and I. Shain, Anal Chem., 36, 706 (1964)

35. E. G. Janzen, J. B. Pickett, J. W. Happ and W. DeAngelis, submitted to J. Org. Chem., (1969)

36. E. G. Janzen, private communication

37. "Electrochemistry at Solid Electrodes", R. N. Adams, Marcel Dekker, Inc., New York (1969)

38. G. L. Booman and D. T. Pence, Anal. Chem, 36, 1366 (1965)

39. D. L. Maricle and W. G. Hodgson, Anal. Chem., 37, 1562 (1965)

40. M. E. Peover and B. S. White, Electrochim. Acta, 11, 1061 (1966)

41. N. J. Turro, "Molecular Photochemistry", W. A. Benjamin, Inc., New York, 1965

42. W. R. Ware, J. Am. Chem. Soc., 83, 4374 (1961)

43. T. H. Forster, "Fluoreszenz Organisher Verbindungen", Vandenhoeck and Ruprecht, Gottingen, 1951

44. L. N. Nekrasov, Electrokhimiya, 2, 438 (1966)

45. J. R. Totter, Private Communication

46. I. B. C. Matheson and J. Lee Spectroscopy Letters, 2, 117 (1969)

47. K. Weber, Z. Physik. Chim., B51, 100 (1941)

48. "Photochemistry", J. G. Calvert and J. W. Pitts, Jr., John Wiley and Sons, Inc., New York, 1967

49. H. Leonhardt and A. Weller in "Luminescence of Organic and Inorganic Materials", Ed. by H. D. Kappmann and G. M. Spruch, John Wiley and Sons, Inc., New York, 1962

50. E. Bauer, Z. Phys, Chem., B16, 465 (1932)

51. J. Weiss and H. Fischgold, Z. Phys. Chem., B32, 135 (1936)

52. K. Watanabe, J. Chem. Phys., 26, 542 (1957)

53. Ibid, 1773

54. R. W. Kiser, U. S. Atmoic Energy Comm. Report, TID-6142 (1960)

Biographical Note

The author was born February 19, 1943 in Ogdensburg, New York. He attended public schools in Endwell and Dansville, New York, graduating from Dansville Central High School in 1960. He entered Union College, Schenectady, New York in 1960, from which he received the B.S. degree in Chemistry in June 1964.

After graduation from Union College, he was employed by the Cabot Corporation, Boston, Massachusetts during the summer of 1965. He entered M.I.T. in September 1964 as a candidate for the degree of Doctor of Philosophy.

While at M.I.T. he married the former Ardelle M. Fullerton.

The author is a member of the American Chemical Society.